The ghrelin axis in the skeletal microenvironment

Safraz Mohamed Omer

BSc (Hons) Biomedical Science

University of Lincoln (UK)

Institute of Health and Biomedical Innovation

Translational Research Institute

Faculty of Health

Queensland University of Technology

Thesis submitted for the award of the degree of Master of Applied Science (Research) at Queensland University of Technology

Keywords

Ghrelin, acyl ghrelin, des-acyl ghrelin, growth hormone secretagogue receptor type 1a (GHSR1a), ghrelin *O* acyl transferase (GOAT), growth hormone receptor (GHR), trabecular bone, cortical bone, micro-computed tomography, immunohistochemistry, chondrocytes, osteoblasts, osteoclasts.

Abstract

Ghrelin is a 28 amino acid peptide hormone that is acylated on the third amino acid residue of serine. The ghrelin axis, comprising ghrelin and its receptor, is expressed by cells of the bone and cartilage microenvironments indicating that it may modulate skeletal metabolism. Positive correlations have been observed between ghrelin levels and bone mineral density (BMD) in several human populations, and administration of ghrelin increases BMD in rodents. Ghrelin receptor (GHSR1a) knockout (GHSR$^{-/-}$) mice have shown significantly weaker bone micro-architectures with ageing due to increased osteoclast activity. As GHSR1a only partly mediates acyl ghrelin signalling, the first part of this project aimed to characterise the bone microarchitecture of adult GOAT$^{-/-}$ mice, which do not produce the acylated form of ghrelin. Micro-computed tomography (micro-CT) was used to evaluate the trabecular and cortical bone micro-architecture of the femora and tibiae of female GOAT$^{-/-}$ mice and wildtype (WT) control mice aged 6, 9 and 18 months. The results showed that the trabecular bone microarchitecture of GOAT$^{-/-}$ mice aged 6 months had significantly less ($p<0.05$) bone volume fraction (BV/TV) as a result of decreased ($p<0.05$) trabecular connectivity, indicating that acyl ghrelin is involved in the regulation of physiological bone remodelling, by affecting the microarchitecture of trabecular bone. The trabecular BMD was not significantly different ($p>0.05$) in the GOAT$^{-/-}$ mice, indicating that acyl ghrelin signalling contributes to maintaining bone strength by affecting the microstructural property of trabecular bone rather than the mineralisation of the trabecular bone of adult mice. Reduced connectivity density may be a result of increased osteoclast activity due to the lack of acyl ghrelin signalling as reported with GHSR$^{-/-}$ mice. Trabecular BMD and BV/TV were not significantly ($p>0.05$) different in the 9 and 18 month old GOAT$^{-/-}$ mice compared to WT, however, the GOAT$^{-/-}$ mice at these ages were significantly heavier, and therefore the results may have been compromised. The cortical bone compartment of the GOAT$^{-/-}$ mice demonstrated distinctly different regulatory patterns to the trabecular bone compartment. Cortical BMD of the femora and tibiae of 6 month old GOAT$^{-/-}$ mice was significantly greater ($p\leq0.05$) than the WT controls, indicating that lack of acyl ghrelin signalling improves mineralisation. The resistance of cortical bone in the mid-diaphyses

(pMOI) of the femora of GOAT$^{-/-}$ mice at 6 months was not significantly different (p>0.05) compared to WT controls, however, the tibiae showed significantly reduced pMOI compared to WT controls. The periosteal apposition was not affected in the absence of acyl ghrelin as indicated by the lack of difference (p<0.05) in the GOAT$^{-/-}$ mouse femora and tibiae compared to WT controls. The endosteal resorption was reduced as the endosteal perimeter showed a significantly reduced (p<0.05) endosteal perimeter in the femora and tibiae of GOAT$^{-/-}$ mice. This suggests that osteoclast activity may be reduced in the cortical compartment of GOAT$^{-/-}$, unlike the trabecular compartment which suggested that the osteoclast activity enhanced in the GOAT$^{-/-}$ mice.

Rat chondrocytes and human immortalised chondrocytes have been shown to express ghrelin, but lack GHSR1a. In the second part of this project, we investigated whether ghrelin and GHSR1a is expressed by chondrocytes of the first trimester human fetal skeleton and mouse embryos and fetuses by immunohistochemistry. Ghrelin immunoreactivity was not seen in the chondrocytes of the first trimester human fetal upper limbs, lower limbs and vertebrae, suggesting that an autocrine/ paracrine ghrelin signalling pathway may be absent in the cartilage microenvironment. GHSR1a immunoreactivity was observed in the chondrocytes of the first trimester human fetal upper limbs, lower limbs and vertebrae, and mouse embryos/ fetuses aged E14.5, E16.5 and E18.5. Immunoreactivity was seen in the proliferating and mature hypertrophic chondrocytes identified based on morphology. Furthermore, ghrelin is associated with GH release and GH signals through GHR. GHR has been reported to be expressed by second trimester human fetal chondrocytes. Therefore, we further investigated, by immunohistochemistry whether GHR is expressed by chondrocytes of first trimester human fetal tissues and mouse embryos/ fetuses. GHR immunoreactivity was not observed in the chondrocytes of the first trimester human fetal chondrocytes, however, chondrocytes of E14.5, E16.5 and E18.5 mouse embryos/fetuses showed immunoreactivity. This project has shown that the ghrelin axis has a role in the regulation of the bone and cartilage microenvironments. Further work is necessary to determine whether the role in bone is direct (independent of other hormones such as GH) and whether pharmacological applications such as ghrelin mimetics have the potential to improve the bone microarchitecture in models of bone loss. Further work on determining expression of GHSR1a and GHR in chondrocytes based on the stages of endochondral ossification between the human and mouse embryos/fetuses will provide knowledge of the GHR and GHSR1a signalling commencement during skeletal development.

Table of Contents

List of Figures

List of Tables

List of abbreviations

-/- , KO	Knockout
µA	Micro-amps
µm	Micrometre
2D	Two dimensional
3D	Three dimensional
BMD	Bone mineral density
BV/TV	Bone volume fraction
C.Den	Connectivity density
cAMP	Cyclic adenosine mono-phosphate
cBMD	Cortical bone mineral density
ccm/cm^3	Cubic centimetre
CT	Computerised tomography
Ct.Ar	Cortical bone area
Ct.pm	Cortical perimeter
Ct.Th	Cortical thickness
Ec.pm	Endosteal perimeter
g	Grams
GH	Growth hormone
GHR	Growth hormone receptor
GHSR	Growth hormone secretagogue receptor
GOAT	Ghrelin *O* acyl transferase
GPCR	G protein coupled receptor
HA	Hydroxyapatite
IGF	Insulin like growth factor
kV	Kilovolts
MBOAT	Membrane bound *O* acyl transferase
mg	Milligrams
micro-CT, µCT	micro-computed tomography

mm	Millimetre
mm^2	Millimetre squared
mm^4	Millimetre to the power four
mRNA	Messenger RNA
p	Probability
PC	Pro-hormone convertase
pMOI	Polar moment of inertia
Ps.pm	Periosteal perimeter
ROI	Region of interest
RT-PCR	Reverse transcription polymerase chain reaction
S.E.M	Standard error of mean
Tb.N	Trabecular number
Tb.Sp	Trabecular separation
Tb.Th	Trabecular thickness
VOI	Volume of interest
WT	Wildtype

Acknowledgements

I would like to first thank my principal supervisor Dr. Laura Gregory for giving me the opportunity to undertake this project. I thank Dr. Laura Gregory and my associate supervisors Associate Professor Lisa Chopin and Dr. Penny Jeffery for their useful supervision, guidance and support in the direction of the project and project outcomes. I would like to additionally thank Dr. Penny Jeffery for providing the GOAT$^{-/-}$ mice and helping with human fetal tissue extraction and immunohistochemistry for this project; Dr. Laura Gregory for teaching me *in vivo* techniques, micro-CT and bone biology; and Associate Professor Lisa Chopin for her experienced supervision, leadership, direction, support with ethics applications and assistance writing of the thesis.

I thank Lisa Foster and Ben Harvie at Pharmacy Australia Centre for Excellence, animal facility staff at the Translational Research Institute and animal facility staff at the Mater Medical Research Institute for their support with the housing and maintenance of the mice used in this project. I thank Dr. Rebecca Pelekanos at the University of Queensland Centre for Clinical Research, for providing me with the first trimester human fetuses and mouse embryos to investigate the ghrelin axis in the cartilage microenvironment. I thank Associate Professor Mia Woodruff (Institute of Health and Biomedical Innovation, QUT), Ms. Crystal Chang (University of Queensland Diamantina Institute) and Ms. Helen O'Connor (QUT) for their support with the histology facilities and services for this project. I acknowledge the support of Dr. Roland Steck for his help with the micro-CT scanning and evaluations.

Finally I would like to thank my parents, brother, relatives and friends for their continuous, never changing, unconditional encouragement, love and support.

Statement of Original Authorship

"The work contained in this thesis has not been submitted previously to meet requirements for an award at this or any other higher education institution. To the best of my knowledge and belief, the thesis contains no material previously published or written by another person except where due reference is made."

QUT Verified Signature

Signature: .

Date: August 2014

Chapter 1

General Introduction

1.1 <u>Bone Structure and Function</u>

Bone diseases represent a major health and economic burden for society with increasing demand for effective therapies. Some of these diseases include osteoporosis, Paget's disease of bone, rickets, osteomalacia and osteogenesis imperfecta (*Bone Health and Osteoporosis: A Report of the Surgeon General*, 2004). Osteoporosis is a major metabolic bone disease and is estimated to affect 200 million women worldwide and 75 million people in Europe, USA and Japan (International Osteoporosis Foundation, 2013). The annual treatment cost for osteoporotic fractures in the workplace in the USA, Canada and Europe is almost US$48 billion (International Osteoporosis Foundation, 2013). The regulation of the bone microenvironment is under the influence of environmental, mechanical and endogenous chemical activity. Understanding the physiology of the regulation of the bone microenvironment by endogenous chemicals (hormones, growth factors and cytokines) may lead to progress in effective therapeutic and management strategies for metabolic bone diseases.

Bone is a complex, metabolically dynamic, specialised connective tissue which is composed of cells and extracellular matrix, like all connective tissues. The extracellular matrix of bone is made up of organic components (~ 30%), such as collagenous fibres, (90% of which is type I collagen), proteoglycans, glycosaminoglycans, glycoproteins, osteonectin (which anchors bone mineral to collagen) and osteocalcin (Clarke, 2008; Gentili & Cancedda, 2009). Almost 70% of bone is inorganic material which is mainly composed of the bone mineral composite, hydroxyapatite ($Ca_5[PO_4]_3[OH]$), which is the storage form of calcium and phosphate (Clarke, 2008). The main types of cells in bone tissue are osteoblasts, which produce the organic matrix (osteoid), osteoclasts, which break down bone tissue (bone resorption), and osteocytes which act as mechanosensory and endocrine cells (Crockett, Rogers, Coxon, Hocking, & Helfrich, 2011). Macroscopically, there are two types of bone tissue: the cortical bone, which constitutes approximately 80% of the skeleton and the trabecular bone (which comprises ~20% of skeleton). Cortical bone is dense and solid, consisting of compact collagenous fibres positioned in concentric sheets, or lamellae which run in perpendicular planes around osteons containing blood vessels and nerves in a central canal (Clarke, 2008). Trabecular bone is composed of a honeycomb-like network of bony plates or rods interspersed in the bone marrow compartment (Clarke, 2008).

Bone tissue functions to provide structural support, permit movement and locomotion by providing levers for muscles, to protect vital internal organs, provide maintenance of mineral homeostasis and acid-base balance, serve as a reservoir of growth factors and cytokines, and provide the environment for haematopoiesis within the marrow spaces (Chappard, Baslé, Legrand, & Audran, 2008; Taichman, 2005). Based on size, bones can be classified as long, short, flat or irregular bones. Short bones are cuboidal in shape and many examples are located in the foot (tarsals) and wrist (carpals) (Kulkarni, 2012). Long bones are tubular in shape with a hollow shaft and two ends and are located in the upper and lower limbs. The gross structure of long bones consists of two main regions: the epiphyses (often paired)and diaphysis (Figure 1.1-1). The diaphysis is the main shaft of the long bone, composed mainly of cortical bone, where it provides strength and high resistance to bending and torsion. The epiphyses are the upper and lower ends of long bones. The funnel-shaped regions of the diaphysis closest to the epiphyses at both ends is referred to as the metaphyses. The epiphyses and metaphyses are composed of a thin layer of cortical bone tissue, encapsulating a dense trabecular bone network.

The trabeculae follow lines of stress changes and realign in the direction of stress to attenuate the compressive forces and help the bone maintain its shape (Clarke, 2008; Feng & McDonald, 2011& Premkumar, 2011). In 1892, Wolff found that the orientation of trabeculae coincides with the direction of stress trajectories and proposed that bone loading is sensed in the bone microenvironment and that bone adapts its structure accordingly. This principle of functional adaptation is known as Wolff’s Law (Altenbach, 2013). It occurs in conditions of disuse, such as during immobility, space flight and long term bed rest, when bone is lost, and in overloading such as increased exercise regimes, which causes a gain in bone mass (Altenbach, 2013). It also occurs in growth, when the refined trabecular bone in childhood is changed to a coarser trabecular morphology in maturity (Altenbach, 2013), after fracture healing and in relation to orthopaedic implant incorporation (Altenbach, 2013).

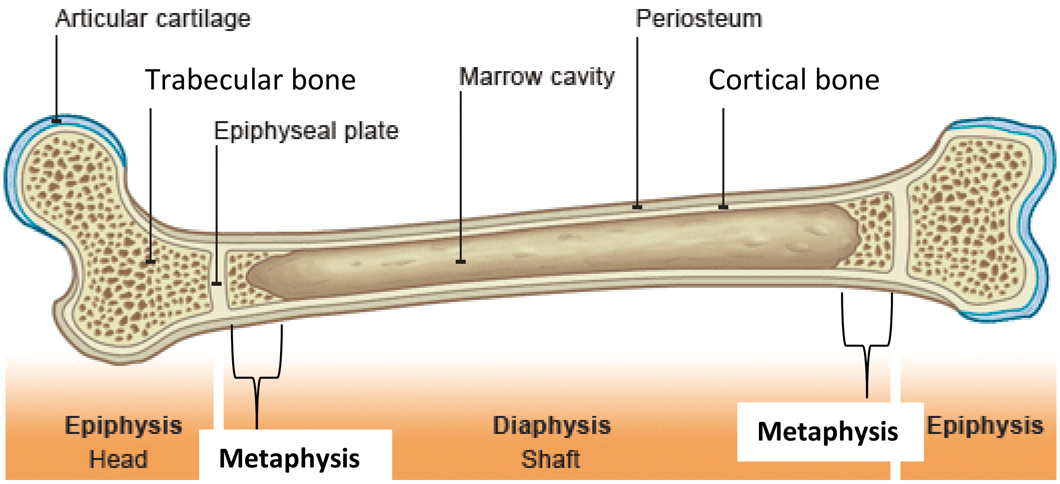

Figure 1.1-1: Typical structure of a long bone showing the epiphyses, metaphyses and diaphysis (Adapted from http://www.bbc.co.uk/schools/gcsebitesize/pe/appliedanatomy/2anato my_skeleton__rev4.shtml).

1.2 Bone modelling and remodelling

Bone continuously adapts to physiological influences (including hormones, growth factors and cytokines) and environmental influences (such as mechanical strains) (Feng & McDonald, 2011; Kini & Nandeesh, 2012). The ability of bone to adapt to mechanical load is brought about by continuous cycles of bone resorption and bone formation activity. If these processes occur at different locations, by the uncoupled independent actions of osteoclasts and osteoblasts, the bone morphology (structure, size and shape) is altered in order to maintain its mechanical integrity, and this process is known as bone modelling (Frost, 1990a). During growth bone modelling is the predominant process which affects the size and shape of bones, especially in long bones as they grow in length (Brandi, 2009). Modelling also occurs throughout life in response to changing mechanical loads, and particularly in the cortical bone of the mid-shaft of long bones (Burr & Allen, 2014; Brandi 2009). In the late 1980s, Frost proposed a conceptual model, which he called the *mechanostat theory* to mathematically explain bone adaptation to mechanical signals. He proposed that the strain magnitude is a mechanical stimulus for bone functional adaptation. Strain is the relative change in length of bone, or deformation of bone tissue that occurs with loading (Burr & Allen, 2014; Frost 1990). The mechanostat theory has been further modified to include more strain-related characteristics which stimulates bone functional adaptation such as strain rate, the frequency of loading cycles, the amount of rest between loading cycles and bouts of loading, and the distribution of strain within the bone structure (Skerry, 2006).

In addition to bone modelling, bone remodelling serves to maintain bone strength and mineral homeostasis by the coupled action of osteoclasts and osteoblasts. Remodelling occurs firstly through resorption of bone by osteoclasts, followed by formation of bone by osteoblasts in a tightly coupled manner, so that the net effect maintains bone strength and mineral homeostasis (Burr & Allen, 2014). The remodelling process consists of four major distinct phases; activation, resorption, reversal and formation (Figure 1.2-1). Remodelling sites may develop randomly, but many sites are targeted to areas that require repair (Clarke, 2008). Activation involves the recruitment and activation of mononuclear monocyte-macrophage osteoclast precursors from the circulation to the bone surface (Bruzzaniti & Baron, 2006). This leads to the differentiation, migration and fusion of the large multinucleated osteoclasts to the mineralised bone surface to initiate resorption (Clarke, 2008; Kini & Nandeesh, 2012; Parra-Torres, Valdés-Flores, Orozco, & Velázquez-Cruz, 2013). During the resorption phase, osteoclasts break down the matrix at the attached interface between the osteoclasts and bone, resulting in resorption pits (Crockett et al., 2011; Seeman, 2009). The release of growth factors contained within the matrix and by osteocytes results in the recruitment of mesenchymal stem cells and osteoprogenitor cells to the resorption pits (Figure 1.2-1) (Crockett et al., 2011; Feng & McDonald, 2011). The reversal and formation phases involve the proliferation and differentiation of osteoprogenitor cells into osteoblasts. Osteoblasts then deposit unmineralised bone matrix (osteoid) onto the surface of the cavities, and differentiate further into osteocytes which then reside in lacunae in the matrix. The osteoid becomes mineralised to complete the remodelling cycle (Figure 1.2-1) (Crockett et al., 2011; Feng & McDonald, 2011; Parra-Torres et al., 2013; Seeman, 2009).

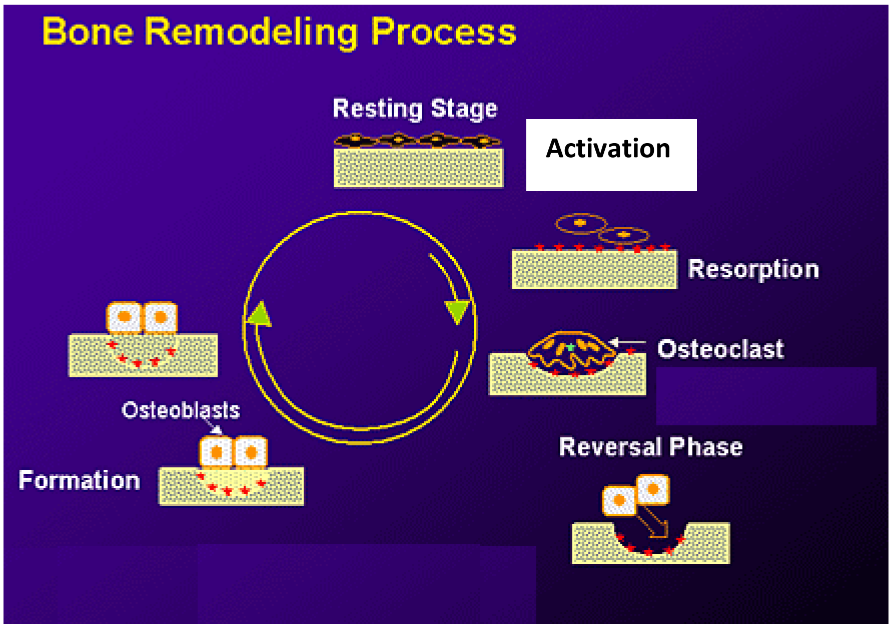

Figure 1.2-1: The bone remodelling process. The remodelling process consists of four major distinct phases: Phase 1: activation of bone remodelling at a specific site from the resting state, Phase 2: bone resorption by osteoclasts, Phase 3: reversal phase in which osteoclast activity halts and osteoblast activity begins, Phase 4: formation of bone by osteoblasts (Adapted from Sebba, 2013).

In normal bone remodelling, there is no net change in bone mass and strength after each remodelling cycle due to temporal and spatial alignment of osteoclast and osteoblast activity (Feng & McDonald, 2011). Any disturbance to this tightly regulated system causes an uncoupling of the activity of osteoclasts and osteoblasts and results in either significant bone loss or more rarely an increase in bone mass. With increasing age, the rate of the formation phase for bone renewal is unable to compensate for the increased activity of osteoclasts in the resorption phase. This results in decreased bone mass and an alteration of the micro-architecture, which results in decreased bone strength, increased bone fragility and increased risk of fracture (Parfitt, 1984; Seeman, 2013). These features are typical of age-related metabolic bone disease such as osteoporosis (Chen, Zhou, Fujita, Onozuka, & Kubo, 2013; Seeman, 2013).

Bone strength is determined by bone geometry, cortical thickness and porosity, trabecular bone morphology, and intrinsic material properties of bone tissue, such as mineralisation (Ammann & Rizzoli, 2003). Changes in microarchitecture with increasing age are reflected in trabecular bone through the decline in the bone volume fraction, trabecular number, connectivity density and trabecular thickness, and an increase in trabecular separation (defined in Table 1.2-1), although the degree of change is site-specific (Parkinson & Fazzalari, 2013). Furthermore, the cortical bone of the diaphysis of long bones undergoes significant age-related changes, including a decrease in cortical thickness (Chen et al., 2013; Parfitt, 1984) and increases in periosteal (outer) and endosteal (inner) circumferences (Clarke, 2008). This results in altered geometric properties, including changes in the area moment of inertia and polar moment of inertia. The area and polar moments of inertia are the distribution of bone tissue around the axis of bending and torsion, respectively, and they indicate the bone's resistance to bending/torsion and the ability to resist fracture under these conditions (Brandi, 2009).

Table 1.2-1: Definition of three dimensional trabecular bone microarchitectural indices as measured in computed tomography (adapted from Bouxsein et al., 2010).

Indices	**Definition**
Bone volume fraction	Ratio of the bone tissue volume to the total tissue volume of the region of interest
Trabecular number	Measure of the average number of trabeculae per unit length normalised by tissue volume
Trabecular thickness	Mean thickness of trabeculae
Trabecular separation	Mean distance between trabeculae
Connectivity density	Measure of the degree of connectivity of trabeculae

The metabolic activity of osteoblasts, osteoclasts and osteocytes is regulated by mechanical strain and a complex network of endogenous chemicals (hormones, growth factors, cytokines and neurotransmitters) for bone modelling and remodelling to maintain skeletal integrity. Examples of these endogenous chemicals include growth hormone (GH), insulin like growth factor-I (IGF-I), oestrogen, parathyroid hormone, 1,25-dihydroxy vitamin D, thyroid hormone, bone morphogenetic proteins (BMPs), prostaglandins and calcitonin (Oxlund, Ejersted, Andreassen, Torring, & Nilsson, 1993; Parra-Torres et al., 2013; Raisz, 1999). Emerging evidence suggests that the peptide hormone ghrelin may also be a key endogenous factor involved in regulating bone metabolism (P. J. D. Delhanty, van der Eerden, & van Leeuwen, 2013).

1.3 Osteogenesis and chondrogenesis

There are two distinct mechanisms of bone formation, or osteogenesis; intramembranous ossification and endochondral ossification (Olsen, Reginato, & Wang, 2000). Intramembranous ossification mainly occurs during the development of the flat bones of the skull, the mandible, maxillae and clavicles. It is also an essential process in appositional bone growth at the periosteum and the process of bone repair in the healing of bone fractures. It begins through the development of a fibrous membrane which is derived from the differentiation of mesenchymal stem cells into osteoprogenitor cells. The osteoprogenitor cells then differentiate further into osteoblasts and this leads to the formation of new bone tissue (Clarke, 2008).

Endochondral ossification mainly occurs during the development of the vertebral column, pelvis and bones of the upper and lower limbs and during postnatal longitudinal growth at the epiphyseal growth plates. It is also involved in the healing of fractures at sites of high mobility and/or poor vascularisation following trauma. During development, endochondral ossification involves the initial formation of a cartilage template (chondrogenesis) by the condensation and differentiation of mesenchymal stem cells into chondroblasts (Clarke, 2008; Mackie, Ahmed, Tatarczuch, Chen, & Mirams, 2008). The cartilage template consists of morphologically distinct chondrocytes which rest, proliferate, mature (hypertrophy) and undergo apoptosis. Chondrocytes undergoing hypertrophy secrete angiogenic factors such as vascular endothelial growth factors (VEGF), to induce vascular invasion of the cartilage-template to allow delivery of osteoprogenitor cells and the subsequent formation of ossification centres. This results in the gradual replacement of the cartilage template with newly formed bone (Mackie, Tatarczuch, & Mirams, 2011). Chondrogenesis and endochondral ossification are controlled exquisitely by cellular interactions, growth and differentiation factors, and other environmental factors that initiate or suppress cellular signalling pathways and the transcription of specific genes in a temporo-spatial manner (Tuan, 2004). Endogenous mediators, such as growth hormone, IGF-I, thyroid hormone, parathyroid hormone, bone morphogenetic proteins and fibroblast growth factors are involved in the regulation of chondrogenesis and endochondral ossification (Mackie et al., 2008; Stevens & Williams, 1999) and there is growing evidence that the ghrelin axis plays an important role in chondrogenesis and possibly endochondral ossification (Caminos et al., 2005; Gomez, Lago, Gomez-Reino, Dieguez, & Gualillo, 2009; Nakahara et al., 2006).

1.4 Growth hormone in bone remodelling and cartilage metabolism

Growth hormone is a 191 amino acid hormone which is secreted in a pulsatile pattern from the anterior pituitary in response to regulatory hormones such as growth hormone releasing hormone (GHRH), somatostatin and ghrelin. It functions by signalling through the growth hormone receptor (GHR) and it has a role as an anabolic regulator of energy metabolism and growth (DiGirolamo et al., 2007). GH plays an important role in bone remodelling, stimulating bone formation and bone resorption. GH regulates remodelling directly by binding to GHR on osteoblasts and osteoclasts, and indirectly by stimulating IGF-I release, which in turn regulates cellular activity in bone. GH stimulates osteoblast proliferation and activity, stimulating bone formation. GH also stimulates osteoclast differentiation to regulate bone resorption (Chihara & Sugimoto, 1997).

GH deficiency in children and adults affects skeletal mineralisation (Drake, Howell, Monson, & Shalet, 2001; Litwack, 2008; Root & Root, 2002). GH treatment initially increases bone resorption, leading to an increase in bone remodelling sites, with the subsequent stimulation of bone formation (Gotherstrom et al., 2001; Koranyi et al., 2001; Litwack, 2008; Ohlsson, Bengtsson, Isaksson, Andreassen, & Slootweg, 1998). This leads to a net increase in bone mass, but only when GH treatment is continued for a prolonged period (Gotherstrom et al., 2001; Koranyi et al., 2001; Litwack, 2008; Ohlsson et al., 1998). This is known as the biphasic model of growth hormone action on bone. The results of studies in non-GH deficient osteoporotic patients treated with GH are contradictory. GH has a positive effect on bone mass in postmenopausal women (Landin-Wilhelmsen, Nilsson, Bosaeus, & Bengtsson, 2003; Litwack, 2008) and in men with idiopathic osteoporosis, but in another study a decrease in bone mineral density (BMD) was reported (Gillberg, Mallmin, Petrén-Mallmin, Ljunghall, & Nilsson, 2002). The potential therapeutic benefits of GH are dependent on the dose, frequency and duration of the treatment (Litwack, 2008). Treatment with GH secretagogues, which stimulate GH release, could provide a more successful therapeutic approach (Litwack, 2008). Ghrelin, the endogenous GH secretagogue, has also been investigated for its therapeutic potential as a growth hormone releasing agent (Arvat et al., 2001).

Studies on growth hormone receptor (GHR) expression have been performed during chondrogenesis using human fetal tissues (Werther, Haynes, Edmonson, et al., 1993; Werther, Haynes, & Waters, 1993; Werther, Haynes, Barnard, & Waters, 1990). These studies showed that GHR is expressed by chondrocytes of the developing sternum and costal cartilages of human fetuses aged 15-20 weeks (Werther, Haynes, & Waters, 1993; Werther et al., 1990) and infants aged 3 days to 8 months (Werther, Haynes, & Waters, 1993). This indicates that growth hormone signalling may regulate the embryological development of the skeleton through endochondral ossification. It is possible that the GHR could be targeted for the treatment of endochondral skeletal abnormalities such as skeletal dysplasias. There have not, however, been any reports describing the expression of GHR receptors on other chondrogenic sites such as limbs or vertebrae. Studying the expression of GHR would determine whether the expression patterns are site- or cell type dependent.

1.5 The ghrelin axis

Ghrelin is a pleiotropic 28 amino acid peptide hormone (Kojima et al., 1999) which has roles in Gh release release (Kojima et al., 1999), appetite regulation (Wren et al., 2000) and energy balance (Kirchner, Heppner, & Tschop, 2012); and it has been demonstrated to play roles in bone metabolism and formation (Amini et al., 2013; Choi et al., 2013; P. J. Delhanty et al., 2006; P. J. D. Delhanty et al., 2013; Deng, Ling, Ma, Liu, & Zhang, 2008), and cartilage metabolism (Caminos et al., 2005; Gomez et al., 2009). Emerging evidence indicates that ghrelin signalling has a potential anabolic regulatory role in bone homeostasis through the dual regulation of osteoblasts and osteoclasts (Choi et al., 2013; Costa et al., 2011; Fukushima et al., 2005; van der Velde et al., 2012). Ghrelin signalling also improves bone tissue healing through intramembranous ossification (Deng et al., 2008) and has been shown to be involved in the regulation of chondrocyte metabolism (Caminos et al., 2005), suggesting that it could also have regulatory roles in endochondral ossification. Thus, an understanding of ghrelin physiology has the potential to offer new therapeutic strategies for metabolic diseases of bone and cartilage.

The ghrelin gene (*GHRL*) is located on the chromosomal locus 3p25.6-3p26.2 and encodes the 117 amino acid preproghrelin peptide (Kang, Zmuda, & Sleeman, 2011; Kojima et al., 1999; Kojima & Kangawa, 2005). Preproghrelin gives rise to a number of products through alternative splicing and post-transcriptional processing. The N-terminal, 23 amino acid signal peptide is cleaved to leave a 94 amino acid segment termed proghrelin (Fig 1.5-2). Proghrelin is cleaved further by prohormone convertases (PC) 1/3, furin and PC2 (Takahashi et al., 2009; Zhu, Cao, Voogd, & Steiner, 2006) to give rise to the 28 amino acid ghrelin and a 66 amino acid C-terminal peptide termed C-ghrelin (Fig 1.5-2). C-ghrelin gives rise to a 23 amino acid peptide hormone, obestatin (B. Liu, Garcia, & Korbonits, 2011; Zhang et al., 2005). Both C-ghrelin and obestatin are present in the circulation, with obestatin circulating at lower concentrations than ghrelin, while C-ghrelin circulates at higher concentrations (Bang, Soule, Yandle, Richards, & Pemberton, 2007; Mondal, Toshinai, Ueno, Koshinaka, & Nakazato, 2008; Pemberton, Wimalasena, Yandle, Soule, & Richards, 2003). Ghrelin circulates as a post-translationally modified form, acyl ghrelin, and an unacylated form, desacyl ghrelin (Hosoda, Kojima, Matsuo, & Kangawa, 2000). Desacyl ghrelin is present in the circulation in higher concentrations than acyl ghrelin and represents approximately 80% of total circulating ghrelin (Date et al., 2000; Hosoda et al., 2000). The addition of the octanoyl group to the serine-3 residue of proghrelin by the enzyme ghrelin *O*-acyl transferase (GOAT) produces acyl ghrelin (Gutierrez et al., 2008; Yang, Brown, Liang, Grishin, & Goldstein, 2008). GOAT is a member of the membrane-bound *O*-acyltransferase (*MBOAT*) superfamily and is encoded by the *MBOAT4* gene (Gutierrez et al., 2008; Yang et al., 2008). GOAT octanoylates serine-3 of proghrelin in the endoplasmic reticulum lumen and can use a range of fatty acid substrates, with the most likely acyl donors being acyl-CoAs (Al Massadi, Tschop, & Tong, 2011; Gahete et al., 2014; Nishi et al., 2005).

The action of acyl ghrelin, including the stimulation of growth hormone release, is mediated largely through the growth hormone secretagogue receptor 1a (GHSR1a) (Howard et al., 1996; Kojima et al., 1999), although an additional, alternative ghrelin receptor is widely hypothesised (Caminos et al., 2005; Muccioli et al., 2004; Thielemans et al., 2007; Volante et al., 2003). The GHS-R1a is a 366 amino acid G protein-coupled receptor (GPCR) with the characteristic seven transmembrane-spanning domains (Howard et al., 1996). The *GHSR* gene is located on chromosome 3q26.31 (Howard et al., 1996) and is transcribed into two GHSR mRNA isoforms, GHSR1a and GHSR1b (Chan & Cheng, 2004; McKee et al., 1997). GHSR1b is a 5 transmembrane, truncated protein and is widely considered to be non-functional, although there is evidence that it modifies GHSR1a trafficking and signalling (Chow et al., 2012; Leung et al., 2007). GHSR1a forms heterodimers with GHSR1b within the endoplasmic reticulum and this has a dominant-negative effect on ghrelin receptor function (Chow et al., 2012; Leung et al., 2007).

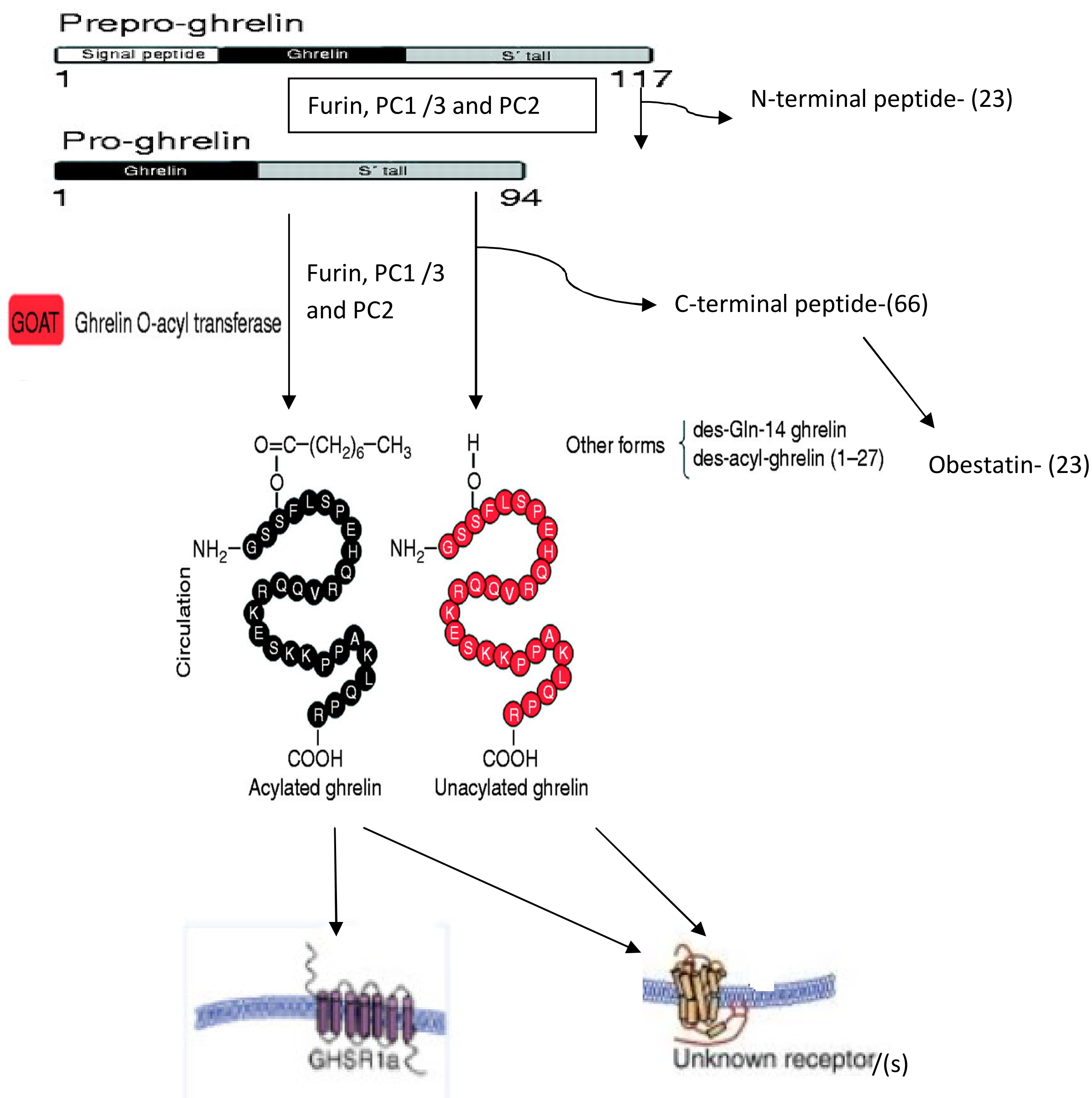

Figure 1.5-1: The ghrelin axis includes the two major circulating forms of ghrelin, desacyl and acyl ghrelin, GOAT and the GHSR1a. Acyl ghrelin is formed by the post-translational esterification of *n*-octanoyl group to the Ser-3 residue of the peptide by the enzyme GOAT. Acyl ghrelin signals through GHSR1a, however, both desacyl ghrelin and acyl ghrelin can signal through unknown receptors. (Adapted from Romero et al., 2010).

The GHSR1a exhibits unusually high constitutive activity, as it signals with ~50% of its maximal capacity in the absence of acyl ghrelin (Holst, Cygankiewicz, Jensen, Ankersen, & Schwartz, 2003). Ghrelin acts through the GHSR1a to have many regulatory effects on physiology and behaviour, such as the mediation of growth hormone release (Arvat et al., 2000; Kojima et al., 1999), regulation of appetite and secretion of gastric acid and gut motility, the regulation of cell proliferation, apoptosis, bone homeostasis, fat accumulation, the enhancement of memory and learning, neuroprotection, immune function, blood glucose control, potentiation of drug and food addiction, and cardiovascular and renal protection (Arvat et al., 2000; Chopin et al., 2011; P. J. D. Delhanty et al., 2013; Gahete et al., 2014; Jeffery, Herington, & Chopin, 2003; Kishimoto, Tokudome, Hosoda, Miyazato, & Kangawa, 2012; Kojima et al., 1999; Sato et al., 2011; Skibicka, Hansson, Egecioglu, & Dickson, 2012; Takeda et al., 2006; Tschop, Smiley, & Heiman, 2000).

Ghrelin also has functions in cells that do not express GHSR1a, and it stimulates proliferation and signalling in the human erythroleukaemic cell line (HEL) and HepG2 cell line, which lack GHSR1a expression (Muccioli et al., 2004; Thielemans et al., 2007). Non-GHSR1a ghrelin binding sites have been demonstrated in many tissues including cartilage (Caminos, et al., 2005), normal thyroid glands, thyroid tumours and thyroid cancer cell lines (Volante et al., 2003), indicating the presence of an alternative receptor or receptors for acyl ghrelin. Desacyl ghrelin does not bind with a high affinity to GHSR1a, but has many important physiological effects such as the regulation of proliferation, apoptosis, appetite, adipogenesis and cardioprotective effects (P. J. Delhanty et al., 2006; Granata et al., 2007; Seim, Josh, Cunningham, Herington, & Chopin, 2011). This property of desacyl ghrelin suggests that unidentified receptors are present through which both desacyl ghrelin and acyl ghrelin signal.

Ghrelin, GHSR1a and GOAT are expressed by a wide variety of tissues (Table 1.5-1). Ghrelin and GOAT are most abundantly expressed in the stomach (Date et al., 2000; Sakata et al., 2009) and GHSR1a is abundantly expressed by the somatotroph pituitary cells of the anterior pituitary gland (Litwack, 2007).

Table 1.5-1. Ghrelin, GOAT and GHSR1a mRNA and protein are expressed in human, mice and rat tissues, including bone and cartilage; ✓ -expression has been documented and U- expression uncertain (Chopin et al., 2011; Date et al., 2000; Kojima & Kangawa, 2005; Lim, Kola, Grossman, & Korbonits, 2011; Lim, Kola, & Korbonits, 2011; Sun, Garcia, & Smith, 2007)

Tissue	Ghrelin		GHSR1a		GOAT	
	mRNA	Protein	mRNA	Protein	mRNA	Protein
Bone	✓	✓	✓	✓	✓	U
Cartilage	✓	✓	U	U	✓	U
Small & large intestine	✓	✓	✓	✓	✓	U
Pituitary & hypothalamus	✓	✓	✓	✓	✓	U
Adrenal gland	✓	✓	✓	✓	✓	U
Thyroid	✓	✓	✓	✓	✓	U
Pancreas	✓	✓	✓	✓	✓	✓
Adipose tissue	✓	✓	✓	✓	✓	U
Stomach	✓	✓	✓	✓	✓	✓
Brain	✓	✓	✓	✓	✓	U
Heart	✓	✓	✓	✓	✓	U
Kidney	✓	✓	✓	✓	✓	U
Liver	✓	✓	✓	✓	✓	U
Lung	✓	✓	✓	✓	✓	U
Lymph node	✓	✓	✓	✓	✓	U
Prostate & Testes	✓	✓	✓	✓	✓	✓
Spleen & Thymus	✓	✓	✓	✓	✓	U

1.5.1 The ghrelin axis in bone

Ghrelin has been reported to have both direct and indirect effects on bone (Fukushima et al., 2005; van der Velde, Delhanty, van der Eerden, van der Lely, & van Leeuwen, 2008). Ghrelin stimulates pituitary GH release synergistically with growth hormone releasing hormone (GHRH) (Kojima *et al*., 1999) and the GH axis may mediate some of the effects of the ghrelin axis in bone. GH enhances bone metabolism directly, by acting through the growth hormone receptor (GHR) and indirectly, by stimulating the release of insulin like growth factor-I (IGF-I), predominantly from the liver and also at the epiphyseal growth plate in cartilage and bone (Cannata, Vijayakumar, Fierz, & LeRoith, 2010). GH and IGF-I are essential determinants of longitudinal bone growth, skeletal maturation and acquisition of bone mass and are important in maintaining bone mass and density by regulating bone modelling and remodelling (Cannata, Vijayakumar, Fierz, & LeRoith, 2010; Giustina, Mazziotti, & Canalis, 2008; Wit & Camacho-Hubner, 2011).

While the role of GH and IGF-I in bone is well established, there is also evidence that ghrelin has GH-independent effects on bone and cartilage. The intraperitoneal injection of ghrelin at a dose of 50µg/kg/day in GH deficient spontaneous dwarf rats for 4 weeks, for example, increased the bone mineral density of the cortical and trabecular bone of the femur (Fukushima et al., 2005), suggesting that ghrelin has a GH-independent role in bone metabolism.

1.5.2 Expression of the ghrelin axis in bone, bone-derived cell lines and cartilage

The ghrelin axis is expressed in bone and bone-derived cell lines, indicating that it may play a role in bone tissues. Human and rodent osteoblasts express ghrelin and GHSR1a (P. J. Delhanty et al., 2006; Fukushima et al., 2005; Kim et al., 2005; Liao L. & Wang, 2010; Maccarinelli et al., 2005). Ghrelin mRNA is expressed in human bone biopsies and in the SV-HFO human pre-osteoblastic cell line (P. J. Delhanty et al.,

2006) and the TE-85 and MG-63 human osteosarcoma cell lines (Pacheco-Pantoja, Ranganath, Gallagher, Wilson, & Fraser, 2011). Ghrelin and GHSR1a mRNA and protein have been detected in cultured human osteoblasts (Liao L. & Wang, 2010) and the MG-63 and Sa-OS2 human osteosarcoma cell lines (Kim et al., 2005). Ghrelin and GHSR1a mRNA and protein are expressed in primary osteoblast-like cells cultured from 21 day fetal rat calvaria (Fukushima et al., 2005; Maccarinelli et al., 2005), in the MC3T3-E1 primary mouse osteoblastic cell line, and the UMR-106 and ROS-17/2.8 rat osteosarcoma cell lines (Kim et al., 2005). Although expression has been described in osteoblasts in a number of studies, there have been few studies describing expression in osteoclasts. Ghrelin and GHSR1a mRNA transcript expression has been demonstrated in mouse osteoclasts, indicating a possible role in bone resorption (van der Velde et al., 2012).

The ghrelin axis is also expressed in chondrocytes and may play a role in chondrogenesis. The ghrelin peptide and mRNA are expressed in human and rodent chondrocytes (Caminos et al., 2005). Immunoreactive ghrelin is mainly expressed in the proliferative and maturative zones of the epiphyseal growth plate (Caminos et al., 2005). Although GHSR1a, transcripts were not identified in this study by RT-PCR, studies demonstrating positive ^{125}I ghrelin binding (Caminos et al., 2005) suggest that ghrelin may exert its effects in cartilage via alternative ghrelin receptors.

1.5.3 Functional effects of the ghrelin axis in bone – *in vitro* studies

Studies *in vitro* have shown that ghrelin administration increases bone formation by enhancing the differentiation, proliferation and activity of osteoblasts (Costa et al., 2011; P. J. Delhanty et al., 2006; Fukushima et al., 2005; Kim et al., 2005; Maccarinelli et al., 2005). Exogenous ghrelin administration stimulates a dose-dependent increase in proliferation in human SV-HFO pre-osteoblastic cells (P. J. Delhanty et al., 2006), human primary osteoblasts (Costa et al., 2011), primary osteoblasts cultured from 21 day rat calvariae (Fukushima et al., 2005; Maccarinelli et al., 2005) and in the MC3T3-

E1 primary mouse osteoblast cell line (Kim et al., 2005). Ghrelin treatment increases differentiation of osteoblasts by the expression of osteoblast differentiation markers such as Runx2 and collagen type α1 in primary rat calvarial cells *in vitro* (Fukushima et al., 2005). Administration of ghrelin also increases osteoblast activity, and increases alkaline phosphatase and osteocalcin production (markers of osteoblast differentiation and matrix production) in primary mouse osteoblast MC3T3-E1 cells (Kim et al., 2005) and primary rat calvaria *in vitro* (Fukushima et al., 2005; Maccarinelli et al., 2005), indicating that ghrelin may play a role in the differentiation and proliferation of osteoblasts.

In contrast to studies on the effect of ghrelin on osteoblasts, a few studies report the role of ghrelin in osteoclasts (which resorb bone). Rat osteoclasts isolated from the long bones of 1-2 day old rats and co-incubated with ghrelin *in vitro* on bovine bone slices induced an increase in bone resorption (Costa et al., 2011), suggesting a role of ghrelin in enhancing osteoclast activity. As ghrelin has been shown to regulate osteoblastic and osteoclastic cells, a dual regulatory role on bone formation and resorption is suggested (Costa et al., 2011). Also, osteoclastogenesis is increased in marrow derived osteoclast cultures of GHSR knockout mice at 3 month of age compared to the wildtype control mice (van der Velde et al., 2012).

1.5.4 Functional effects of ghrelin in bone homeostasis– clinical and *in vivo* studies

A number of studies have indicated that ghrelin has effects on bone mineral density (BMD) in human populations (Misra et al., 2005; Napoli et al., 2011; Nouh, Abd Elfattah, & Hassouna, 2012; Oh et al., 2005; Weiss, Langenberg, & Barrett-Connor, 2006). Ghrelin secretion predicts bone density independent of body composition, the GH-IGF-I axis, cortisol, or oestradiol status in healthy girls (Misra et al., 2005). A significant positive correlation was found between ghrelin and BMD at the vertebral column, hip and radius of perimenopausal and postmenopausal women compared to premenopausal women (Nouh et al., 2012). Serum ghrelin was positively correlated with trabecular BMD of the tibia in a cohort of elderly healthy Italian women and correlated in men, however the latter did not reach statistical significance (Napoli et al., 2011). A beneficial association between circulating ghrelin concentration and bone density was found in women in the Newfoundland (a Canadian) population (Amini et al., 2013), with higher serum ghrelin concentrations correlated with higher bone density measurements in the vertebral column, femoral neck and hip. This association was independent of confounding factors including body mass index, physical activity, age, alcohol consumption and smoking (Amini et al., 2013) indicating that ghrelin plays a role in regulating bone homeostasis *in vivo*. In contrast, ghrelin levels are elevated in girls with anorexia nervosa, and ghrelin secretion does not predict bone density in the lumbar spine and hip, independent of body composition, the GH-IGF-I axis, cortisol, or oestradiol (Misra et al., 2005). In girls with Rett's syndrome, serum ghrelin levels were significantly higher than in age matched healthy subjects, with no association between ghrelin levels and BMD (Caffarelli et al., 2012). This suggests that ghrelin levels are elevated in anorexia nervosa and Rett's syndrome in a compensatory manner and patients with these conditions are likely to be ghrelin resistant.

Serum ghrelin levels were not correlated with the BMD of the lumbar vertebrae and femoral neck of middle-aged males (Oh et al., 2005). Ghrelin also did not show an association with BMD or short-term change in BMD in older males and females (Weiss et al., 2006), however, ghrelin was inversely associated with the bone resorption marker N-terminal telopeptide of collagen (NTX) in males and positively associated with NTX in females, indicating that ghrelin plays a role in bone turnover (Weiss et al., 2006). This suggests that ghrelin may regulate bone metabolism differently in males compared to females.

There are difficulties associated with the accurate measurement of plasma ghrelin levels, however, and accurate measurement is critically dependent on the protocols used in the preparation of samples and the assays. There are no international standards for the measurement of ghrelin levels, and therefore, the results from different laboratories tend to vary widely depending on the protocols used (Chopin et al., 2012).

Studies from GHSR knockout mice suggest that ghrelin signalling may play an important role in maintaining bone mass and micro-architecture with progressing age (van der Velde et al., 2012). Densitometry analysis of bone mineral density (BMD) in ghrelin-null mice at 8 weeks of age (Sun, Ahmed, & Smith, 2003) and GHSR-null mice at 24 weeks of age (Sun, Wang, Zheng, & Smith, 2004) showed no change in bone mineral density compared to their wildtype littermates at the same ages. BMD is, however, a material property which partly contributes to bone strength, therefore, ghrelin signalling may affect the bone strength by affecting other material properties such as its organic or structural properties. Three dimensional (3D) micro-architectural analysis of the bone tissue through micro-CT would provide a more sensitive method for the analysis of the micro-structural effects on bone tissue in the knockout animals (D'Elia, Caracchini, Cavalli, & Innocenti, 2009). This method showed reduced trabecular bone volume fraction, trabecular number, cortical volume and polar moment of inertia on the femora of 6 month old GHSR knockout mice (van der Velde et al., 2012). There were no differences in these morphometric parameters at 3 months of age between the $GHSR^{-/-}$ and wild-type (WT) mice (van der Velde et al., 2012). This study indicates that ghrelin, signalling through GHSR1a, may play an important role in maintaining bone micro-architecture with progressing age through the regulation of the bone microenvironment (van der Velde et al., 2012). Furthermore, the osteoclast numbers on the bone surface of the 6 month old $GHSR^{-/-}$ mice were higher than the WT controls and no differences were observed in the 3 month old $GHSR^{-/-}$ mice compared to the WT controls, suggesting that a compensatory pathway is present at younger ages, which overrules the local stimulation of osteoclast activity (van der Velde et al., 2012). The bone formation marker, procollagen type 1 amino-terminal propeptide (P1NP), was unaltered in the $GHSR^{-/-}$ compared to WT (van der Velde et al., 2012). This indicates that the microarchitectural differences seen in $GHSR^{-/-}$ mice are mainly a result of altered osteoclast activity and not altered osteoblast activity, and therefore, the effects of acyl ghrelin signalling may result from regulation of osteoclast activity more than osteoblast activity.

Ghrelin (both acyl and desacyl forms) may also signal through hypothesised alternative receptors in bone in the absence of GHSR1a (Caminos et al., 2005; Muccioli et al., 2004; Thielemans et al., 2007; Volante et al., 2003). Ghrelin signalling, therefore, may also occur in GHSR$^{-/-}$ mice through alternative receptors.

As GHSR1a also possesses a high level of constitutive activity (Holst et al., 2003), the findings in the GHSR1a knockout mice (van der Velde et al., 2012) do not confirm that acyl ghrelin signalling through GHSR1a is solely responsible for the observed effects and further studies are required. Studies using GOAT$^{-/-}$ mice, which are unable to produce acyl ghrelin, would provide additional information on the relative contributions of acyl ghrelin, desacyl ghrelin and the GHSR1a and their role in maintaining bone micro-architecture with age.

1.6 The role of the ghrelin axis in osteogenesis and chondrogenesis

In addition to studies supporting the effect of ghrelin on regulating bone homeostasis (Amini et al., 2013; Choi et al., 2013), ghrelin appears to have a role in bone development (osteogenesis) and repair (Deng et al., 2008). In a ghrelin supplementation model in rats, increased bone formation was observed in calvarial bone defects in animals treated with ghrelin, suggesting that ghrelin enhances intramembranous ossification during bone healing (Deng et al., 2008). Ghrelin may also play a role in chondrogenesis (Caminos et al., 2005; Gomez et al., 2009). Ghrelin, stimulates cAMP production in cartilage cells (chondrocytes) *in vitro*, and induces a significant increase in the gene expression of chondroitin sulphate type IV (a proteoglycan synthesis gene) in human and murine chondrocytes (Caminos et al., 2005). An increase in cAMP is linked with increased chondrocyte apoptosis and it is hypothesised that ghrelin may play a regulatory role in chondrocyte metabolism, promoting hypertrophic processes by increasing proteoglycan synthesis and programmed cell death (Caminos et al., 2005).

GHSR1a mRNA and protein are expressed in rat fetal ribs (Nakahara et al., 2006), but expression has not been localized to particular cell types. GHSR1a may be expressed in osteoblasts and/ or osteoclasts of costal cartilage, which are present at the sternal ends of the ribs. It is unclear from the study by Nakahara et al. (2006) whether GHSR1a plays a role in chondrogenesis or osteogenesis and this remains to be clarified. It has been reported that ghrelin (peptide and mRNA) are expressed by a mouse immortalised chondrocyte cell line (ATDC-5), juvenile human immortalised chondrocyte cell lines (T/C-28a2, C-20/A4 and C-28/I2) and rat epiphyseal growth plate chondrocytes (in fetal and postnatal rats aged 1 day, 15 days and 25 days) (Caminos et al., 2005). GOAT is also expressed in cultured primary human chondrocytes (derived from human articular cartilage), human immortalised chondrocyte cell lines (T/C-28a2 and C-28/I2) and immortalised mouse chondrocytes (ATDC-5) (Gomez et al., 2009). Although these reports indicate that acylated ghrelin is synthesised and secreted by chondrocytes, the study (Caminos et al., 2005) failed to identify GHSR1a mRNA in chondrocytes of the rat epiphyseal growth plates (in fetal and postnatal rats aged 1 day, 15 days and 25 days) and human immortalised chondrocyte cell lines (T/C-28a2, C-20/A4 and C-28/I2) (Caminos, et al., 2005). Binding studies (using ^{125}-I ghrelin) in human immortalised chondrocytes (T/C-28a2) suggested the presence of alternative ghrelin binding receptors (Caminos et al., 2005). Ghrelin treatment also increased cAMP production and inhibited chondrocyte metabolic activity in human (T/C-28a2) and mouse (ATDC-5) immortalised chondrocytes (Caminos et al., 2005). These reports indicate that chondrocytes produce desacyl and acyl ghrelin which signal through alternative receptors and modulate chondrocyte metabolism in the cartilage template for endochondral ossification. The failure to detect GHSR1a in chondrocytes is challenged by data on Geo Profiles in NCBI showing that human osteoarthritic chondrocytes in monolayer and matrix cultures express GHSR (http://www.ncbi.nlm.nih.gov/geoprofiles/67009914). Therefore, it is necessary to further explore the expression of the ghrelin axis in chondrocytes.

Osteogenesis and chondrogenesis are essential processes involved in skeletal development (Olsen et al., 2000). Therefore, the ideal model for studying the expression of the components of the ghrelin axis on cells involved in osteogenesis and chondrogenesis are fetuses at different stages of development.

1.7 Significance, Hypothesis and Aims

Metabolic bone diseases are a significant health burden in society and understanding bone physiology could lead to improvements in therapeutic and management strategies. Endogenous chemicals regulate bone metabolism and the ghrelin axis could have an association with the regulation of the bone microenvironment. Characterisation of the bone microarchitecture by 3D micro-computed tomography (micro-CT) in GHSR1a knockout mice indicates that ghrelin, signalling through GHSR1a, may play an important role in maintaining bone microarchitecture with progressing age (van der Velde et al., 2012). However, the high level of constitutive activity of GHSR1a (Holst et al., 2003) and presence of alternative receptors through which acyl ghrelin and des acyl ghrelin could signal in the absence of GHSR1a (Caminos et al., 2005; Muccioli et al., 2004; Thielemans et al., 2007; Volante et al., 2003), provide doubt whether or not \ acyl ghrelin signalling through GHSR1a is solely responsible for the microarchitectural changes observed. Therefore, we proposed that the characterisation of the bone phenotype of GOAT knockout mice at different ages would contribute critical information regarding whether acyl ghrelin signalling through GHSR1a is responsible for regulating microarchitecture of bone with increased age. We hypothesise that acyl ghrelin signalling through GHSR1a plays a key role in maintaining the micro-architecture of both trabecular and cortical bone (Caminos et al., 2005; Muccioli et al., 2004; Thielemans et al., 2007; Volante et al., 2003).

There is evidence that the ghrelin axis plays a role in chondrogenesis and further investigation may lead to opportunities to target the axis for treating cartilage disorders such as articular cartilage injuries and developmental disorders of cartilage metabolism, such as chondrodysplasias. Ghrelin is expressed in human and mouse cell lines *in vitro* and on rat chondrocytes of the epiphyseal growth plate (Caminos et al., 2005). Chondrogenesis is a key process involved in the establishment of the framework for endochondral bones in the skeleton during fetal development. The expression of the ghrelin axis (with the exception of GOAT), has not been investigated in primary human chondrocytes (Clarke, 2008; Mackie et al., 2008), which may be a more clinically relevant model for investigating the therapeutic potential of the ghrelin axis for cartilage disorders. We hypothesise that the ghrelin axis is expressed in primary human chondrocytes and plays a regulatory role in chondrogenesis. GHR is expressed by chondrocytes of the primordial sternum and costal cartilages of human fetuses in the second trimester (Clarke, 2008; Mackie et al., 2008; Werther, Haynes, Edmonson, et al., 1993; Werther, Haynes, & Waters, 1993; Werther et al., 1990). Therefore, we hypothesise that both GHR and the ghrelin axis are expressed in first trimester chondrocytes in the endochondral bones of the human skeleton.

Due to ethical limitations and the scarcity of human fetal tissues, investigations of bone formation and the regulators of endochondral bone formation have been widely carried out *in vitro* and on animal models. This presents the challenge of translating the outcomes of *in vitro* and animal experiments to the physiological regulation of endochondral bone formation in humans. We hypothesise that the GH axis and the ghrelin axis together play a role during fetal skeletal development in humans and rodents (mouse).

The overall aims of this project to test the above hypotheses were:

Aim 1: Characterise the microarchitecture of trabecular and cortical bone of GOAT$^{-/-}$ mice with advancing age in comparison to wild type mice.

Aim 2: Compare the expression of ghrelin, GHSR1a and GHR in fetal skeletal chondrocytes of human endochondral bones from the first trimester and murine cartilage templates at E14.5, E16.5 and E18.5.

Chapter 2

General Materials and Methods

2.1 Ethics and source of materials

2.1.1 Source of animals and animal ethics

Aim1

C57BL/6 wildtype (WT) and ghrelin *O*-acyl transferase knockout ($GOAT^{-/-}$) mice were used to characterise the bone morphology of $GOAT^{-/-}$ mice. Animal use was approved by the Animal Ethics Committee of the University of Queensland and approval was ratified by the Queensland University of Technology University Animal Ethics Committee (UAEC approval number TRI/509/12/QUT). C57BL/6J WT female mice aged 6 months (n=7), 9 months (n=5) and 18 months (n=4) were obtained from the University of Queensland Biological Resources Centre or the Animal Resources Centre, Western Australia. $GOAT^{-/-}$ mice (on a C57BL/6J background) were generated at Taconic animal laboratories (US) and were provided under a material transfer agreement between Dr Jeffery and Eli Lilly (Indiana, USA and Professor Matthias Tschop). The mice were re-derived and bred at the Mater Medical Research Institute and Translational Research Institute (TRI). The genotypes of the mice were confirmed by PCR and ghrelin ELISA by Dr Jeffery. Female $GOAT^{-/-}$ mice aged 6 months (n=5), 9 months (n=5) and 18 months (n=7) were available for this project.

On a normal diet, $GOAT^{-/-}$ mice gain weight normally, however, they gain less weight than WT mice on a high fat diet. The phenotype of this strain has been published previously by our collaborators (Kirchner et al., 2009). Although previously unreported, GOAT-/- mice are susceptible to stress and displayed greatly reduced fecundity after transfer to TRI, hence sample numbers and timepoints had to be reduced.

Aim 2

C57BL/6J mouse embryos aged 14.5 days (n=3), 16.5 days (n=3) and 18.5 days (n=3) post conception were provided by Dr. Rebecca Pelekanos (University of Queensland Centre for Clinical Research, Royal Brisbane Hospital). Ethics was approved by the Animal Ethics Committee of the University of Queensland (Ethics approval: University of Queensland Centre for Clinical Research project number 2009000508-NHMRC).

2.1.2: Human ethics

Products of human conception (6-12 week old embryos/fetuses, n=9) following termination of pregnancy by vacuum aspiration were provided by Dr. Rebecca Pelekanos (University of Queensland Centre for Clinical Research, Royal Brisbane Hospital). Ethics was approved by The Human Research Ethics Committee of the Royal Brisbane and Women's Hospital (Ethics approval: University of Queensland Centre for Clinical Research project number 2009000508-NHMRC).

2.2.1 Characterisation of bone microarchitecture of GOAT$^{-/-}$ mice

To determine a role of acyl ghrelin signalling in the regulation of the bone micro-environment with age, the microarchitecture of femoral and tibial trabecular and cortical bone tissues were compared between GOAT$^{-/-}$ and WT mice at different ages using micro-computed tomography (micro-CT). For this project, female GOAT$^{-/-}$ and WT mice of three age categories (6, 9 and 18 months; n=4-7 mice per group) were used to analyse the bone tissue phenotypes at different stages of the adult mouse lifecycle. The desired sample size of for each group at each age was 7 which was determined by using the power calculation [(21.0*SD2)/(mean1-mean2)^2], with a substantive difference of 20% based on data for callus size from Ekholm, et al., 2002 and for chondrocyte proliferation from (Z. Liu, Lavine, Hung, & Ornitz, 2007). The numbers, however, were not even due to the challenge of maintaining the GOAT$^{-/-}$ mice as a result of increased susceptibility to stress and greatly reduced fecundity. The normality tests used for analysis, the Kolmogorov-Smirnov test requires 5 or more values. The Shapiro-Wilk test requires 7 or more values and the D'Agostino test requires 8 or more values. The Kolmogorov-Smirnov test was used for parameters of mice with sample numbers of more than 5, and this resulted in a $p>0.05$, showing that the data are not inconsistent with a Gaussian distribution. Normal distribution was assumed for sample numbers less than 4 as previous studies such as van der Velde et al, 2012 showed that the distribution of parameters in the ghsr1a mice follow normal distribution. With smaller data sets the normality tests do not have much power to detect modest deviations from the Guassian ideal (Harvey, 2013).

2.2.2: Housing, Injections, Euthanasia and Tissue Sampling

Animal experimentation was carried out at the vivarium at Pharmacy Australia Centre for Excellence (PACE) and the Mater Medical Research Institute (MMRI) following a week's acclimatisation after the introduction to the animal facilities. All animals were housed in a maximum of 4 per cage, had unlimited access to chow diet and water, and a daily diurnal light cycle of 12 hours. Female GOAT$^{-/-}$ mice and WT mice aged 6 months (n=5), 9 months (n=5) and 18 months (n=7) were sacrificed by carbon dioxide asphyxiation. This involved placing each mouse in an empty enclosed chamber and introducing carbon dioxide gas. Euthanasia was confirmed by observing the cessation of a number of vital signs, including the lack of respiration. The mice were radiographed on a Kodak, *in vivo* X-ray machine to visualise any skeletal abnormalities.

The lower limbs of each mouse were extracted by removing the fur and skin from the hip joints to the feet, removing muscles and cutting around the hip joint. The tibiae and femora were separated and the length of each bone was measured with a ruler. To allow fixative to enter the medullary cavity, the femoral head and distal tibial epiphysis were removed with scissors. The tissues were fixed in freshly prepared 4% paraformaldehyde (PFA) in 0.1M PBS for 18-24 hours at 4◦ C. Following fixation, the right femora and tibiae were transferred to 70% ethanol for micro-CT scanning and processing for dynamic histomorphometry and the left femora and tibiae were transferred to 14% EDTA in distilled water (pH=7.2) for decalcification for 3 week with changes to fresh EDTA every 3 days.

2.2.3: Micro-computed tomography scanning and evaluation

The right femora and tibiae were scanned and analysed using the Scanco µCT 40 desktop microCT scanner (Scanco Medical, Brüttisellen, Switzerland). The samples were wrapped in bench cloth moistened with 70% ethanol, to prevent the sample from moving and drying out during the scan. Samples were contained within a sample tube with an internal diameter of 10mm containing 70% ethanol. The samples were scanned with an X-ray power of 55kV and tube current of 144µA to achieve a scanning resolution of 12µm. The femora were scanned from the distal end of the femoral neck to the distal articular surface of the femur (as shown in Figure 2.2.3-1) and the tibiae were scanned from the proximal articular surface of the tibia to the distal part of the tibia where the fibula attaches (as shown in Figure 2.2.3-1). Following scanning, the trabecular and cortical bone tissues were evaluated for the following parameters from reconstructed cross-sectional images, in order to distinguish between the microarchitectural and material properties between the trabecular and cortical compartments of GOAT$^{-/-}$ and WT mice.

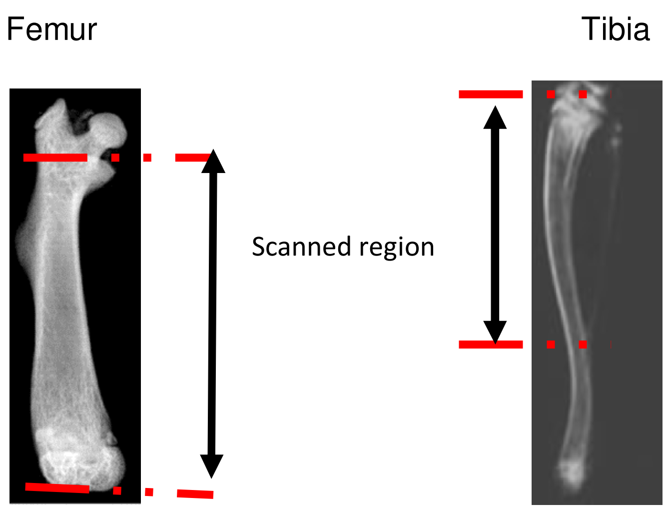

Figure 2.2.3-1. Scanned regions of femora and tibiae for microCT analysis. Each radiograph is an anteroposterior view.

Trabecular bone measurements: The regions of interest for trabecular bone measurements were the secondary spongiosa of the distal femoral metaphysis and proximal tibial metaphysis. These regions were defined by firstly excluding the 40 scan slices (each slice = 12µm) immediately adjacent to the epiphyseal growth plate within the diaphysis of each bone. This region corresponds to the primary spongiosa where new bone is generated from the active epiphyseal growth plate (which is the site of longitudinal bone growth). Second, the subsequent 150 (1.8mm) serial slices of the metaphysis were selected for evaluation. The area of interest of each slice was selected by drawing contour lines around the trabecular bone tissue along the inner margin of the cortical bone to exclude the cortex (as shown in Figure 2.2.3-2). Material bone mineral density (BMD), bone volume fraction (BV/TV), trabecular number (Tb.N), trabecular thickness (Tb.Th), trabecular separation (Tb.Sp) and connectivity density (Conn. Den) were determined using the direct model of the in-built evaluation script for trabecular measurements of the Scanco µCT 40 desktop microCT scanner.

Cortical bone measurements: The region of interest for cortical measurements was the mid-diaphyses of the femur and tibia. The start of this region was selected by dividing the total number of slices of the specimen by 2 and substracting 10 slices towards the distal femoral growth plate for the femur or the proximal tibial growth plate for the tibia. From this point 20 slices towards the proximal femoral growth plate for the femora and 20 slices for the distal tibial growth plate for tibiae were evaluated for material bone mineral density (BMD) and polar moment of inertia (pMOI) using the evaluation script for cortical measurements.

One mid-slice of each region of interest was exported to the Osteomeasure software (Osteometrics, Atlanta, Georgia, USA) in TIFF format converted to RGB using GIMP2 software. Contour lines were drawn around the cortical perimeter and marrow perimeter of each slice (as shown in Figure 2.2.3-2) to obtain values for cortical bone area, mean cortical width, endosteal circumference and periosteal circumference.

2.2.4 Statistical Data analysis

All data was analysed using GraphPad Prism 6, statistics analysis software program (San Diego, CA). The Kolmogorov-Smirnov test was used for parameters of mice with sample numbers of more than 5, and this resulted in a $p>0.05$, showing that the data are not inconsistent with a Gaussian distribution. Guassian distribution was assumed for sample sizes less than 5 as previous studies such as van der Velde et al., 2012 have shown that these parameters show a normal distribution. Comparison of the results between GOAT$^{-/-}$ and WT was performed using independent Student's t-test and comparison between the ages for each group was performed using the one-way ANOVA with Tukey's *post hoc* analysis. Probability values of $p<0.05$ were considered statistically significant and $0.1>p>0.05$ was considered marginally significant (Gregory, et al., 2006). Results were expressed as the mean value± standard error of mean (S.E.M).

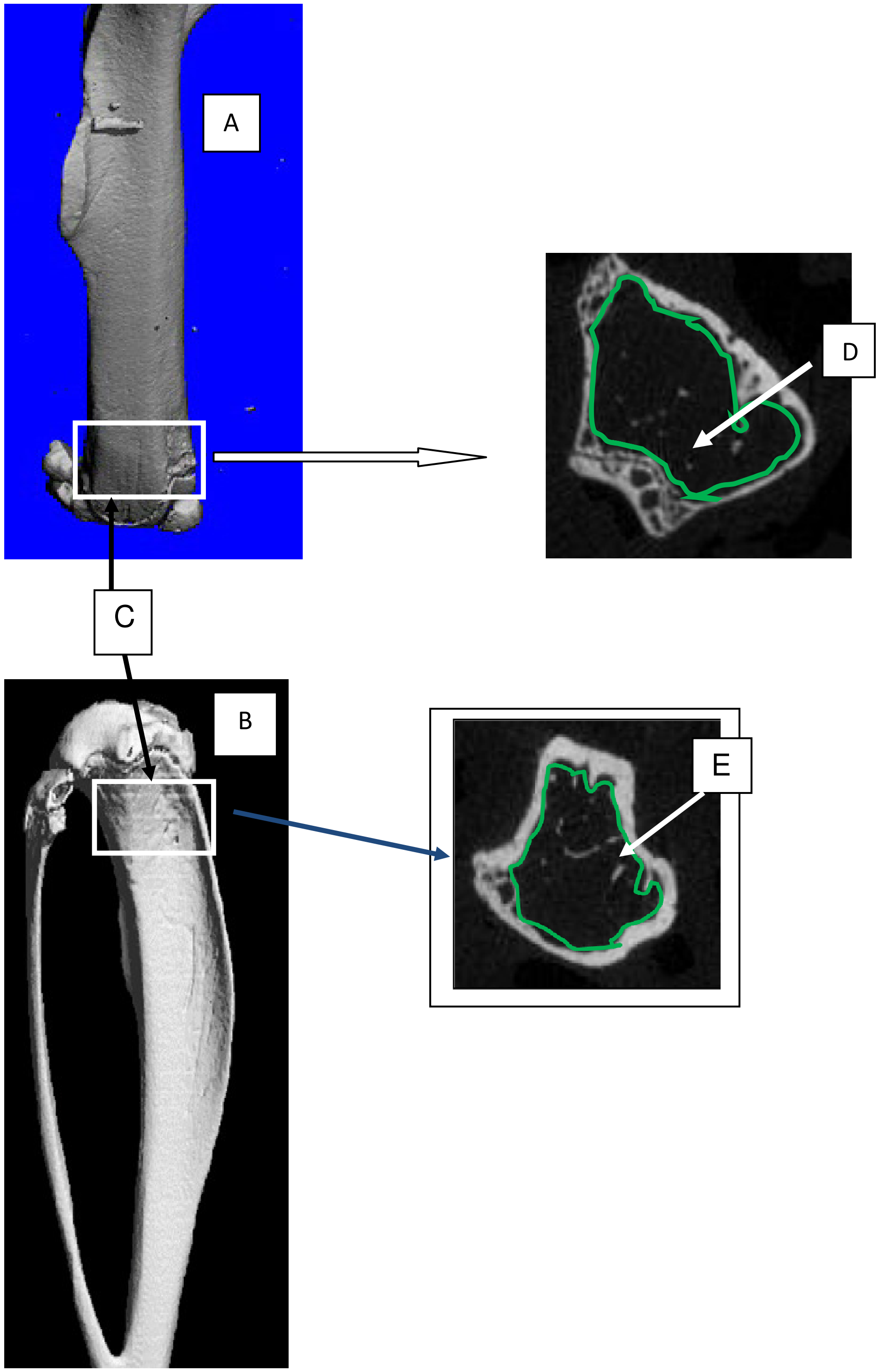

Figure 2.2.3-2. Three dimensional images of the femur (A) and tibia (B) showing the selected region of interest for trabecular measurements (C) and 2D cross sectional slice from the ROI in the femur (D) and tibia (E) showing the green contour lines drawn to define the area of interest in the cross sections.

2.3 Immunohistochemistry and Tartrate Resistant Acid Phosphatase staining

2.3.1: Optimisation of primary antibodies for immunostaining mouse bone tissue sections

Decalcified left femora and tibiae were processed, paraffin embedded and 3µm sections mounted on Superfrost slides. Sections of 8 day old, 8 week old and 6 month old wild type (WT) mice were immunostained to optimise primary antibody dilutions for the expression of ghrelin, GHSR1a, GOAT, osteocalcin, and runx2. The sections were deparaffinised in Solv21C (Muraban Laboratories, Brisbane), followed by rehydration in a series of graded ethanol (3 times in 100%, 90% and 70% ethanol) then phosphate buffered saline (PBS). Antigen retrieval was performed by microwave heating the sections in 10mM sodium citrate buffer pH 6.0 containing 0.05% (v/v) Tween-20 for 20 minutes. After cooling, endogenous peroxidase activity was blocked with 3% H_2O_2 for 10 minutes at room temperature. The sections were washed in PBS and non-specific antibody binding was blocked by incubating the sections in 1% BSA in PBS+0.1% Tween for 1 hour at room temperature. The sections were then incubated with the primary antibodies diluted in blocking buffer at 4℃ overnight, with antibody dilutions of 1:100, 1:250, 1:500 and 1:1000 for rabbit polyclonal anti-mouse ghrelin (Phoenix Pharmaceuticals Inc., H-031-31), goat polyclonal anti-human GHSR1a diluted 1:100 (Santa Cruz Biotechnology, F-16), goat anti-human GOAT antibody (Abcam, ab-170690), goat anti-human MBOAT4 antibody (Santa Cruz Biotechnology, sc-98001), anti-human runx2 antibody (Abcam, ab23981) and anti-human osteocalcin (Santa Cruz Biotechnology, sczsc-30044). Antibody dilutions of 1:100, 1:250, 1:500, 1:1000 were used. Negative control tissue used were GOAT$^{-/-}$ mouse stomach tissues for GOAT antibodies and for all antibodies the primary antibody was replaced with normal goat IgG diluted 1:100 (Santa Cruz Biotechnology, sc-2755), or rabbit IgG 1:100 (Santa Cruz Biotechnology, sc-2763) for GHSR1a, ghrelin, osteocalcin and runx2 antibodies. Sections were washed in PBS+0.1% Tween (PBST) and incubated with horse radish peroxidase (HRP) rabbit or goat polymer conjugates (Biocare Medical) for 30 minutes. Sections were washed with PBST and stained with the chromogen diaminobenzidine (DAB, Invitrogen). All immunostained sections were lightly counterstained with Mayers haematoxylin, air dried overnight and coverslipped using DPX mounting medium (Sigma Aldrich). Sections were visualised under a standard light microscope for the staining patterns.

2.4.2: Tartrate resistant acid phosphatase (TRAP) staining and osteoclast quantification

One section of the left tibia and femur of each WT and GOAT$^{-/-}$ mouse aged 6 month old, 9 month old and 18 month old were TRAP stained to determine osteoclast number on the trabecular bone surface in the secondary spongiosa of the distal femoral metaphysis and proximal tibial metaphysis. This was done to determine whether osteoclast activity is altered in the absence of acyl ghrelin signalling. GHSR$^{-/-}$ mice have been reported to have increased osteoclast numbers on the trabecular bone surface at 6 months of age (van der Velde et al., 2012). Naphthol-ASTR phosphate (Sigma, N-6125) was made to a concentration of 10mg/ml in N, N-dimethyl formamide and 4ml was mixed in 60 ml of 0.05M Tris-HCl (staining buffer, pH 9.0). Pararosaniline-HCl (Sigma, P-3750) at concentration of 40mg/ml and sodium nitrite at a concentration of 40mg/ml in distilled water was mixed in equal volumes (total volume= 10% of staining mixture) and added to the staining mixture. The mixture was stirred and 10% sodium tartrate (Sigma, S-8640) was added to the mixture and the pH was adjusted to 5.0 with 10M sodium hydroxide. The mixture was filtered into a coplin jar through a No. 1 Whatman filter paper. The sections were de-waxed in xylene (3 washes at 5 minutes each), rehydrated in a graded series of alcohols (3 X 100% ethanol, 2 X 90% ethanol, 1 X 70% ethanol, 1 X 50% ethanol for 5 minutes each) to running distilled water for 5 minutes. The sections were incubated in the TRAP mixture at 37℃ in an oven for 20-30minutes for colour development. Colour development (presence of red stained osteoclasts) was checked at 20, 25 and 30 minutes under a light microscope. Once colour development was confirmed, the sections were washed in running tap water for 10 minutes, lightly counterstained with Mayer’s haematoxylin for 5 minutes and washed in running tap water for 10 minutes. The sections were dried overnight and coverslipped with an aqueous mounting medium (CC/Mount^{TM}, Sigma, C9368).

Osteoclast numbers on the trabecular bone surface of the secondary spongiosa of the distal femoral metaphysis and proximal tibial metaphysis of the stained sections were determined by obtaining images of each section at a magnification of 200x using a light microscope (Zeiss), connected to a computer installed with the Osteomeasure program (Osteometrics, Atlanta, Georgia, USA). The secondary spongiosa of each section was chosen by excluding 350µm from the lowest end of the growth plate and selecting the subsequent 1.5mm of the adjacent region of the metaphysis. The trabecular bone perimeter of the secondary spongiosa of the image on the Osteomeasure program was defined by drawing around the surface using a digitised pen and selecting the osteoclasts on the surface to define osteoclast numbers on the trabecular bone surface.

2.5 Expression of the growth hormone secretagogue receptor 1a (GHSR1a) and the growth hormone receptor (GHR) in human and mouse fetal chondrocytes

Vertebral columns, upper limbs and lower limbs were harvested from human fetuses (n=8) with a gestational age of 6-12 weeks. The human tissues, together with mouse embryos at post-conception age 14.5 (n=3), 16.5 (n=3) and 18.5 (n=3) were fixed in 4% PFA for 24 hours at 4˚C. The tissues were processed and embedded in paraffin by the histology services at Queensland Institute of Medical Research (QIMR) or University of Queensland Diamantina Institute (UQDI).

2.5.1 Immunohistochemistry for protein expression on human fetal chondrocytes

The paraffin-embedded tissue blocks were sectioned at 5µm thickness on a rotary microtome (Leica RM2235) onto Superfrost slides (HDScientific, HD41800) and deparaffinised in Solv21C (Muraban Laboratories, Brisbane), followed by rehydration in a series of graded ethanol (3 times in each solution of 100%, 90% and 70% ethanol) to phosphate buffered saline (PBS). Antigen retrieval was performed by microwave heating the sections in 10mM sodium citrate buffer pH 6.0 containing 0.05% (v/v) Tween-20 for 20 minutes. After cooling, endogenous peroxidase activity was blocked with 3% H_2O_2 for 10 minutes at room temperature. The sections were washed in PBS and non-specific antibody binding was blocked by incubating the sections in 1% BSA in PBS+0.1% Tween for 1 hour at room temperature. The sections were then incubated with the primary antibodies diluted in blocking buffer with optimised antibody concentrations of 1:100, 1:250, 1:500 and 1:1000 diluted in the blocking buffer (1% BSA in PBS+0.1% Tween). The final antibody dilutions as shown in Table 2.3-1 were rabbit polyclonal anti-ghrelin diluted 1:500 (Phoenix Pharmaceuticals Inc., H-031-31; cross reactive with human, mouse and rat ghrelin), rabbit polyclonal growth hormone receptor antibody diluted 1:100 (Santa Cruz Biotechnology, H-300; cross-reactive with human, mouse and rat GHR) and goat polyclonal anti-GHSR1a diluted 1:100 (Santa Cruz Biotechnology, F-16; cross reactive with human, mouse and rat GHSR1a) at 4˚C overnight. For negative controls the primary antibody was replaced with normal goat IgG diluted 1:100 (Santa Cruz Biotechnology, sc-2755), or rabbit IgG 1:100 (Santa Cruz Biotechnology, sc-2763). Sections were washed in PBS+0.1% Tween (PBST) and incubated with horse radish peroxidase (HRP) rabbit or goat polymer conjugates (Biocare Medical) for 30 minutes. Sections were washed with PBST and stained with the chromogen diaminobenzidine (DAB, Invitrogen). All immunostained sections were lightly counterstained with haematoxylin, air dried overnight and coverslipped using DPX mounting medium (Sigma Aldrich). Mouse brain tissues were immunostained for use as positive controls for anti-GHSR1a and mouse liver tissues were immunostained for positive control as growth hormone receptor antibody. The GHSR1a antibody has been previously validated on GHSR knockout mice (Shin et al., 2010) and in mammalian cells by our group (Fung et al., 2013). Mouse stomach, which is known to express high levels of ghrelin and GOAT, was used as positive control for anti-ghrelin antibody and anti-GOAT antibodies.

Table 2.5-1: Primary antibodies and dilutions used in immunohistochemistry for human tissues and mouse embryos

Antibody and species specificity	Host species	Optimised dilution	Supplier & catalogue number
Anti-mouse ghrelin	Rabbit	1:500	Phoenix Pharmaceuticals Inc (H031-31)
Growth hormone receptor (human) antibody	Rabbit	1:100	Santa Cruz Biotechnology (H300)
anti-human growth hormone secretagogue receptor 1a	Goat	1:100	Santa Cruz Biotechnology (F16)
IgG	Rabbit	1:100	Santa Cruz Biotechnology (sc2763)
IgG	Goat	1:100	Santa Cruz Biotechnology (sc2755)

2.3.2 Safranin O/Fast green staining

To determine the morphology of chondrocytes in order to identify the cells that were immunostained, safranin O/fast green staining was performed on the fetal sections. The sections were deparaffinised in xylene and rehydrated in a graded series of ethanol (100% X3, 90%, 70%) to distilled water. The sections were stained with freshly made Weigert's haematoxylin (1.5% aqueous ferric chloride 1ml HCL mixed in equal amounts with 1% haematoxylin) for 10 minutes, washed in distilled water and differentiated in 0.5% acid alcohol. The sections were washed in distilled water, blued in 0.1% ammonia and stained with 0.2% fast green solution (Sigma Aldrich) for 5 minutes. The sections were then rinsed in 1% acetic acid, stained with 0.1% Safranin O for 1 minute and dehydrated in a graded series of ethanol (70%, 90% and 3 X 100%) to xylene. The stained sections were mounted using DPX mounting medium (Sigma Aldrich) and visualised by light microscopy.

Chapter 3

The microarchitecture of bone in GOAT knockout mice

3.1 Introduction

The ghrelin axis has many roles in physiological processes including the regulation of growth hormone secretion (Kojima et al., 1999), appetite (Wren et al., 2000) and energy balance (Kirchner et al., 2012). Accumulating evidence from recent reports indicates that ghrelin may have a positive regulatory role in bone metabolism (Amini et al., 2013; Costa et al., 2011; Fukushima et al., 2005; Kim et al., 2005; van der Velde et al., 2012). Several studies on human populations (particularly in females) have shown a positive correlation between circulating ghrelin levels and bone mineral density (BMD), independent of confounding factors such as body mass index (BMI), physical activity, age, alcohol consumption and smoking (Amini et al., 2013; Misra et al., 2005; Napoli et al., 2011; Nouh et al., 2012; Oh et al., 2005; Weiss et al., 2006).

Ghrelin and GHSR1a are expressed by osteoblasts (P. J. Delhanty et al., 2006; Fukushima et al., 2005; Kim et al., 2005; Liao L. & Wang, 2010; Maccarinelli et al., 2005) and ghrelin has positive effects on the proliferation of rat, mouse and human osteoblasts (Costa et al., 2011; P. J. Delhanty et al., 2006; Fukushima et al., 2005; Kim et al., 2005; Liao L. & Wang, 2010; Maccarinelli et al., 2005) and differentiation of mouse and rat osteoblasts (Fukushima et al., 2005). In contrast to osteoblasts, only a few studies have reported that ghrelin has a role in osteoclast function. Ghrelin and GHSR1a are expressed by mouse osteoclasts (van der Velde et al., 2012) and ghrelin has been reported to increase rat osteoclast resorption (Costa et al., 2011). These studies suggest that ghrelin may directly regulate the function of both osteoblasts and osteoclasts.

In vivo, ghrelin administration has been shown to have an anabolic effect on bone in Sprague Dawley rats aged 6 weeks as it increases BMD (Fukushima et al., 2005). The anabolic effects of ghrelin administration is contradicted by reports that BMD is not affected in 8 week old ghrelin deficient (Sun et al., 2003) and 24 week old GHSR deficient (Sun et al., 2004) mice compared to age matched, WT controls. This suggests that ghrelin may contribute to the short-term improvement in bone strength by affecting the material properties of bone.

In vivo, ageing has been shown to have a significant impact on the activity of ghrelin as indicated by the microarchitecture of GHSR-deficient ($GHSR^{-/-}$) mice (van der Velde et al., 2012). Three dimensional (3D) micro-CT analyses of the trabecular and cortical bone microarchitecture of the left femora of $GHSR^{-/-}$ mice aged 3 and 6 months have shown that the 6 month old $GHSR^{-/-}$ mice have reduced trabecular bone volume fraction, trabecular number, cortical volume and polar moment of inertia compared to age matched WT controls (van der Velde et al., 2012). The microarchitecture of $GHSR^{-/-}$ mice aged 3 months was not significantly different to the WT controls (van der Velde et al., 2012). Furthermore, this study showed that the $GHSR^{-/-}$ mice showed a higher number of osteoclasts compared to WT controls in both 3 and 6 month old animals. Since the micro-architectural differences were observed at only 6 months, this may indicate that a systemic or central process overrides the local stimulation of osteoclast activity at younger ages (van der Velde et al., 2012). Ghrelin may also signal through alternative receptors (Caminos et al., 2005; Thielemans et al., 2007; Volante et al., 2003) in bone in the absence of GHSR1a. The possibility that ghrelin signalling may have continued through compensatory pathways in these GHSR knockout mice cannot be excluded. As GHSR1a also possesses a high level of constitutive activity (Holst et al., 2003), the findings in the $GHSR^{-/-}$ mice do not confirm that acyl ghrelin signalling through GHSR1a is solely responsible for the observed effects and further studies are required. We hypothesise that employing $GOAT^{-/-}$ mice, which are unable to produce acyl ghrelin may provide additional information on the relative contributions of acyl ghrelin, desacyl ghrelin and the GHSR1a and their role in maintaining bone micro-architecture with age. This study aimed to characterise the trabecular and cortical bone microarchitecture of female $GOAT^{-/-}$ mice at different adult ages through µCT.

3.2 Methods

This study was carried out as detailed in Chapter 2 section 2.2.2 and 2.2.3. In brief, female C57/BL6 $GOAT^{-/-}$ and C57/BL6 WT mice aged 6, 9 and 18 months were euthanised and weighed. The right femora and tibiae were harvested, fixed and scanned in ethanol using a Scanco µCT 40 desktop microCT scanner (Scanco Medical, Brüttisellen, Switzerland). Trabecular micro-architectural measurements were carried out on the secondary spongiosa of the distal femoral metaphysis and proximal tibial metaphysis of reconstructed cross-sectional images using the in-built Scanco µCT 40 script for trabecular measurements. Cortical bone measurements were carried out on the mid-diaphyses of the femora and tibiae of reconstructed cross-sectional images and the cortical material BMD and polar moment of inertia were evaluated using the in-built Scanco µCT 40 script for cortical measurements. Osteomeasure software was used to measure other cortical parameters such as cortical bone area, mean cortical width, periosteal perimeter and endosteal perimeter from mid-diaphyseal cross-sections.

3.3 Results

3.3.1 Phenotype of $GOAT^{-/-}$ and WT mice

The weight of each mouse was measured at the time of sacrifice using an electronic scale to ensure that weight was matched between the $GOAT^{-/-}$ (KO) and WT mice as weight differences would influence the microarchitectural strength of bone. Compared to WT control mice, the $GOAT^{-/-}$ mice used in this study were significantly heavier at 9 (38.76g ±2.28, p=0.002) and 18 months of age (36.15g ±0.85, p=0.03) , however, there were no significant differences in weights between the WT and $GOAT^{-/-}$ at 6 months of age (Figure 3.3-1A). WT mice showed an increase in weight with age with a statistically significant increase between 9 (28.94g ± 0.26) and 18 months of age (32.3g ±1.36, p=0.028). $GOAT^{-/-}$ mice showed an earlier increase in weight with increasing age than WT mice, where a significant increase was observed in $GOAT^{-/-}$ mice between 6 and 9 months (p=0.007).

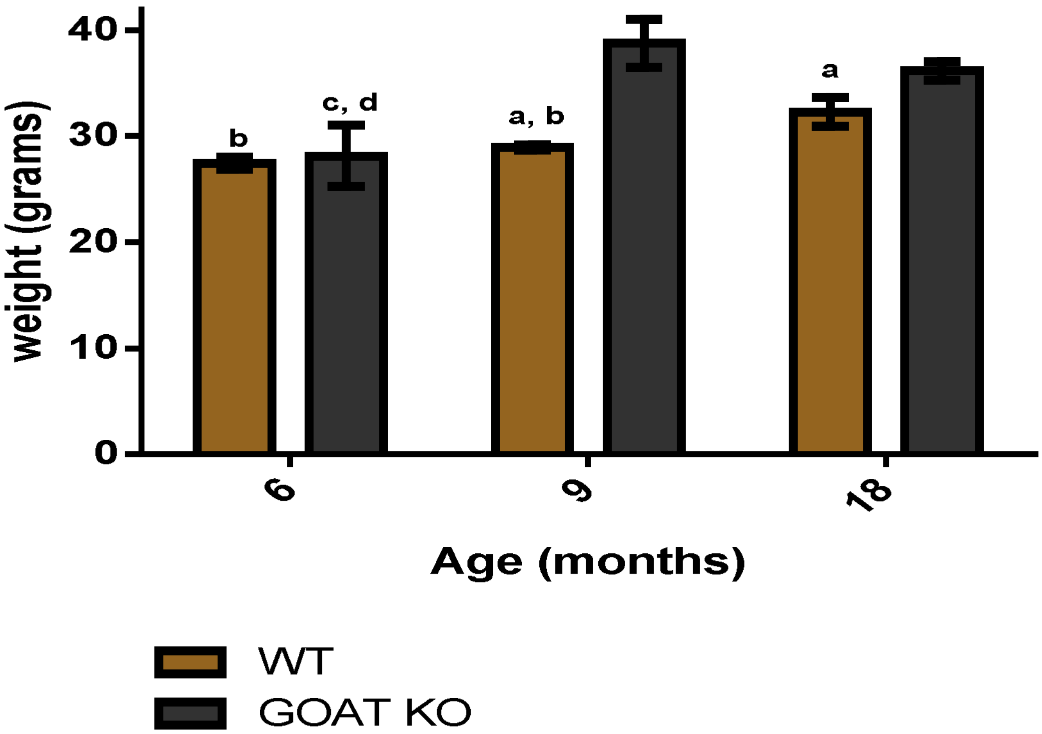

Figure 3.3-1A: Weights (g) of GOAT$^{-/-}$ (KO) and wildtype (WT) mice at 6, 9 and 18 months of age measured at time of sacrifice. Statistically significance differences between means of GOAT$^{-/-}$ and WT mice was determined using independent Student's t tests (GraphPad) and between the ages for each group using one-way ANOVA with Tukey's *post hoc* analysis (GraphPad). Data represented as mean +/- standard error of the mean (SEM) and p<0.05 accepted as significant; a= p<0.05 compared to GOAT$^{-/-}$ at same age, b=p<0.05 compared to WT at 18 months of age, c=p<0.05 compared to 9 month old GOAT$^{-/-}$, d=p<0.05 compared to 18 month old GOAT$^{-/-}$.

Radiographic (X-ray) images of the skeletons were taken at PACE at time of sacrifice to investigate presence of macroscopic phenotypic changes in the skeleton such as fractures, skeletal deformities or skeletal dysplasia or aplasia in the GOAT$^{-/-}$ and WT mice at 6 and 9 months of ages (Figure 3.3-1B). X-ray imaging could not be performed for the 18 month old GOAT$^{-/-}$ and WT mice as the necessary radiographic equipment was unavailable at the Mater Medical Research Institute (MMRI) where the 18 month old mice were housed. No differences in the upper limbs, lower limbs, vertebral columns, skulls or thorax, were observed in the radiographs between the GOAT$^{-/-}$ and WT mice aged 6 and 9 months.

3.3.2 Trabecular bone micro-architecture of secondary spongiosa of the distal femoral metaphysis and proximal tibial metaphysis.

In order to determine if acyl ghrelin affects bone microarchitecture, both femora and tibiae were chosen for evaluation of the trabecular micro-architecture. Representative 3D CT volume-rendered models (Figures 3.3-2) demonstrated the trabecular bone present in the region of interest in the distal metaphyses of the femora (Figures 3.3-2A) and proximal metaphyses of the tibiae (Figure 3.3-2B) in the GOAT$^{-/-}$ and WT mice. A notable decline was observed in the trabecular bone volume fraction with advancing age between 6 and 9 months in the WT femora (Figure 3.3-2A) and tibiae (Figure 3.3-2B). A smaller amount of trabecular bone occupied the volume of interest (VOI) in the GOAT$^{-/-}$ femora and tibiae compared to WT at 6 months of age (Figure 3.3-2).

Bone mineral density (BMD) is a measure of the degree of mineralisation of the bone tissue and therefore represents the inorganic material properties of the bone which contributes to the strength of bone. The BMD of the trabecular bone was measured on the reconstructed cross sectional images from the microCT scan in the secondary spongiosa of the distal femoral metaphyses and the secondary spongiosa of the proximal tibial metaphyses, using the in-built evaluation script for trabecular measurements of the Scanco µCT 40 desktop microCT scanner. The material BMD of

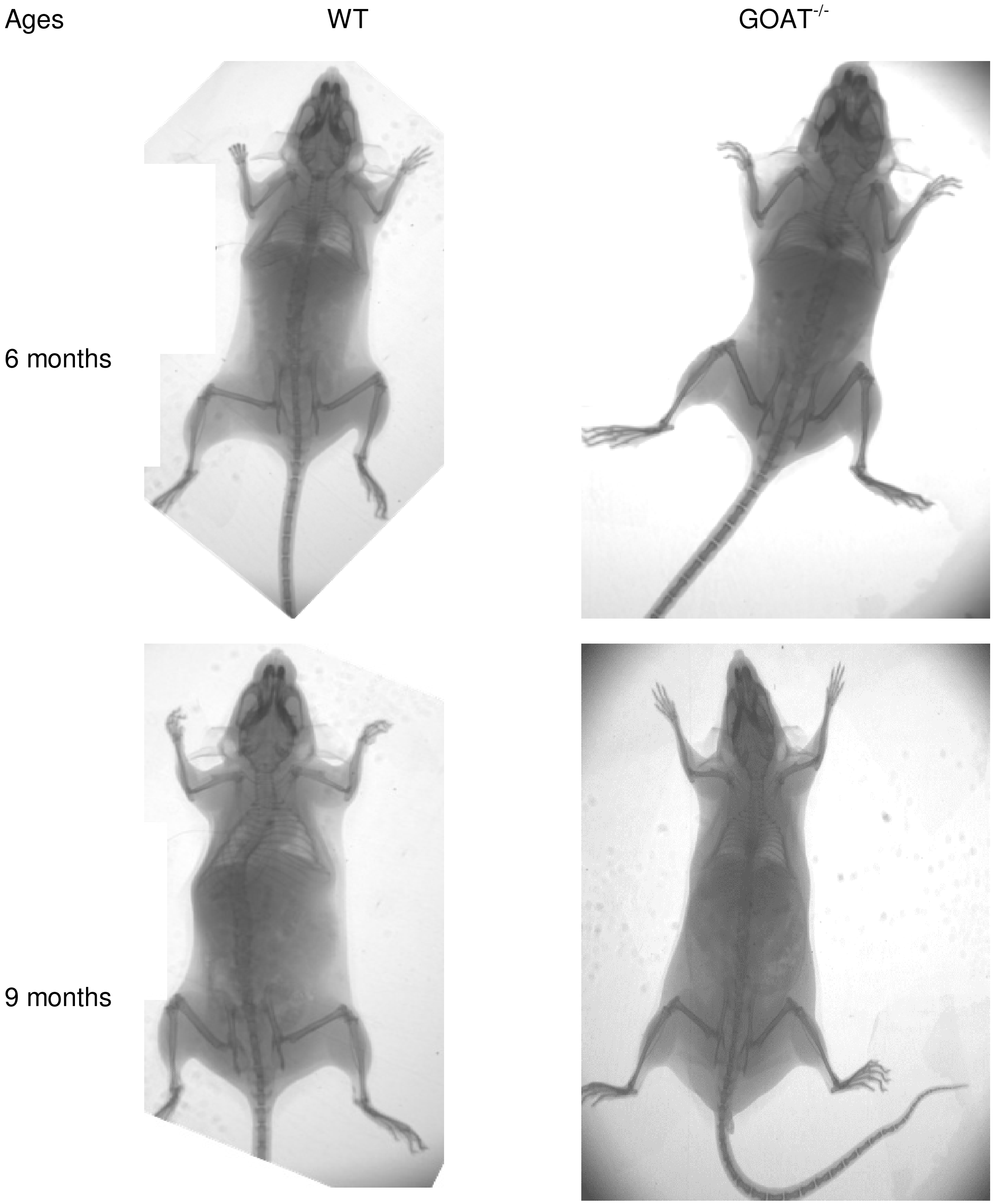

Figure 3.3-1B: Representative radiographic (X-ray) images of 6 and 9 month old C57BL/6J GOAT$^{-/-}$ and WT mice. Mice are in a prone position on the film receptor. Abnormalities such as fractures, aplasias or dysplasias are not observable in the axial or appendicular skeletons of either GOAT$^{-/-}$ or WT mice.

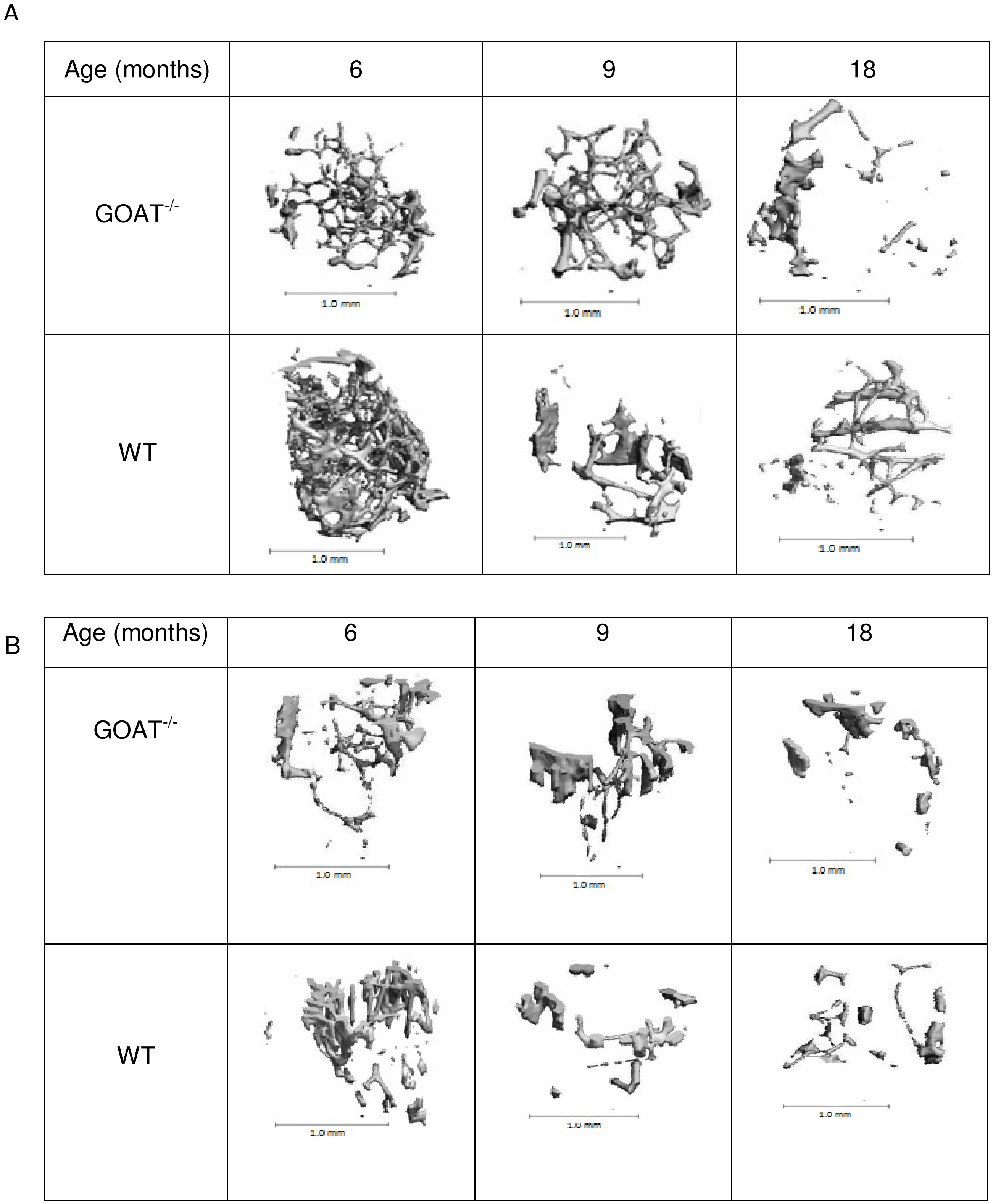

Figure 3.3-2- Representative 3D micro-CT volume-rendered models of the secondary spongiosa of: A) the distal femoral metaphyses; and B) proximal tibial metaphyses of GOAT$^{-/-}$ and WT mice aged 6, 9 and 18 months. Note that these models represent the trabecular compartment only with the cortical shell extracted. Scale bar = 1.0mm.

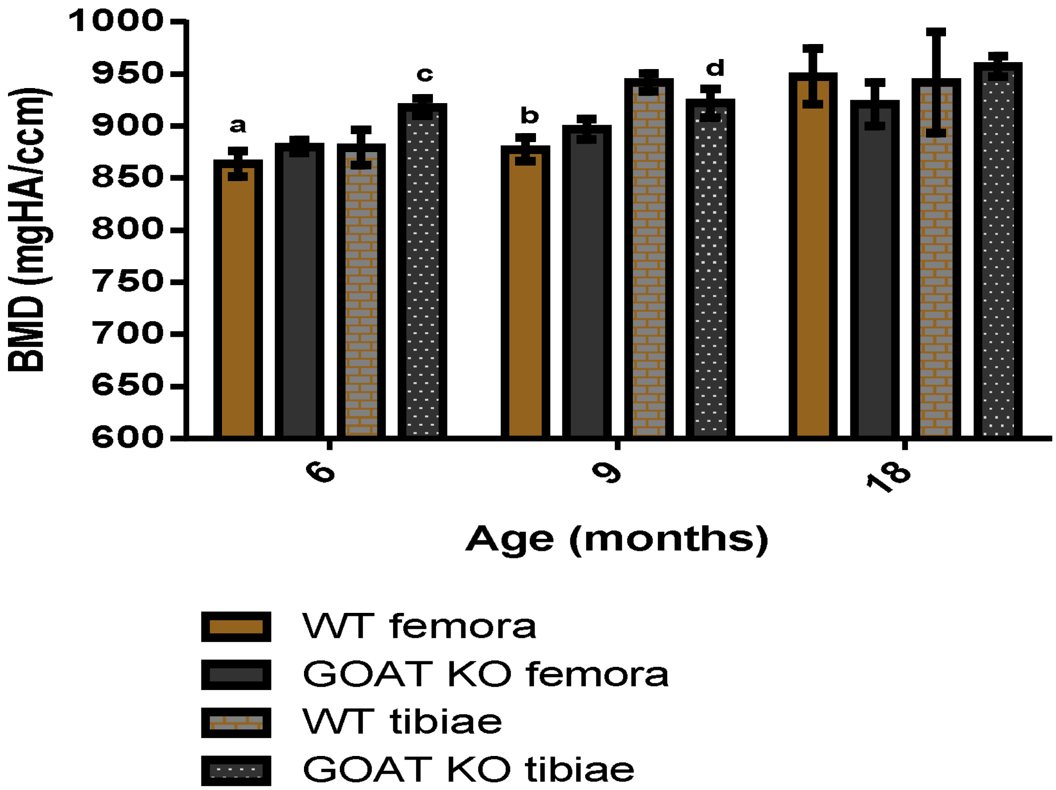

Figure 3.3-3: Material bone mineral density (BMD, mgHA/ccm) of trabecular bone of the secondary spongiosa of the distal metaphyses of the right femora and proximal metaphyses of right tibiae of GOAT KO and WT mice aged 6, 9 and 18 months. Statistical significance between means of GOAT KO and WTs was determined using independent Student's t tests (GraphPad) and between the ages for each group using one-way ANOVA with Tukey's *post hoc* analysis (GraphPad). Significance accepted at $p<0.05$ and marginal significance accepted at $p<0.1$;, data represented as mean +/- standard error of the mean (SEM); a=$p<0.05$ compared to 18 months old WT femora, b=$p<0.1$ compared to 18 month old WT femora, c=$p<0.05$ compared to 18 month old GOAT KO tibiae, d=$p<0.1$ compared to 18 month old GOAT KO tibiae.

the secondary spongiosa of the distal metaphyses of the femora in WT mice showed a significant increase (p=0.01) in BMD with advancing age from 6 (864.05±12.58mgHA/ccm) to 18 months (947.88±26.86mg/HA/ccm), with greatest change observed between 9 (877.61±11.53mgHA/ccm) and 18 months (p=0.05) (Figure 3.3-3); no significant age-related change in BMD was observed in WT tibiae. The BMD of the secondary spongiosa of the proximal metaphyses of the tibiae of GOAT$^{-/-}$ mice showed a significant increase with advancing age from 6 (879.61±16.84 mgHA/ccm)) to 18 (941.87± 48.84mgHA/ccm) months (p=0.014), and between 9 (941.80±8.630 mgHA/ccm) and 18 months (p=0.07) (Figure 3.3-3); no significant age-related change in BMD was observed in GOAT$^{-/-}$ femora. No significant differences were observed between the trabecular BMD of GOAT$^{-/-}$ and WT mice in the tibiae and femora at 6, 9 and 18 months of age.

Trabecular bone volume fraction (BV/TV) is the volume of trabecular bone occupying the total volume of interest and is an indicator of overall bone mass. Due to the large surface area of trabecular bone tissue, changes in bone remodelling rates and altered bone cell function as a result of altered physiology, affects the bone volume fraction. BV/TV of the secondary spongiosa of the distal metaphyses of the right femora in GOAT$^{-/-}$ mice at 6 months of age (3.1% ±0.5) was significantly lower (p=0.005) compared to WT (6.2% ±0.6) controls (Figure 3.3-4). Similarly, BV/TV of the proximal metaphyses of the right tibiae of GOAT$^{-/-}$ mice aged 6 months (1.68% ±0.2) was significantly lower (p=0.007) compared to WT control mice (6.3% ±1.2) of the same age (Figure 3.3-4). BV/TV significantly decreased with advancing age in the femora of WT from 6 (6.2% ±0.6) to 9 months (3.0% ±0.8; p=0.02) and in the tibiae of WT mice from 6 (6.3% ±1.2) to 9 months (2.3% ±0.8; p= 0.05) (Figure 3.3-4). No significant differences in BV/TV were observed in the tibiae and femora of GOAT$^{-/-}$ mice with advancing age.

The number of bone trabeculae present within the tissue volume (trabecular number, Tb.N) contributes to the microstructural strength of bone. The in-built script determines Tb.N by computing the inverse of the mean distance between the mid-axes of adjacent trabeculae (Bouxsein et al., 2010). Tb.N of the femora of 9 month old GOAT$^{-/-}$ mice

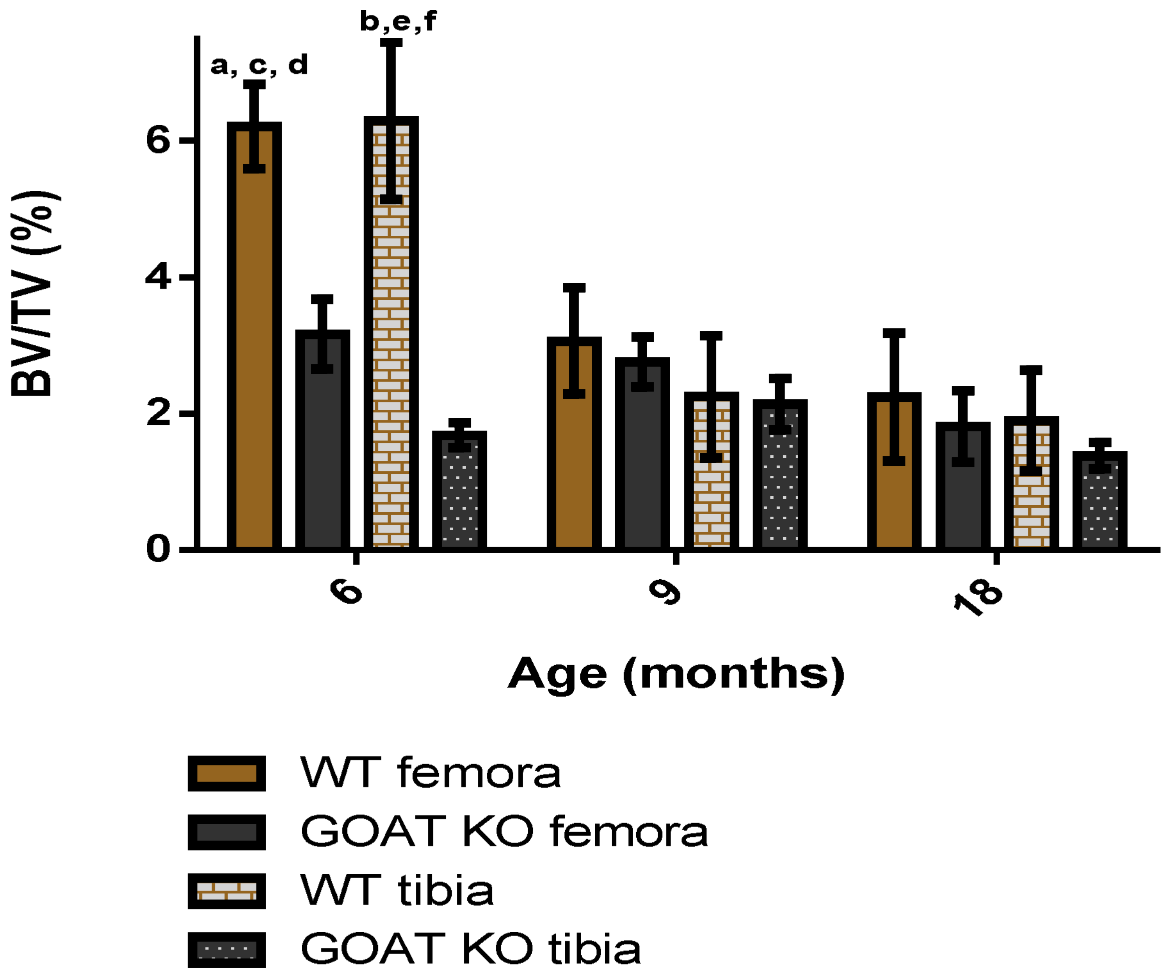

Figure 3.3-4: Trabecular bone volume fraction (BV/TV, %) of the secondary spongiosa of the distal femoral metaphyses of right femora and proximal metaphyses of right tibiae of GOAT KO and WT mice aged 6, 9 and 18 months. Statistical significance between means of GOAT KO and WTs was determined using independent Student's t tests (GraphPad) and between the ages for each group using one-way ANOVA with Tukey's post hoc analysis (GraphPad). Significance accepted at $p<0.05$ and marginal significance accepted at $p<0.1$, data represented as mean +/- standard error of the mean (SEM); a=$p<0.05$ compared to GOAT KO femora at 6 months of age, b=$p<0.05$ compared to GOAT KO tibiae at 6 months of age, c=$p<0.05$ compared to 9 months old WT femora, d=$p<0.05$ compared to 18 months WT femora, e=$p<0.1$ compared to 9 months old WT tibiae f=$p<0.05$ compared to 18 months WT tibiae.

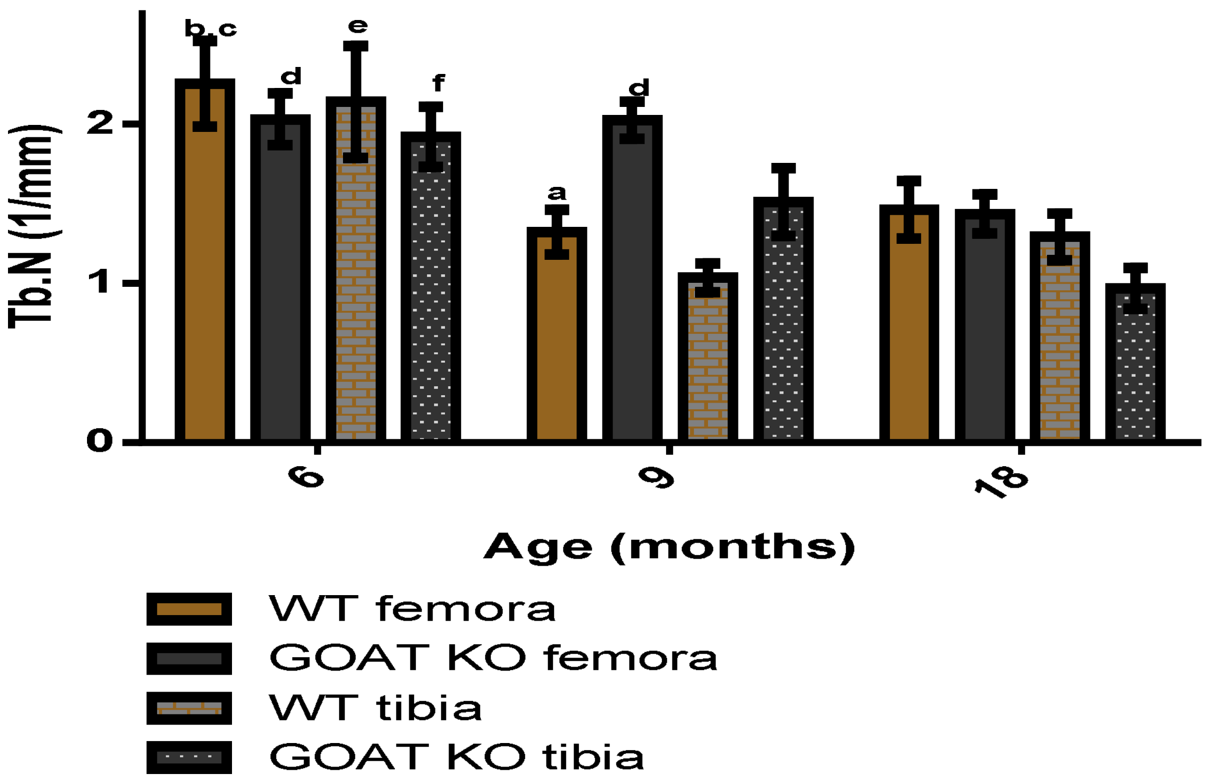

Figure 3.3-5: Trabecular number (Tb.N, #/mm) of the secondary spongiosa of the distal femoral metaphyses of right femora and proximal metaphyses of right tibiae of GOAT KO and WT mice aged 6, 9 and 18 months. Statistical significance between means of GOAT KO and WTs was determined using independent Student's t tests (GraphPad) and between the ages for each group using one-way ANOVA with Tukey's *post hoc* analysis (GraphPad). Significance accepted at $p<0.05$ and marginal significance accepted at $p<0.1$, data represented as mean +/- standard error of the mean (SEM); a=$p<0.05$ compared to GOAT KO femora at 9 months of age, b=$p<0.1$ compared to 18 month old WT femora, c=$p<0.05$ compared to 9 month old WT femora, d=$p<0.05$ compared to 18 month old GOAT KO femora, e=$p<0.1$ compared to 9 month old WT tibiae, f=$p<0.05$ compared to 18 month old GOAT KO tibiae.

2.02 ±0.11mm^{-1}) was significantly greater (p=0.005) than the WT aged 9 months (1.32 ±0.14mm^{-1}) (Figure 3.3-5). Tb.N of the femora significantly decreased with advancing age in the GOAT$^{-/-}$ from 9 (2.02 ±0.11mm^{-1}) to 18 months (1.43 ±0.12mm^{-1}; p=0.01). Tb.N of the WT femora decreased significantly with advancing age from 6 (2.25 ±0.27mm^{-1}) to 9 months (1.32±0.14mm^{-1}; p=0.04). Tb.N of the tibiae in the GOAT$^{-/-}$ mice significantly decreased (p=0.007) with advancing age from 6 (1.91±0.18mm^{-1}) to 18 months (0.96 ±0.1211mm^{-1}) with the greatest decrease being observed with marginal significance (p=0.05) with advancing age in the tibiae of WT from 6 (2.13 ±0.35 mm^{-1}) to 9 months (1.03 ±0.09mm^{-1}) (Figure 3.3-5).

The thickness of trabeculae within the bone volume (trabecular thickness, Tb.Th) is an index of the trabecular microstructure that provides strength to bone and reflects changes in the balance of osteoblastic and osteoclastic activity at bone remodelling sites. The micro-CT measurement is based on a sphere fitting method, where for Tb.Th measurement, the spheres are fitted to the trabecular struts. The diameter of the largest sphere that can be fitted through each voxel and is completely contained within the object is used to average the diameters and yield the Tb.Th value (Bouxsein et al., 2010). Tb.Th of the trabeculae in the distal femoral metaphyses of GOAT$^{-/-}$ mice (0.05 ±0.002 mm) was significantly lower (p=0.001) compared to WT (0.06 ±0.002 mm) mice at 9 months of age (Figure 3.3-6). Similarly, Tb.Th of the trabeculae in the proximal metaphyses of the tibiae was significantly lower (p=0.09) in the GOAT$^{-/-}$ (0.05 ±0.004 mm) compared to WT mice (0.06 ±0.002 mm) aged 9 months (Figure 3.3-6).

The trabecular separation (Tb.Sp) is an index that represents the distance between adjacent trabeculae and therefore the thickness of the marrow spaces within the trabecular bone microstructure. It therefore gives an indication of the porosity of the trabecular bone tissue. The algorithm used for measurements of the Tb.Sp is based on 3D calculations, namely, a sphere fitting method, where the spheres are fitted to the marrow space (Bouxsein et al., 2010). The diameter of the largest sphere that can be fitted through each voxel and is completely contained within the background is used to average the diameters and yield Tb.Sp values (Bouxsein et al., 2010). Tb.Sp of the distal femoral metaphyses and the proximal tibial metaphyses.

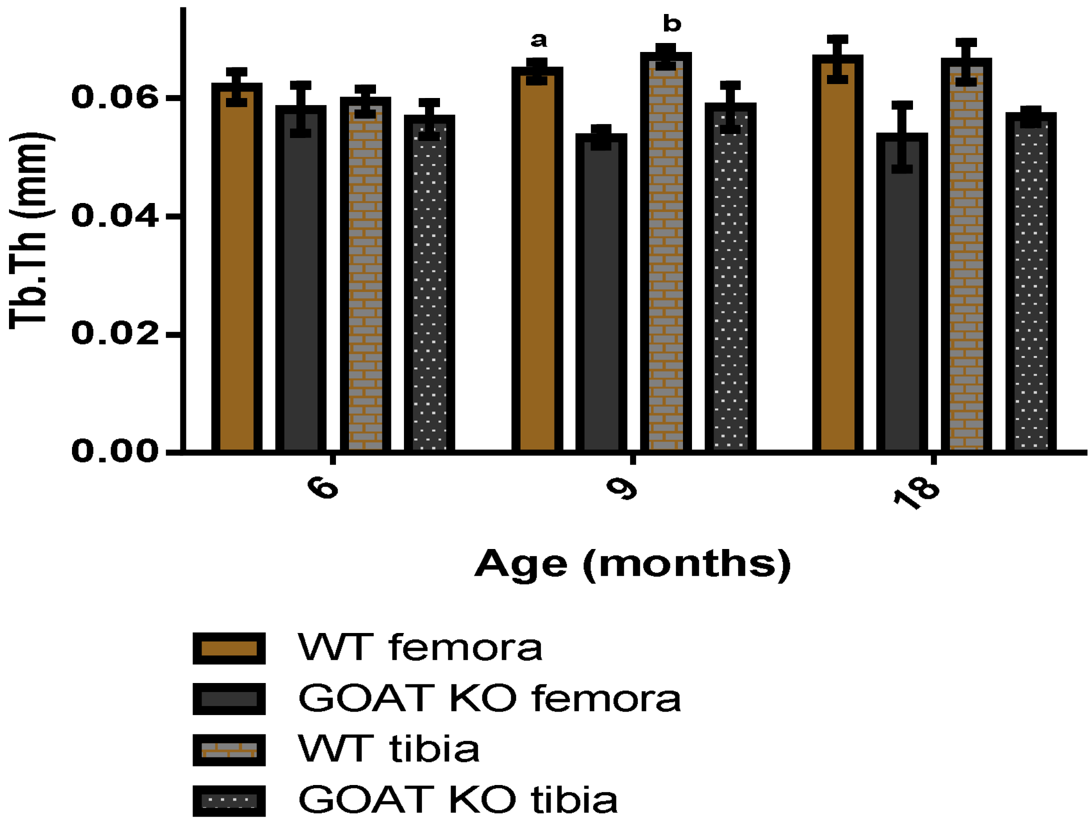

Figure 3.3-6: Trabecular thickness (Tb.Th, mm) of the secondary spongiosa of the distal femoral metaphyses of right femora and proximal metaphyses of right tibiae of GOAT KO and WT mice aged 6, 9 and 18 months. Statistical significance between means of $GOAT^{-/-}$ and WTs was determined using independent Student's t tests (GraphPad) and between the ages for each group using one-way ANOVA with Tukey's *post hoc* analysis (GraphPad). Significance accepted at $p<0.05$ and marginal significance accepted at $p<0.1$, data represented as mean +/- standard error of the mean (SEM); a=$p<0.05$ compared to GOAT KO femora at 9 months, b=$p<0.1$ compared to $GOAT^{-/-}$ tibiae at 9 months.

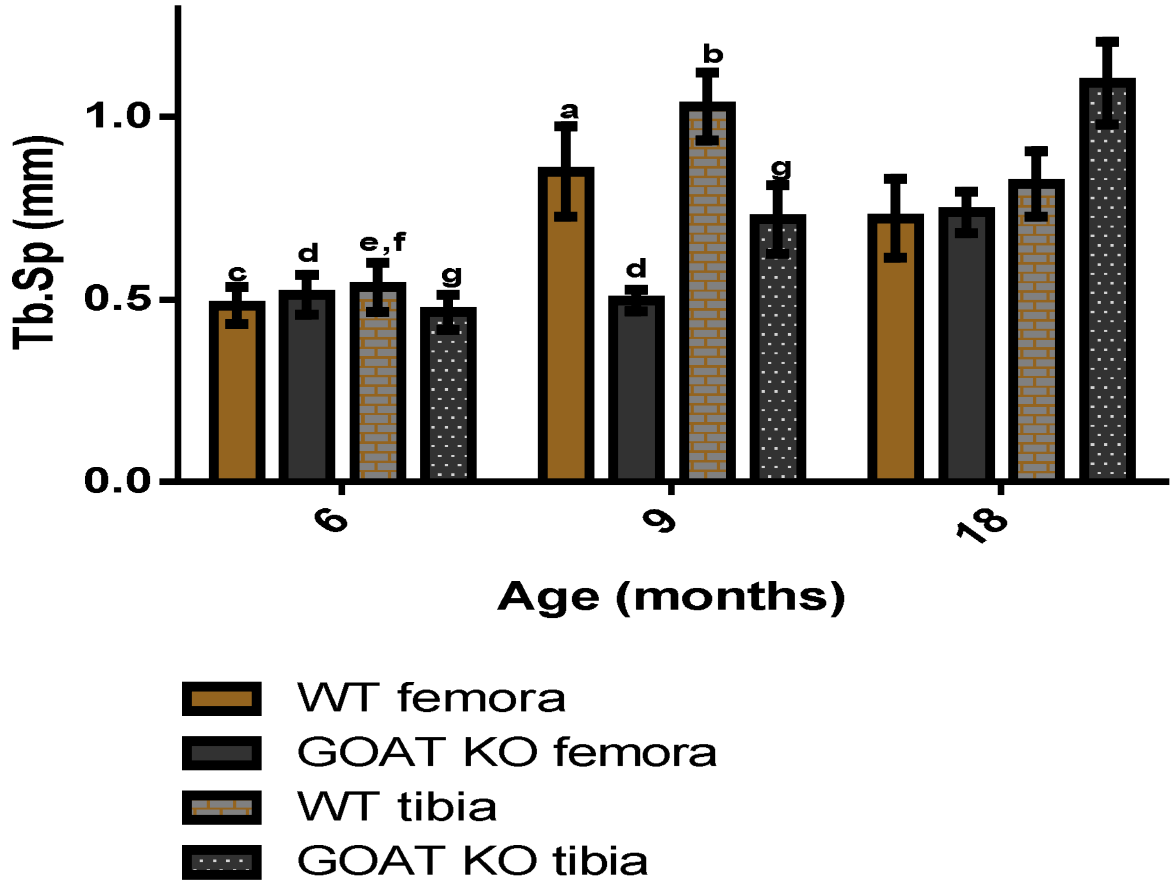

Figure 3.3-7: Trabecular separation (Tb.Sp, mm) of the secondary spongiosa of the distal femoral metaphyses of right femora and proximal metaphyses of right tibiae of GOAT KO and WT mice aged 6, 9 and 18 months. Statistical significance between means of GOAT KO and WTs was determined using independent Student's t tests (GraphPad) and between the ages for each group using one-way ANOVA with Tukey's *post hoc* analysis (GraphPad). Significance accepted at $p<0.05$ and marginal significance accepted at $p<0.1$, data represented as mean +/- standard error of the mean(SEM); a=$p<0.05$ compared to GOAT KO femora at 9 months of age, b=$p<0.1$ compared to GOAT KO tibiae at 9 months of age, c=$p<0.05$ compared to 9 month WT femora, d=$p<0.05$ compared to 18 month old GOAT KO femora, e=$p<0.05$ compared to 9 month old WT tibiae, f=$p<0.05$ compared to 18 month old WT tibiae, g=$p<0.05$ compared to 18 month old GOAT KO tibiae.

Tb.Sp of the distal femoral and proximal tibial metaphyses in GOAT$^{-/-}$ mice at 9 months (0.49 ±0.02 mm and 0.71 ±0.09 mm, respectively) of age was significantly smaller (*p*=0.05 and *p*=0.01, respectively) than the WT controls at 9 months of age (0.85 ±0.12 mm and 1.02 ±0.09 mm, respectively) (Figure 3.3-7). The GOAT$^{-/-}$ mice showed an increase in the trabecular separation at the distal metaphyses of femora with advancing age, from 9 (0.498 ±0.028) to 18 months (0.73 ±0.05mm) (*p* =0.0122) (Figure 3.3-7). GOAT$^{-/-}$ mice showed a significant steady increase in the trabecular separation at the proximal metaphyses of tibiae with advancing age, from 6 (0.46 ±0.04mm) to 18 months (1.09 ±0.11mm; *p*= 0.0009), with the greatest decrease observed between 9 (0.719 ±0.093) and 18 months (1.093 ±0.11mm; *p*=0.0300) (Figure 3.3-7). WT mice showed an increase in the trabecular separation at the distal femoral and proximal tibial metaphyses with advancing age, from 6 (0.48 ±0.05mm and 0.53±0.06mm, respectively) to 9 months (0.85 ±0.12mm and 1.02 ±0.09mm, respectively) (*p*=0.025 and *p*=0.0019) (Figure 3.3-7).

Connectivity density (C.Den) indicates the connectedness of the trabeculae in the trabecular bone network. Trabecular connections are critical for the maintenance of the trabecular microarchitecture and is a major determinant of bone strength. C.Den in both the trabecular network of the distal femoral metaphyses and the proximal tibial metaphyses of GOAT$^{-/-}$ mice (6.20 ±0.83 mm^{-3} and 0.85 ±0.34 mm^{-3}, respectively) were significantly lower (*p*=0.03 and *p*=0.06, respectively) at 6 months of age compared to WT (23.06 ±5.89 mm^{-3} and 26.61 ±10.23 mm^{-3}, respectively) (Figure 3.3-8). No further significant differences were observed in C.Den in the animals studied.

3.3.3 Cortical bone micro-architecture of the mid-diaphyses of the femora and tibiae in GOAT$^{-/-}$ mice.

The representative 2D microCT bone slices of the mid-diaphyses of femora and tibiae shown in Figures 3.3-9A and 3.3-9B, respectively, visually demonstrate that the cortical width (Ct.Wi) of the mid-diaphyses of femora of GOAT$^{-/-}$ mice is greater at 6 and 9

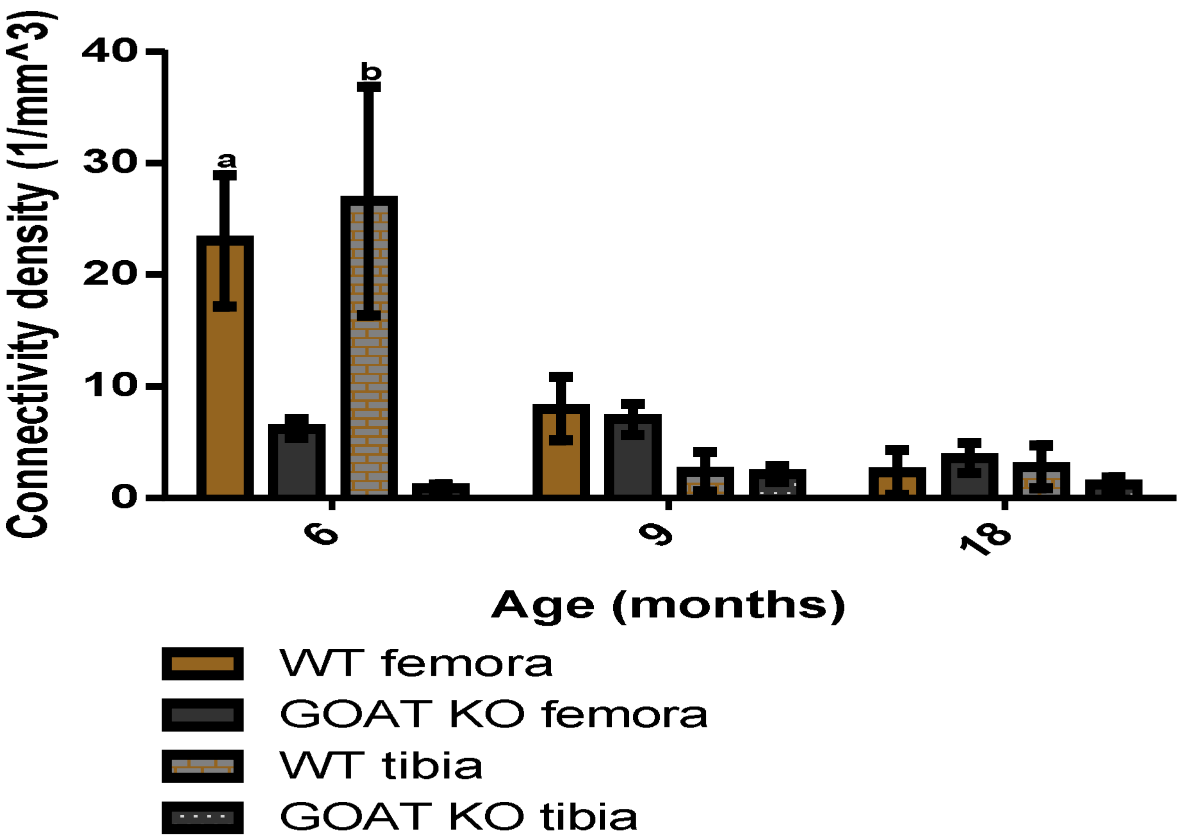

Figure 3.3-8: Connectivity density (per mm^3) of the secondary spongiosa of the distal femoral metaphyses of right femora and proximal metaphyses of right tibiae of GOAT KO and WT mice aged 6, 9 and 18 months. Statistical significance between means of GOAT KO and WTs was determined using independent Student's t tests (GraphPad) and between the ages for each group using one-way ANOVA with Tukey's *post hoc* analysis (GraphPad). Significance accepted at $p<0.05$ and marginal significance accepted at $p<0.1$, data represented as mean +/- standard error of the mean (SEM); a=$p<0.05$ compared to GOAT KO femora at 6 months of age, b=$p<0.05$ compared to GOAT KO tibiae at 6 months of age.

months compared to the WT mice. Ct.Wi is also reduced in 18 month old GOAT$^{-/-}$ femora and tibiae compared to the 9 month old femora and tibiae.

Material bone mineral density in cortical bone (cortical bone mineral density, Ct.BMD) is one of the material properties of the cortical bone and is an indicator of the degree of mineralisation of the cortical bone tissue providing strength to cortical bone. GOAT$^{-/-}$ mice showed a significantly higher Ct.BMD in the mid-diaphyses of the femur (p=0.05) at 6 months (1208.99±17.61 mgHA/ccm) compared to WT (1115.16±16.34 mgHA/ccm). At 6 months of age the GOAT$^{-/-}$ tibiae also had a significantly higher (p=0.04) Ct. BMD (1176.2±10.98 mgHA/ccm) compared to WT (1116.57±22.24). At 9 months of age GOAT$^{-/-}$ femora (1241.22±14.33 mgHA/ccm) had significantly higher (p=0.04) Ct.BMD than WT femora (1197.81±8.77 mgHA/ccm). The GOAT$^{-/-}$ tibiae (1175.5±5.32 mgHA/ccm) at 9 months also had significantly higher (p=0.0003) Ct.BMD than WT tibiae (112.45±2.55 mgHA/ccm) (and , (Figure 3.3-10). The Ct.BMD increased with advancing age in the WT femora between 6 (1115.16±16.34 mgHA/ccm) and 18 months (1238.30±16.80 mgHA/ccm) (p=0.005) (Figure 3.3-10).

The cortical bone width (Ct.Wi) is an indicator of bone modelling of the bone shaft through endosteal resorption and periosteal bone apposition. Ct.Wi was measured by exporting one cross sectional image from the microCT scan of the mid-diaphyses of tibiae and femora of GOAT$^{-/-}$ and WT mice from the Scanco µCT 40 desktop microCT scanner to the Osteomeasure software. Contour lines were drawn around the cortical periosteal perimeter and endosteal perimeter in the Osteomeasure software to generate the mean distance between the two contour lines, equating to Ct.Wi. In the mid-diaphyses of GOAT$^{-/-}$ femora at 6 months (240.79±15.84 µm) and 9 months (222.57±6.54 µm), the Ct.Wi was significantly larger (p=0.0053 and p=0.0103, respectively) than WT femora of the same age (6 month: 174.99±7.17 mm; and 9 month: 179.22±7.28 mm). Similar to the femora, the Ct.Wi of GOAT$^{-/-}$ tibiae at 6 months (202.17±5.67 mm) and 9 months (202.97±3.01 µm) were significantly higher (p=0.01 and p=0.002, respectively) compared to WT (6 months: 168.24±8.63 µm; and 9 months: 166.04±8.47 µm).

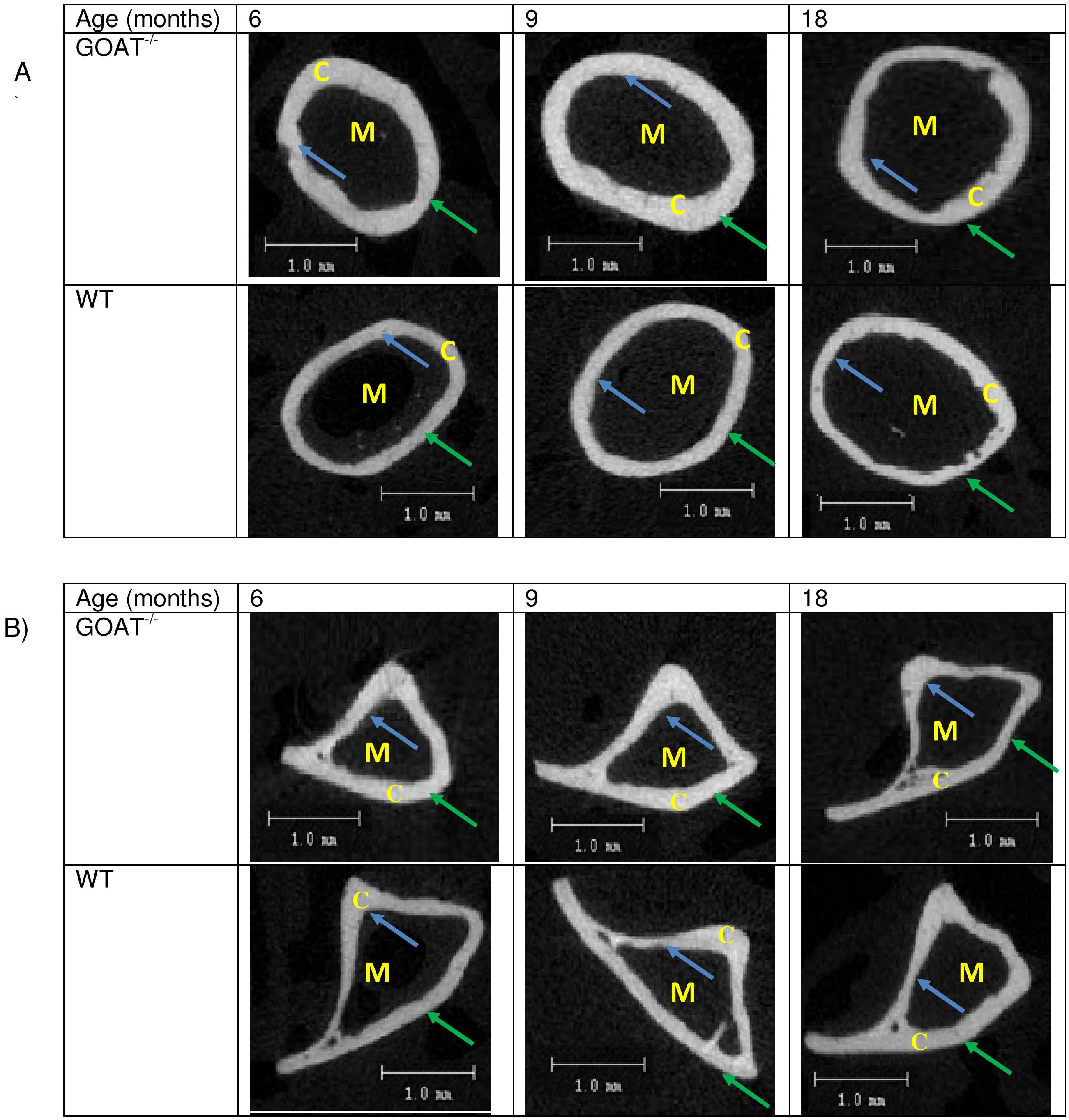

Figure 3.3-9: Representative 2D slices of mid-diaphyses of A) femora and B) tibiae evaluated for cortical bone architecture in GOAT$^{-/-}$ and WT mice aged 6, 9 and 18 months. Scale bar = 1.0 mm, C=cortical bone, M=medullary cavity, green arrow shows the periosteum and blue arrow shows the endosteal surface of the cortex.

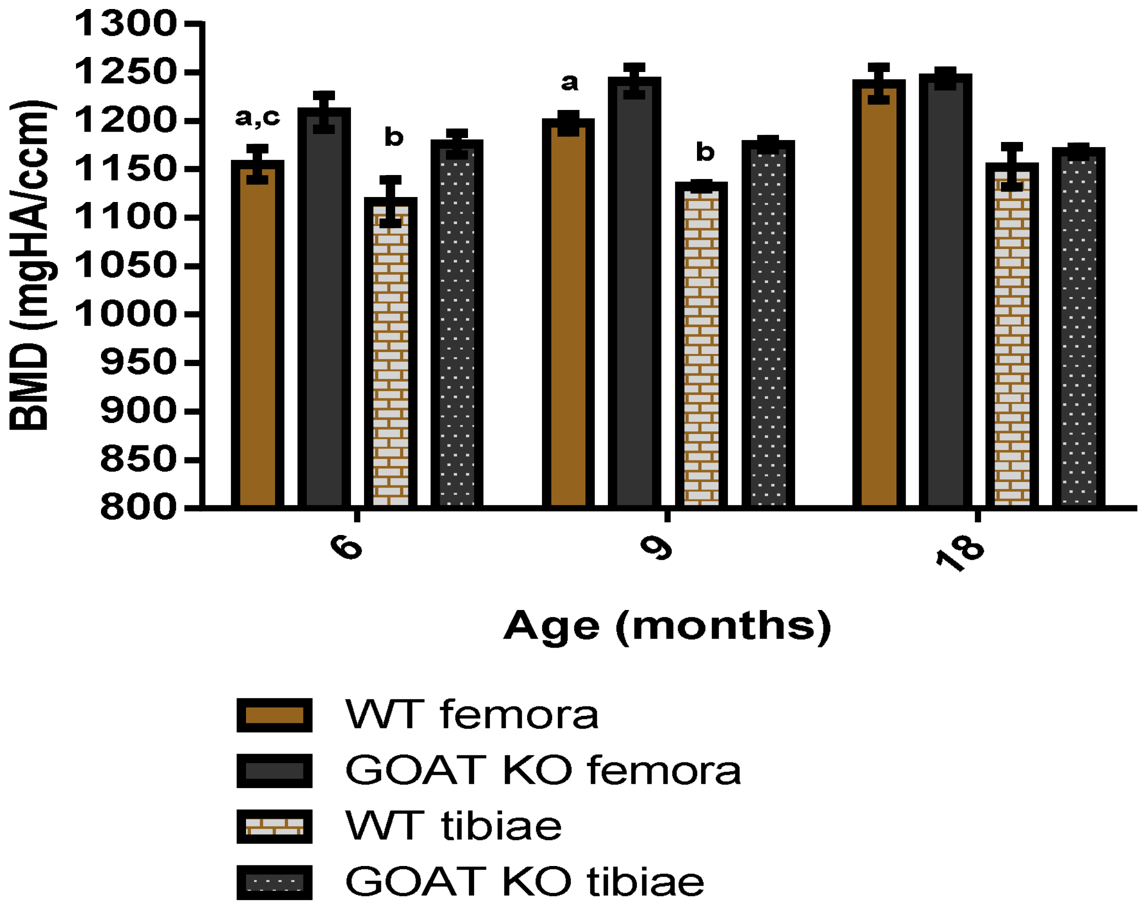

Figure 3.3-10: Material bone mineral density of cortical bone (Ct.BMD, mgHA/cm^3) of the mid-diaphyses of the right femora and right tibiae in GOAT KO and WT mice aged 6, 9 and 18 months. Statistical significance between means of GOAT KO and WTs was determined using independent Student's t tests (GraphPad) and between the ages for each group using one-way ANOVA with Tukey's *post hoc* analysis (GraphPad). Data represented as mean +/- standard error of the mean (SEM), significance accepted at $p<0.05$ and marginal significance accepted at $p<0.1$; a=$p<0.05$ compared to GOAT KO femora at same age, b=$p<0.05$ compared to GOAT KO tibiae at same age, c=$p<0.05$ compared to 18 months old WT femora.

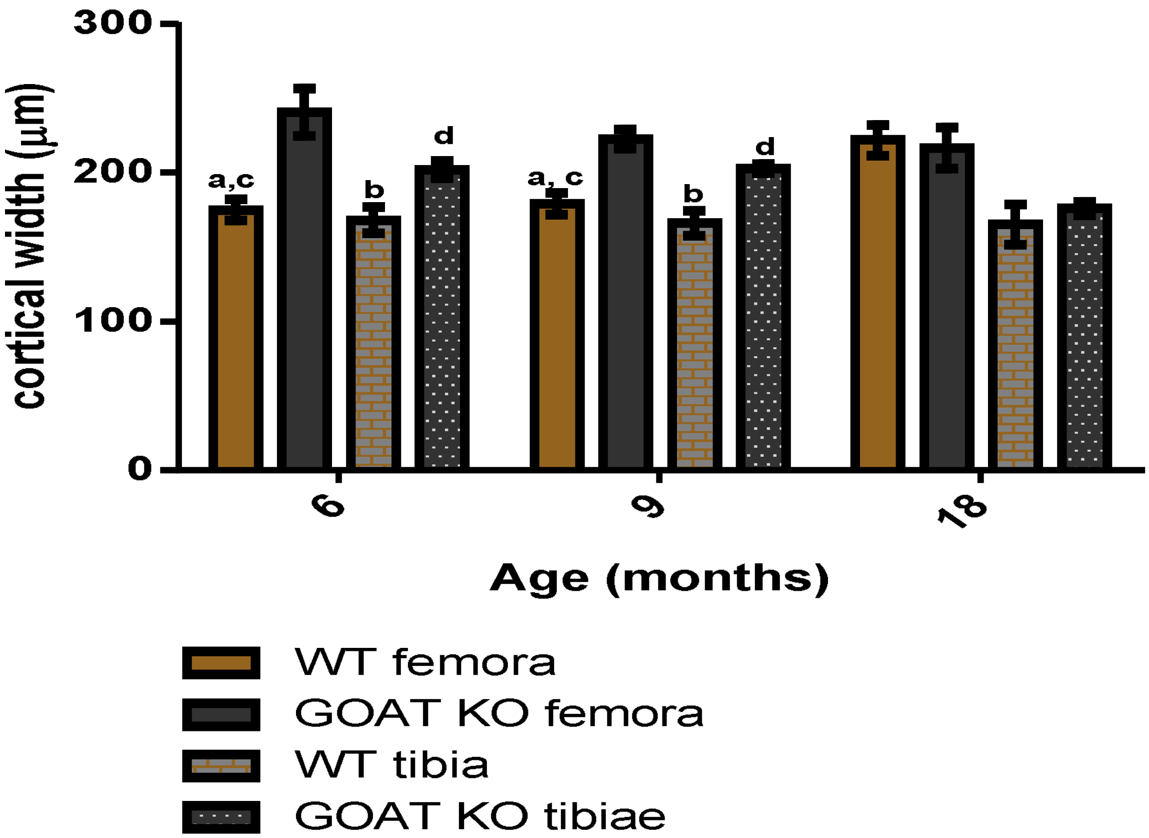

Figure 3.3-11: Cortical width (Ct.Wi, µm) of mid-diaphyses of the right femora and right tibiae in GOAT KO and WT mice aged 6, 9 and 18 months. Statistical significance between means of GOAT KO and WTs was determined using independent Student's t tests (GraphPad) and between the ages for each group using one-way ANOVA with Tukey's *post hoc* analysis (GraphPad). Data represented as mean +/- standard error of the mean (SEM) significance accepted at $p<0.05$ and marginal significance accepted at p<0.1; a=$p<0.05$ compared to GOAT KO femora at same age, b=$p<0.05$ compared to GOAT$^{-/-}$ tibiae at same age, c=$p<0.05$ compared to 18 month WT femora, d=$p<0.05$ compared to 18 month GOAT KO tibiae.

Ct.Wi in the femora of WT mice significantly increased with advancing age from 9 to 18 months (p=0.01) (Figure 3.3-11). The Ct.Wi of the mid-diaphyses of the tibiae in GOAT$^{-/-}$ mice decreased with advancing age from 9 to 18 months (p=0.007) (Figure 3.3-11).

The periosteal bone perimeter (Ps.Pm) is a measure of the periosteal circumference of the mid-diaphyses of long bones. It gives an indication of the bone formation occurring in the cortical bone during appositional growth in response to physiological changes. Ps.Pm was measured on the cross sectional images of the mid-diaphyses of tibiae or femora exported from the microCT scan from the Scanco µCT 40 desktop microCT scanner and imported to the Osteomeasure software. Contour lines were drawn around the cortical perimeter (circumference of the diaphysis) of the bone slice in the Osteomeasure software to generate the Ps.Pm values. Ps.Pm showed a significant increase with advancing age between 9 (8.62±0.39 mm) and 18 months (11.08±0.43 mm; p=0.003) in the mid-diaphyses of tibiae in the GOAT$^{-/-}$ mice (Figure 3.3-12).

The endosteal bone perimeter (Ec.pm) is a measure of the endosteal circumference of the mid-diaphyses of long bones. It gives an indication of the degree of bone resorption occurring on the endosteal surface of the cortical bone in response to physiological changes. Ec.Pm was measured on the cross sectional images of the mid-diaphyses of tibiae or femora exported from the microCT scan from the Scanco µCT 40 desktop microCT scanner and imported to the Osteomeasure software. Contour lines were drawn around the endosteal perimeter of the image in the Osteomeasure software to generate the Ec.Pm values. GOAT$^{-/-}$ mice showed significantly lower Ec.Pm at 6 (p=0.02) and 18 (p=0.03) months of age (5.74±0.26 mm and 6.53±0.20 mm, respectively)of the mid-diaphyses of the femora compared to WT (6.67±0.19 mm and 7.46±0.37 mm, respectively). GOAT$^{-/-}$ tibiae showed a significantly smaller Ec.Pm (p=0.002) of the mid-diaphyses compared to WT (6.53±0.26 mm) at 6 months of age (5.08±0.19 mm) (Figure 3.3-13).

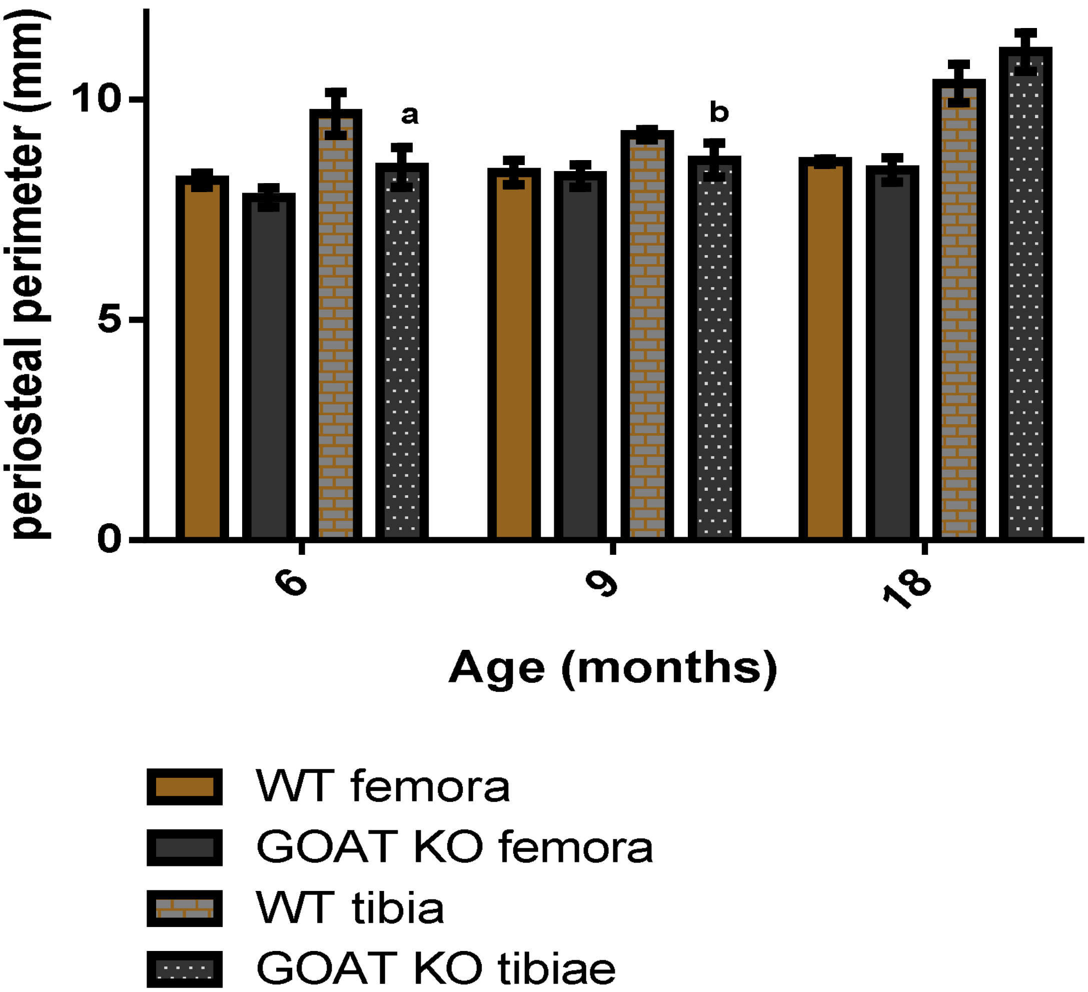

Figure 3.3-12: Periosteal perimeter (Ps.Pm, mm) of the mid-diaphysis of right femora and right tibiae of GOAT KO and WT mice aged 6, 9 and 18 months. Statistical significance between means of GOAT KO and WTs was determined using independent Student's t tests (GraphPad) and between the ages for each group using one-way ANOVA with Tukey's *post hoc* analysis (GraphPad). Data represented as mean +/- standard error of the mean (SEM),significance accepted at $p<0.05$ and marginal significance accepted at $p<0.1$; a=$p<0.05$ compared to 9 month GOAT KO tibiae, b= $p<0.05$ compared to 18 month GOAT KO tibiae.

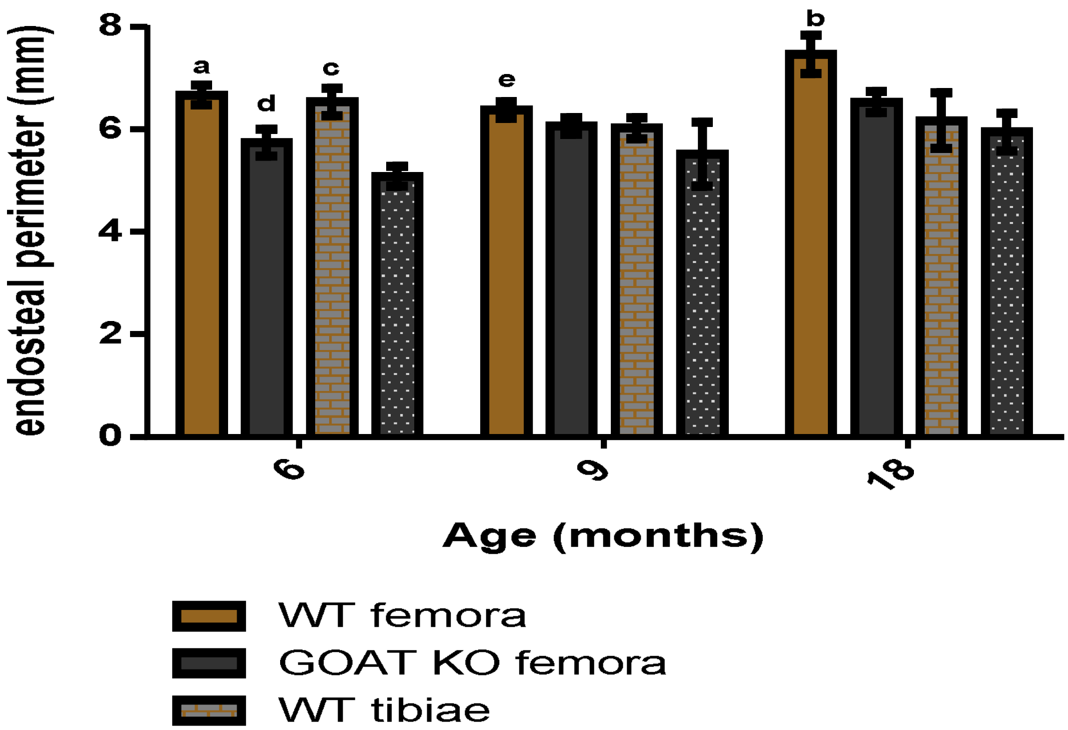

Figure 3.3-13: Endosteal perimeter (Ec.Pm, mm) of the mid-diaphyses of right femora and right tibiae of GOAT KO and WT mice aged 6, 9 and 18 months. Statistical significance between means of GOAT KO and WTs was determined using independent Student's t tests (GraphPad) and between the ages for each group using one-way ANOVA with Tukey's *post hoc* analysis (GraphPad). Data represented as mean +/- standard error of the mean (SEM), significance accepted at $p<0.05$ and marginal significance accepted at $p<0.1$; a= $p<0.05$ compared to GOAT KO femora at 6 months, b= $p<0.1$ compared to GOAT KO femora at 18 months, c= $p<0.05$ compared to GOAT KO tibiae at 6 months, d= $p<0.05$ compared to 18 month old GOAT KO femora, e=$p<0.05$ compared to 18 month old WT femora.

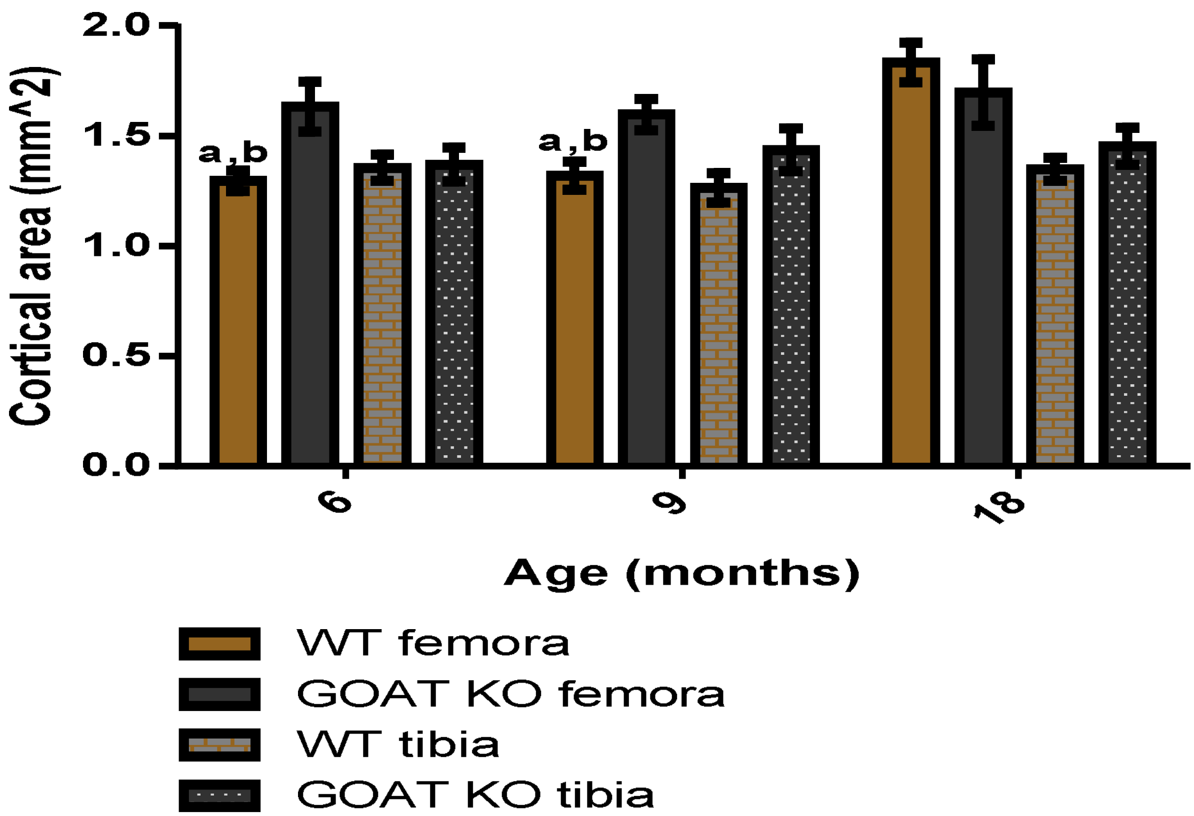

Figure 3.3-14: Cortical bone area (Ct.Ar, mm^2) of the mid-diaphysis of right femora and right tibiae of GOAT KO and WT mice aged 6, 9 and 18 months. Statistical significance between means of $GOAT^{-/-}$ and WTs was determined using independent Student's t tests (GraphPad) and between the ages for each group using one-way ANOVA with Tukey's *post hoc* analysis (GraphPad). Data represented as mean +/- standard error of the mean (SEM), significance accepted at p<0.05 and marginal significance accepted at p<0.1; a=p<0.05 compared to GOAT KO femora at same age, b=p<0.05 compared to 18 month old WT femora.

Ec.Pm of the femora in GOAT$^{-/-}$ mice significantly increased with advancing age from 6 to 18 months (p=0.04), and Ec.Pm significantly increased with age in the femora of WT mice from 9 to 18 months (p=0.03).

Cortical bone area (Ct.Ar) is the area of cortical bone occupying the mid-diaphyseal cross section. It is a similar measure to the Ct.Wi which provides information of the net of periosteal apposition and endosteal resorption occurring in the mid-diaphyses of the femora or tibiae. The Ct.Ar of the mid-diaphyses of GOAT$^{-/-}$ femora was significantly higher (p= 0.01) at 6 months (1.63±0.11 mm^2) compared to WT femora (1.297±0.046). Similarly at 9 months the Ct.Ar of GOAT$^{-/-}$ femora (1.59±0.07 mm^2) was significantly larger (p=*0.*02) than WT femora (1.32±0.06 mm^2). With advancing age the Ct.Ar of the WT femora increased significantly from 9 (1.32±0.06 mm^2) to 18 months (1.83±0.01 mm^2; p=0.0009).

The polar moment of inertia (pMOI) is the distribution of bone around the longitudinal axis and is indicative of the bone's ability to resist fracture under torsion loads. The calculation of pMOI (J= π[radius of outer circle^4 - radius of inner circle^4]/2) of the mid-diaphyses are based on the radius of the diaphyseal cross-sections (Bhavikatti and Rajashekarappa, 1994) and is reliant on the shape and size of the cylinder. The pMOIs of the mid-diaphyses of the femora of GOAT$^{-/-}$ mice (0.51±0.03 mm^4) were significantly lower at 18 months of age (p=0.025) compared to WT (0.69±0.07 mm^4) (Figure 3.2-15) and the tibiae of GOAT$^{-/-}$ mice (0.28±0.02 mm^4, 0.28±0.01 mm^4 and 0.37±0.01 mm^4, respectively) had significantly lower pMOI compared to WT (0.40±0.01 mm^4 , 0.39±0.01 mm^4 and 0.43±0.01 mm^4, respectively) at 6 (p=0.0006), 9 months (p=0.003) and 18 months of age (p=0.028) (Figure 3.2-15). pMOI increased in the WT femora with advancing age from 9 (0.40±0.01 mm^4) to 18 months (0.43±0.01 mm^4; p=0.001) and also in the GOAT$^{-/-}$ femora from 9 (0.39±0.02 mm^4) to 18 months (0.51±0.03 mm^4; p=0.029) (Figure 3.3-15). The pMOI of GOAT$^{-/-}$ tibiae increased with advancing age from 9 (0.28±0.01 mm^4) to 18 months (0.37±0.01 mm^4; p=0.021) (Figure 3.3-15).

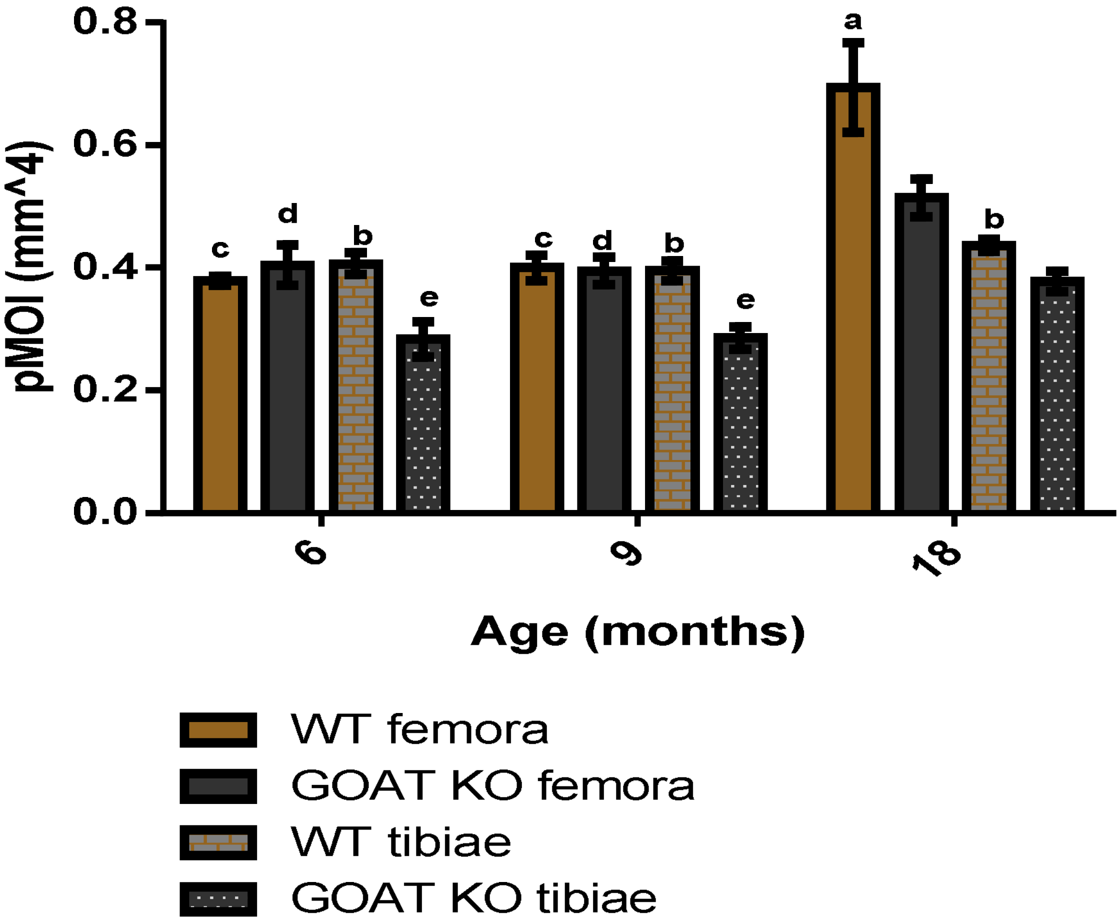

Figure 3.3-15: Polar moment of inertia (pMOI, mm^4) of the mid-diaphysis of right femora and right tibiae of GOAT KO and WT mice aged 6, 9 and 18 months. Statistical significance between means of GOAT KO and WTs was determined using independent Student's t tests (GraphPad) and between the ages for each group using one-way ANOVA with Tukey's *post hoc* analysis (GraphPad). Data represented as mean +/- standard error of the mean (SEM), significance accepted at $p<0.05$ and marginal significance accepted at $p<0.1$; a=$p<0.05$ compared to GOAT KO femora at 18 months, b=$p<0.05$ compared to GOAT KO tibiae at same age, c=$p<0.05$ compared to 18 month WT femora, d= $p<0.05$ compared to 18 month GOAT KO femora, e=$p<0.05$ compared to 18 month GOAT KO tibiae.

4.3 Discussion

In this study the trabecular and cortical bone microarchitecture of the femora and tibiae of female adult GOAT$^{-/-}$ mice aged 6, 9 and 18 months were characterised using high resolution µCT and is the first study to investigate and report the skeletal phenotype of GOAT$^{-/-}$ mice. The study found that the trabecular bone volume fraction of both femora and tibiae of GOAT$^{-/-}$ mice was significantly less at 6 months of age compared to the WT controls. There were no differences in the mineral density of the trabecular bone between the GOAT$^{-/-}$ and WT at 6 months. This suggests that the trabecular bone strength is reduced in the GOAT$^{-/-}$ femora and tibiae at 6 months via the volume of bone being reduced rather than reduced mineralisation. The reduced bone volume fraction in the GOAT$^{-/-}$ mice was due to less trabecular connectivity density in comparison to WT controls. Trabecular number, thickness and separation were not significantly different. Reduced connectivity density could be a result of a decrease in bone formation by osteoblasts relative to resorption by osteoclasts (Van Der Linden, Verhaar, & Weinans, 2001) or an increase in osteoclast activity relative to osteoblast activity, resulting in incomplete filling of resorption cavities and focal perforations in the trabecular struts, similar to osteoporosis (Epstein, 2005). The lack of a change in the trabecular thickness suggests that the osteoblast activity is unchanged and the decrease in connectivity density is more likely a result of increased osteoclast activity in the GOAT$^{-/-}$ trabecular bone. GHSR$^{-/-}$ (partial lack of acyl ghrelin signalling) has been reported to increase osteoclastogenesis in culture, resulting in an increased pool of osteoclasts, without affecting osteoblastogenesis (van der Velde et al., 2012). In addition GHSR$^{-/-}$ mice showed increased osteoclast activity, demonstrated by a significantly higher osteoclast number on the trabecular bone surface at 6 months of age (van der Velde et al., 2012). The decrease in bone volume fraction in the GOAT$^{-/-}$ mice at 6 months of age is similar to the finding that the bone volume fraction of GHSR$^{-/-}$ mice is decreased at 6 months of age compared to WT controls (van der Velde et al., 2012). Although it was attempted to determine osteoclast activity through the osteoclast numbers on the trabecular bone surface of the GOAT$^{-/-}$ mice in this project, due to technical limitations and time constraints we were unable to gather accurate and reliable data for osteoclast activity (see Appendix 6.2).

The loss of trabecular bone volume fraction in the GHSR$^{-/-}$ mice, however, was a result of reduced trabecular number (loss of individual trabecular struts) (van der Velde et al., 2012), whereas the reduced bone volume fraction in the femora and tibiae of GOAT$^{-/-}$ mice was due to less trabecular connectivity density in comparison to WT controls. Trabecular number, thickness and separation were not significantly different in the GOAT$^{-/-}$ femora or tibiae compared to WT. This suggests that the trabecular number may be unchanged in the GOAT$^{-/-}$ mice because the reduced connections may result in greater numbers of separate trabecular struts. The measurements were also taken in the femoral head for the GHSR$^{-/-}$ mice (van der Velde et al., 2012), whereas for the GOAT$^{-/-}$ mice in this study, the measurements were taken at the distal metaphyses of femora and proximal metaphyses of tibiae. Therefore, the loss of trabecular bone volume fraction resulting from loss of trabecular number or connectivity density may be site-specific.

Acyl ghrelin function is mediated largely through GHSR1a (Kojima et al., 1999), however GHSR1a exhibits unusually high constitutive activity (Holst et al., 2003) and acyl ghrelin is capable of signalling in the absence of GHSR1a through alternative receptors (Caminos et al., 2005; Muccioli et al., 2004; Thielemans et al., 2007; Volante et al., 2003). GOAT is the enzyme responsible for the post-translational esterification of ghrelin to produce acylated ghrelin (Gutierrez et al., 2008; Yang et al., 2008) and GOAT$^{-/-}$ mice are characterised by a total absence of acylated ghrelin, with the presence of desacyl ghrelin (Kirchner et al., 2009). The finding of this study that the trabecular bone volume fraction of GOAT$^{-/-}$ mice is reduced at 6 months was also seen in GHSR$^{-/-}$ mice (van der Velde et al., 2012) which had a reduced bone volume fraction at 6 months caused by increased osteoclast activity. This indicates that acyl ghrelin signalling through GHSR1a is responsible for the regulation of the trabecular bone microarchitecture through the regulation of bone metabolism. Lack of GHSR has shown an increase in osteoclast activity, suggesting that GHSR1a signalling may have an inhibitory role on osteoclast activity (van der Velde, et al., 2012). Therefore, it is likely that the lack of acyl ghrelin signalling through GHSR1a in the GOAT$^{-/-}$ mice, may have increased osteoclast activity resulting in the similar observation of the reduced bone volume fraction.

GOAT$^{-/-}$ mice aged 9 and 18 months were not significantly different in the bone volume fractions of the femora and tibiae compared to the WT controls of the same age. Surprisingly, GOAT$^{-/-}$ mice in these older age groups were heavier than the WT controls, potentially due to altered metabolism as the mice age, and this observation has not been published before. Alternatively, the increased weights of GOAT$^{-/-}$ mice in this study may be due to the older GOAT$^{-/-}$ mice being maintained in smaller numbers per cage due to their susceptibility to stress compared to the WTs (Jeffery, P., personal communication). The body compositions of the GOAT$^{-/-}$ were not investigated in this study, however a previous study has shown that older GOAT$^{-/-}$ mice have substantially higher initial body weights and fat mass (Yi et al., 2012).
One of the major functions of trabecular bone is to support the ends of long bones in load bearing (Mow & Huiskes, 2005; Tanck, Homminga, van Lenthe & Huiskes, 2001). The increased weight of the GOAT$^{-/-}$ mice at 9 and 18 months would have increased the mechanical demands on the skeleton, leading to stimulation in bone formation within the trabecular compartment. This process is described by Frost's mechanostat theory, which proposes that adaptive remodelling occurs when strains are above or below the physiological threshold of the animal (Ferretti, Capozza, Mondelo, & Zanchetta, 1993; Frost, 1990b). Although it would be expected that the GOAT$^{-/-}$ mice would have increased trabecular bone volume fraction due to the increased weights and therefore increased functional demand (Tanck, Homminga, van Lenthe, & Huiskes, 2001), this was not observed. The lack of difference in the trabecular bone volume fractions in the femora and tibiae between GOAT$^{-/-}$ and WT at 9 and 18 month of ages may have been due to an inhibition of osteoblast activity in the GOAT$^{-/-}$ mice, as ghrelin has positive effects on differentiation, proliferation and activity of osteoblasts (Costa et al., 2011; P. J. Delhanty et al., 2006; Fukushima et al., 2005; Kim et al., 2005; Liao L. & Wang, 2010; Maccarinelli et al., 2005). Conversely this observation may be due to the increased

osteoclast activity associated with ageing being unopposed in the absence of acyl ghrelin (van der Velde, et al., 2012), such that any stimulation in bone formation in the heavier animals may have been counteracted by increased bone resorption on the GOAT$^{-/-}$ trabecular bone surface.

At 9 months of age the bone volume fraction did not show differences to the WT mice because the GOAT$^{-/-}$ maintained the trabecular number they showed at 6 months of age compared to the decline in trabecular number in the WT controls. Tb.N is computed as the inverse of the mean distance between the mid-axes of adjacent trabeculae (Bouxsein et al., 2010), therefore when the trabecular number is large, there is a high density of individual trabeculae within the volume of interest. A high Tb.N therefore may indicate a higher bone mass or that the trabeculae are distributed evenly across the volume of interest. A high Tb.N could also mean that the Tb.Th has increased resulting in a decreased distance between trabeculae and hence increased Tb.N. A smaller Tb.N can indicate that the trabeculae are far apart and therefore distance between mid-axes is large. This usually means that there are fewer connections between the trabeculae but not necessarily, such as in cases where only a very small amount of bone is remaining (Bouxsein et al., 2010)).

At 9 months of age, the femora of GOAT$^{-/-}$ mice had higher Tb.N, smaller Tb.Th, smaller Tb.Sp, no difference in C.Den and no difference in BV/TV compared to WT. The high Tb.N of the GOAT$^{-/-}$ indicates that the trabeculae are more densely packed, and the low Tb.Sp indicates that there is less marrow space between adjacent trabeculae. These results alone would predict a higher BV/TV in the GOAT$^{-/-}$ mice at 9 months, however, this was not the case. Instead, no difference in BV/TV was observed between the GOAT$^{-/-}$ mice compared to WT mice at 9 months of age. Furthermore, in addition to the changes in trabeculae distribution, the Tb.Th was significantly lower in GOAT$^{-/-}$ mice. Therefore, whilst there was a higher density of trabeculae in the GOAT$^{-/-}$ mice, each trabecula was significantly thinner than WT mice, ultimately resulting in no change to bone volume. Bone remodelling through the tightly coupled activity between osteoclasts and osteoblasts affects the thickness of trabeculae. The reduced thickness indicates that osteoclast activity is greater than osteoblast activity in the GOAT$^{-/-}$ mice in comparison to the WT mice. This suggests that osteoclast activity may be increased in the GOAT$^{-/-}$ mice similar to the increased osteoclast activity seen in the 6 month old GHSR$^{-/-}$ mice (van der Velde et al., 2012), suggesting that acyl ghrelin signalling through GHSR1a may be required for suppressing undesirable osteoclast activity at older ages.

At 18 months of age, there were no differences in the BV/TV, Tb.N, Tb.Th, Tb.Sp and Conn.Den in the femora and tibiae of the GOAT$^{-/-}$ mice compared to WT mice. The bone volume fractions of GOAT$^{-/-}$ mice and WT mice at both 9 and 18 months of age appeared to be very small (approximately 2%). The lack of differences in morphometric parameters between the trabecular bone of GOAT$^{-/-}$ mice and WT mice at 18 months may be mainly attributed to the small amount of bone present in the volume of interest for comparison (Gregory, et al., 2006).

The results of this study demonstrate distinctly different regulatory patterns in the cortical and trabecular bone compartments in the absence of GOAT. Cortical BMD generally decreases or remains unaltered with increasing age in adults (Flaherty, 1999; Furst, et al., 2008). The mineral density of the cortical bone of the mid-diaphyses of the femora and tibiae of GOAT$^{-/-}$ mice was higher at 6 and 9 months of age compared to WT mice. This indicates that the material property (hardness) of cortical bone which provides strength is enhanced in the absence of acyl ghrelin signalling, which suggests that acyl ghrelin signalling may contribute to age-related bone loss by reducing cortical bone density.

The results of this study also demonstrate that the polar moment of inertia (pMOI) of cortical bone (geometric property of strength) in GOAT$^{-/-}$ mice is reduced. The reduced pMOIs were observed in the 18 month old femora and 6, 9 and 18 month old tibiae compared to WT controls. The GHSR$^{-/-}$ mice, however, have been reported to have a lower pMOI in the mid-shaft of the femora at 6 months of age (van der Velde, et al., 2012). This indicates that at 6 months of age the absence of acyl ghrelin does not affect the pMOI of femora, however, the absence of GHSR1a, which partly mediates acyl ghrelin signalling and has constitutive activity, reduces pMOI of femora. This suggests that the constitutive activity may play a modulatory role in providing strength to resist torsion in the femora at 6 months. The pMOI of tibiae, however, were reduced in the GOAT$^{-/-}$ mice at 6, 9 and 18 months of age compared to WT mice. This suggests that the modulation of strength to resist torsion in the mid-diaphyses by acyl ghrelin signalling may be limb-specific. Also, the changes observed in the GOAT$^{-/-}$ mice at 9 and 18 months could be a result of increased weights in the GOAT$^{-/-}$ resulting in altered modelling.

The periosteal perimeter of a cross-section of the mid-diaphyses of the femora and tibiae revealed that there were no differences between the periosteal perimeters between the GOAT$^{-/-}$ mice and WT mice. This indicates that the periosteal apposition (formation of bone on the periosteal surface by osteoblasts) was not affected by the absence of acyl ghrelin. The endosteal perimeter of a cross-section of the mid-diaphyses of the femora and tibiae showed that the endosteal perimeter of GOAT$^{-/-}$ mice is reduced, in the femora at 6 and 18 months and in the tibiae at 6 months. This indicates that at 6 months the endocortical surfaces of the mid-diaphyses of femora and tibiae undergo less resorption. Therefore, this suggests that the osteoclast activity is regulated in a different manner (reduced osteoclast activity) during modelling in the mid-diaphyses of cortical bone in comparison to remodelling in the trabecular bone (increased osteoclast activity). It is unclear whether an endogenous modulator of cortical bone is different to the trabecular bone. For example, Tobias, et al., (1992) found opposite effects of insulin-like growth factor-I (IGF-I) on the formation of trabecular and cortical bone in adult female rats; IGF-I stimulated periosteal bone formation but reduced trabecular bone formation (Heap, et al., 2004). The results of our study also demonstrate that the cortical bone compartment regulation by acyl ghrelin is different to trabecular bone.

Cortical width and cortical area in mid-diaphyses, showed an increase in femora of GOAT$^{-/-}$ mice at 6 and 9 months of age compared to WT mice. The tibiae, however, showed an increase in cortical width and not the cortical areas at 6 and 9 months of age in the GOAT$^{-/-}$ mice compared to WT. The increase of Ct.Wi and Ct.Ar in the femora at 6 months is a result of smaller endosteal perimeters, however, at 9 months the increase in width could be a result of the adaptation to increased load in the GOAT$^{-/-}$ mice. It is unclear, the reason for the Ct.Wi and Ct.Ar difference in the tibiae at 6 and 9 months of age in the GOAT$^{-/-}$ mice.

The regulation of bone metabolism by acyl ghrelin could be a result of the direct action of acyl ghrelin on osteoblasts and osteoclasts, or it could be indirect interactions with other hormones, or could be a combination of both direct and indirect mechanisms (Costa et al., 2011; P. J. Delhanty et al., 2006; Fukushima et al., 2005; Kim et al., 2005; Maccarinelli et al., 2005; van der Velde et al., 2012). One of the major functions of acyl ghrelin is the stimulation of growth hormone release (Kojima et al., 1999). Growth hormone is released in a pulsatile manner under the influence of environmental and physiological changes (Sattler, 2013). A current investigation carried out by Professor Chen Chen's laboratory (University of Queensland) has shown that the pulsatile growth hormone levels of GOAT$^{-/-}$ mice aged 8 weeks are reduced compared to WT (Jeffery, P., personal communication). Growth hormone is a direct and indirect regulator of bone metabolism (Cannata et al., 2010; Giustina et al., 2008; Morel et al., 1993; Wit & Camacho-Hubner, 2011). Reduced pulsatile GH may reduce the pulsatility of other hormones necessary for bone metabolism, such as IGF-1 (Morel et al., 1993). As GH also acts directly on bone to regulate bone metabolism (Cannata, Vijayakumar, Fierz, & LeRoith, 2010), the long-term effect of reduced GH pulsatility might be related to the microarchitectural differences observed in the GOAT$^{-/-}$ mice, especially at 6 months of age in this study.

In conclusion, this study demonstrates that the trabecular bone microarchitecture of bone of GOAT$^{-/-}$ mice aged 6 months has a decreased bone volume fraction as a result of decreased trabecular connectivity, indicating that acyl ghrelin is involved in the regulation of physiological bone remodelling by affecting the micro-structural properties of trabecular bone.. Reduced connectivity density may be a result of increased osteoclast activity due to the lack of acyl ghrelin signalling as reported with $GHSR^{-/-}$ mice (van der Velde et al., 2012).

The mid-diaphyses of the femora and tibiae of cortical bone of 6 month old $GOAT^{-/-}$ mice have increased mineralisation indicating that acyl ghrelin signalling may negatively regulate cortical bone mineralisation. The unaffected periosteal perimeters and reduced endosteal perimeters in the $GOAT^{-/-}$ mice aged 6 months, indicate that osteoclast activity may be reduced. The geometric property providing resistance to fracture by torsion (pMOI) is reduced in the tibiae at an ealier age compared to the femora in the $GOAT^{-/-}$ mice. These results suggest that acyl ghrelin signalling modulates cortical bone metabolism, and tibial cortical bone is affected earlier than femora. The results also indicate that cellular activity is regulated differently during bone remodelling in the trabecular bone compared to bone modelling in the cortical bone.

Chapter 4

Expression of GHSR1a and GHR in chondrocytes of first trimester human fetal skeletons and mouse embryos

4.1 Introduction

Bone formation during embryological development, juvenile growth and bone repair may occur via intramembranous ossification or endochondral ossification, or a combination of both (Cohen, 2006). The main difference between the two processes is that in endochondral ossification, a cartilage model is first formed which is then replaced by new bone tissue, whereas in intramembranous ossification in the embryo, bone is formed directly from mesenchyme without the intermediate cartilage model (Cohen, 2006; Mackie et al., 2008; Olsen et al., 2000; Tuan, 2004). In endochondral ossification the behaviour of chondrocytes in the cartilage template is under the influence of a complex network of interactions between systemic and local endogenous signals such as growth hormone, insulin like growth factor-1, bone morphogenetic protein, fibroblast growth factors, thyroid hormone and parathyroid hormone (Mackie et al., 2008; Tuan, 2004).

Ghrelin has been reported to be expressed by chondrocytes (Caminos et al., 2005). Ghrelin (at the peptide level and mRNA transcript level) are expressed in mouse immortalised chondrocyte cell line (ATDC-5), juvenile human immortalised chondrocyte cell lines (T/C-28a2, C-20/A4 and C-28/I2) and rat epiphyseal growth plate chondrocytes (fetal and postnatal rats aged 1 day, 15 days and 25 days) (Caminos et al., 2005). The octanoylating enzyme, GOAT, is also expressed by cultured primary human chondrocytes (human articular cartilage derived), human immortalised chondrocyte cell lines (T/C-28a2 and C-28/I2) and immortalised mouse chondrocytes (ATDC-5) (Gomez et al., 2009). Although these reports indicate that acylated ghrelin is synthesised and secreted by chondrocytes, the study (Caminos et al., 2005) failed to identify GHSR1a mRNA in chondrocytes of the rat epiphyseal growth plates (fetal and postnatal rats aged 1 day, 15 days and 25 days) and human immortalised chondrocyte cell lines (T/C-28a2, C-20/A4 and C-28/I2). The analysis of ^{125}-I ghrelin binding on human immortalised chondrocytes (T/C-28a2) however, suggested presence of alternative ghrelin binding receptors (Caminos et al., 2005). Ghrelin treatment also increased cAMP production and inhibited chondrocyte metabolic activity in human (T/C-28a2) and mouse (ATDC-5) immortalised chondrocytes (Caminos et al., 2005). These reports indicate that chondrocytes produce acylated ghrelin to signal through alternative receptors and modulate chondrocyte metabolism in the cartilage template for endochondral ossification. The failure to detect GHSR1a in chondrocytes is challenged by data on Geo Profiles in NCBI showing that human osteoarthritic chondrocytes in monolayer and matrix cultures express GHSR (http://www.ncbi.nlm.nih.gov/geoprofiles/67009914). These differences in results could be attributed to the different origins of the chondrocytes as well as detection methods. . Human fetal tissues including pancreas (Chanoine & Wong, 2004) and lung (Volante et al., 2002) express ghrelin and the GHSR1a, however, a major gap in the literature has been the lack of studies examining ghrelin and GHSR1a expression in human fetal chondrocytes.

The growth hormone receptor (GHR) is expressed by chondrocytes of the costal cartilage of human fetuses in the second trimester and in infants between 3 and 8 months (Werther, Haynes, Edmonson, et al., 1993; Werther, Haynes, & Waters, 1993; Werther et al., 1990) indicating a direct action of growth hormone (GH) in chondrification in human fetal development. The expression of the GHR has not been studied in human fetal skeletal sites of endochondral bone development such as vertebrae, and bones of upper and lower limbs, which may indicate whether GHR expression is widespread in the chondrocytes of the human fetal skeleton or just specific to the costal cartilage region. Furthermore, there have been no reports of the expression of the GHR in chondrocytes of the cartilage templates of the first trimester of human fetal skeletal development.

The aim of this study was to investigate the expression of ghrelin, GHSR1a and GHR proteins in chondrocytes of first trimester human fetal primordial vertebrae, and the cartilage templates of the bones of the upper and lower limbs by immunohistochemistry. In addition, this study aimed to compare the expression of GHSR1a and GHR in chondrocytes of the cartilage templates of the first trimester human fetal skeleton cartilage templates to the chondrocytes of the cartilage templates of the mouse fetal skeleton.

4.2 Methods

This study was carried out as detailed in Chapter 2 sections 2.5, 2.5.1 and 2.5.2. In brief, human fetal upper limbs, lower limbs and vertebral columns were harvested, fixed, processed, embedded and sectioned. The sections (n=5) of each tissue were immunostained for ghrelin, GHSR1a and GHR, using primary antibodies that have previously been validated using murine knockout tissues (Shin, et al., 2010; Fung, et al., 2013). Chondrocyte morphology was determined on separate safranin O fast green stained sections to identify the chondrocytes on the immunostained sections. Mouse embryos aged E14.5, E16.5 and E18.5 were fixed, processed, embedded and sectioned. Sections (n=5) of each tissue were immunostained in a similar manner to the human tissue sections for the expression of GHSR1a and GHR. Sections were visualised under light microscopy and one section from each tissue was imaged for presentation.

4.3 Results

4.3.1 Morphology of the cartilage templates

In order to identify the morphology of chondrocytes in cartilage templates, sections of human fetal vertebral column (Figure 4.3-1A), upper limb (Figure 4.3-1B) and lower limb (Figure 4.3-1C) were stained with safranin O fast green. The stained sections demonstrated the presence of proteoglycan-rich cartilage templates (stained pink) for endochondral bone formation. The chondrocytes were present in small cavities (lacunae) and were recognised as resting, proliferating or mature hypertrophic chondrocytes, based on their morphology. Resting chondrocytes were small individual cells present in lacunae, where more than one cell was present in a single lacuna these cells were characterising as proliferating cells and mature hypertrophic chondrocytes were characterised as gigantic cells present in swollen lacunae. The chondrocytes appeared to be arranged in distinct zones, particularly in the upper limb (Figure 4.3-1B) and lower limb (Figure 4.3-1C).

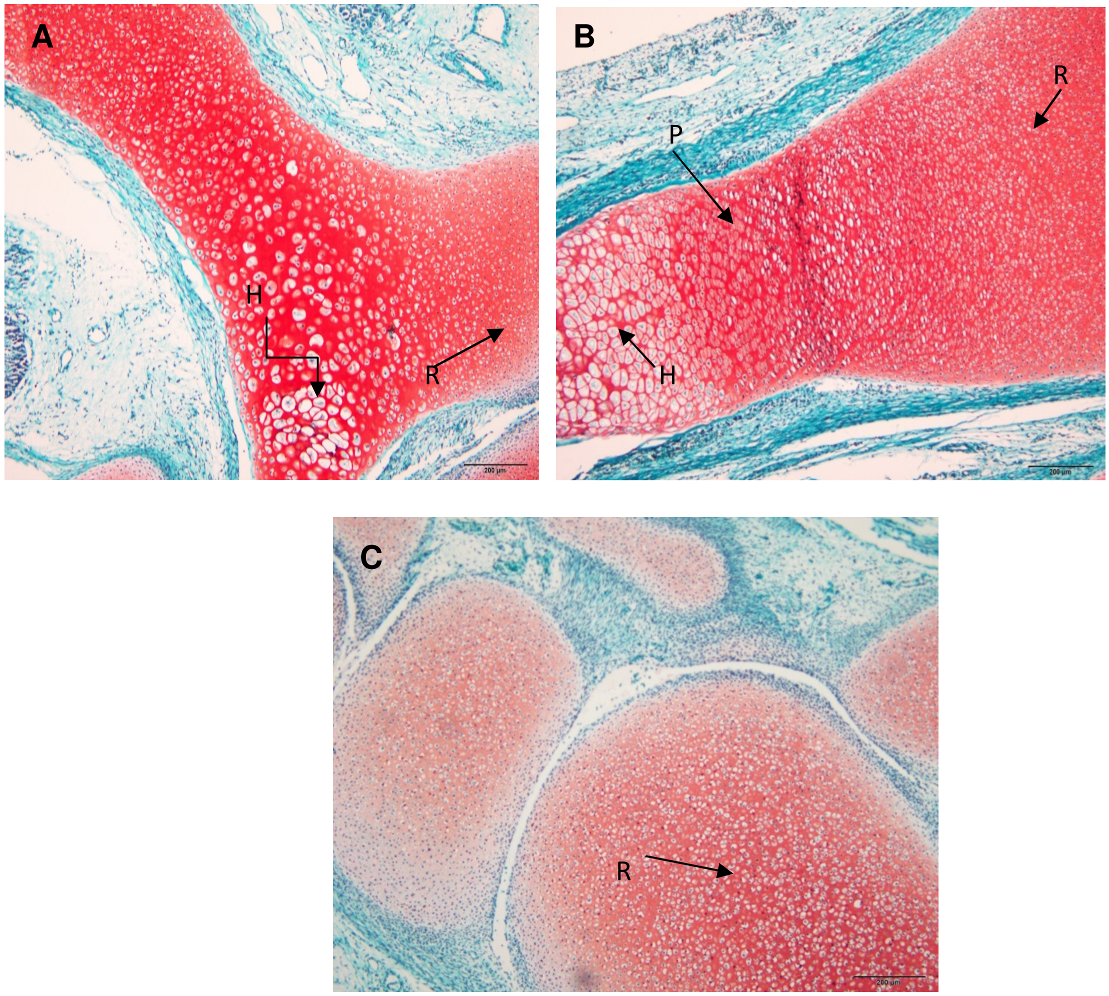

Figure 4.3-1: Human fetal tissues (7-10 weeks gestational age) vertebrae (A), upper limb (B) and lower limb (C) sectioned longitudinally and stained with safranin O fast green, magnification (100x), scale bar=500µm. Red stained tissue indicates cartilage (safranin O binding to proteoglycans) and green stained tissue indicates fibrous connective tissues. Note that three cellular zones based on morphological characteristics were present in each cartilage template (i) resting chondrocytes are indicated by R (seen as small individual cells in lacuna), (ii) proliferating chondrocytes are indicated by P (multiple cells in a single lacuna) and (iii) H indicates mature hypertrophic chondrocytes (enlarged giant sized cells in swollen lacuna).

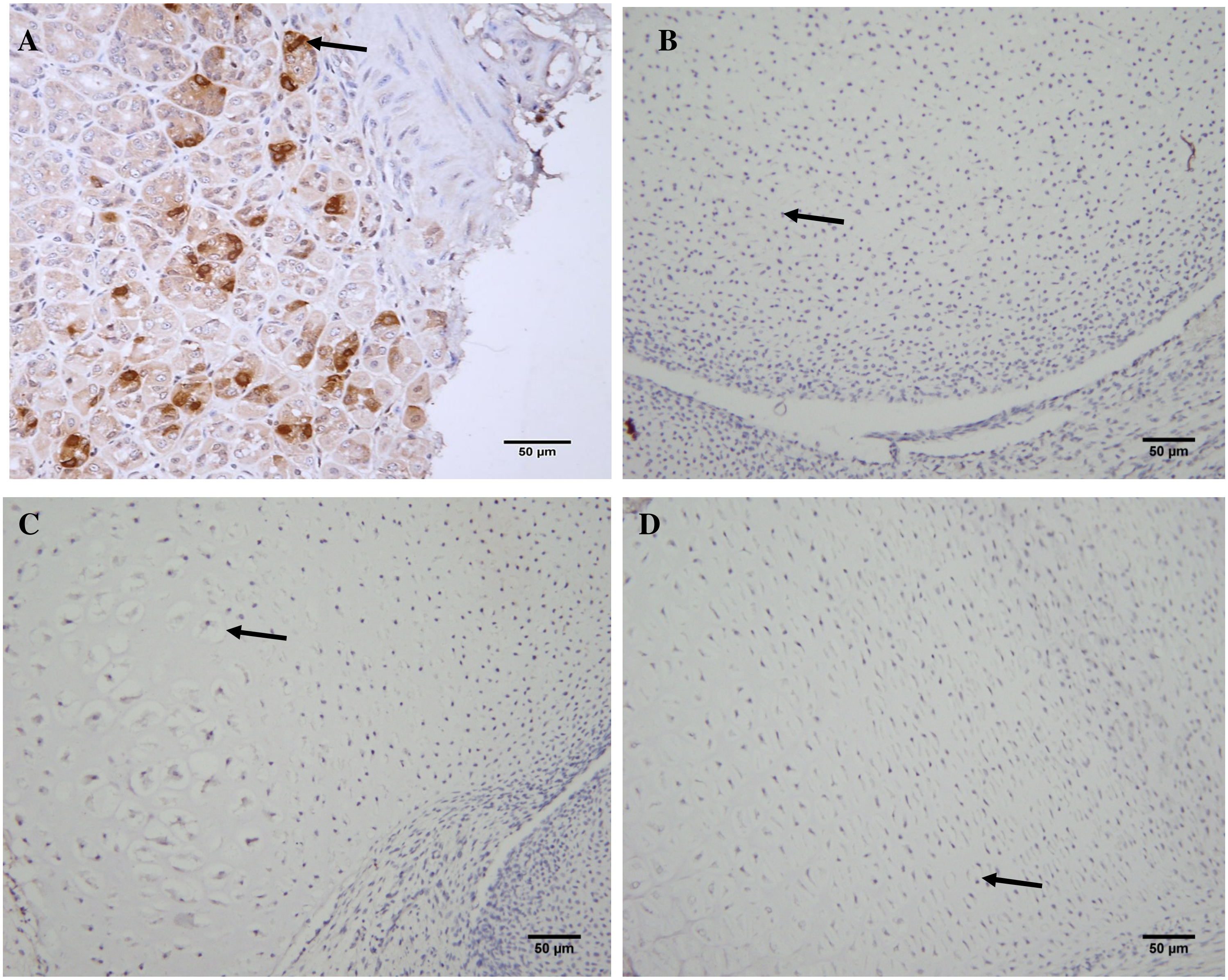

Figure 4.3-2: Immunostaining for ghrelin expression in human tissues with rabbit polyclonal anti-ghrelin antibody (Phoenix Pharmaceuticals Inc., H-031-31). Strong ghrelin immunoreactivity was present in the enteroendocrine cells of the positive control tissue (A), human adult stomach (arrow; 400x). Ghrelin expression was not detected in human fetal (10-12 weeks) chondrocytes of the (B) lower limb (200x, arrow indicates resting chondrocyte) or upper limb. Similarly, (C) vertebral chondrocytes were non-immunoreactive for ghrelin (200x, arrow indicates hypertrophic chondrocyte). Negative controls included non-specific rabbit IgG on (D) upper limb (200x, arrow indicates proliferating chondrocyte) and omission of primary antibody. Scale bars are as shown.

4.3.2 Expression of ghrelin, GHSR1a and GHR in human fetal cartilage

Ghrelin immunoreactivity was not detectable in chondrocytes of first trimester human fetal tissue sections of the vertebral column (Figure 4.3-2C), upper limb (data not shown) and lower limb (Figure 4.3-2B). Positive control sections of human adult stomach immunostained for ghrelin expression demonstrated positive immunoreactivity with enteroendocrine ghrelin expressing cells indicating that the rabbit polyclonal anti-ghrelin antibody (Phoenix Pharmaceuticals Inc., H-031-31) detected ghrelin. Negative control sections of human fetal upper limb immunostained with non-specific rabbit IgG (Figure 4.3-2D) showed no immunoreactivity with the tissue sections, indicating that the primary antibodies which were raised in rabbits did not immunoreact non-specifically with the tissue sections.

Chondrocytes of the human fetal tissues were immunoreactive for GHSR1a. Human fetal tissue sections of vertebrae (Figure 4.3-3A and 4.3-3B), upper limb (Figure 4.3-3C) and lower limb (Figure 4.3-3D) immunostained for GHSR1a showed immunoreactivity with proliferating and hypertrophic chondrocytes of the cartilage templates. A lipid raft staining pattern was observed in the immunoreactive cells (Figure 4.3-2A). Immunoreactivity was not observed in resting chondrocytes of the cartilage templates. Positive control sections of mouse brain immunostained for GHSR1a expression demonstrated positive immunoreactivity with GHSR1a expressing cells indicating that the goat polyclonal anti-GHSR1a antibody (Santa Cruz Biotechnology, F-16) detected GHSR1a (data not shown). Negative control sections of human fetal upper limb immunostained with non-specific goat IgG (Figure 4.3-3 insert C) showed no immunoreactivity with the tissue sections indicating that the primary antibodies which were raised in goats did not immunoreact non-specifically with the tissue sections.

GHR immunoreactivity was not detected in chondrocytes of first trimester human fetal tissues. Human fetal tissue sections of vertebrae (data not shown), upper limb (data not shown) and lower limb (Figure 4.3-4D) immunostained for GHR expression did not show immunoreactivity with chondrocytes of the cartilage templates. Positive control

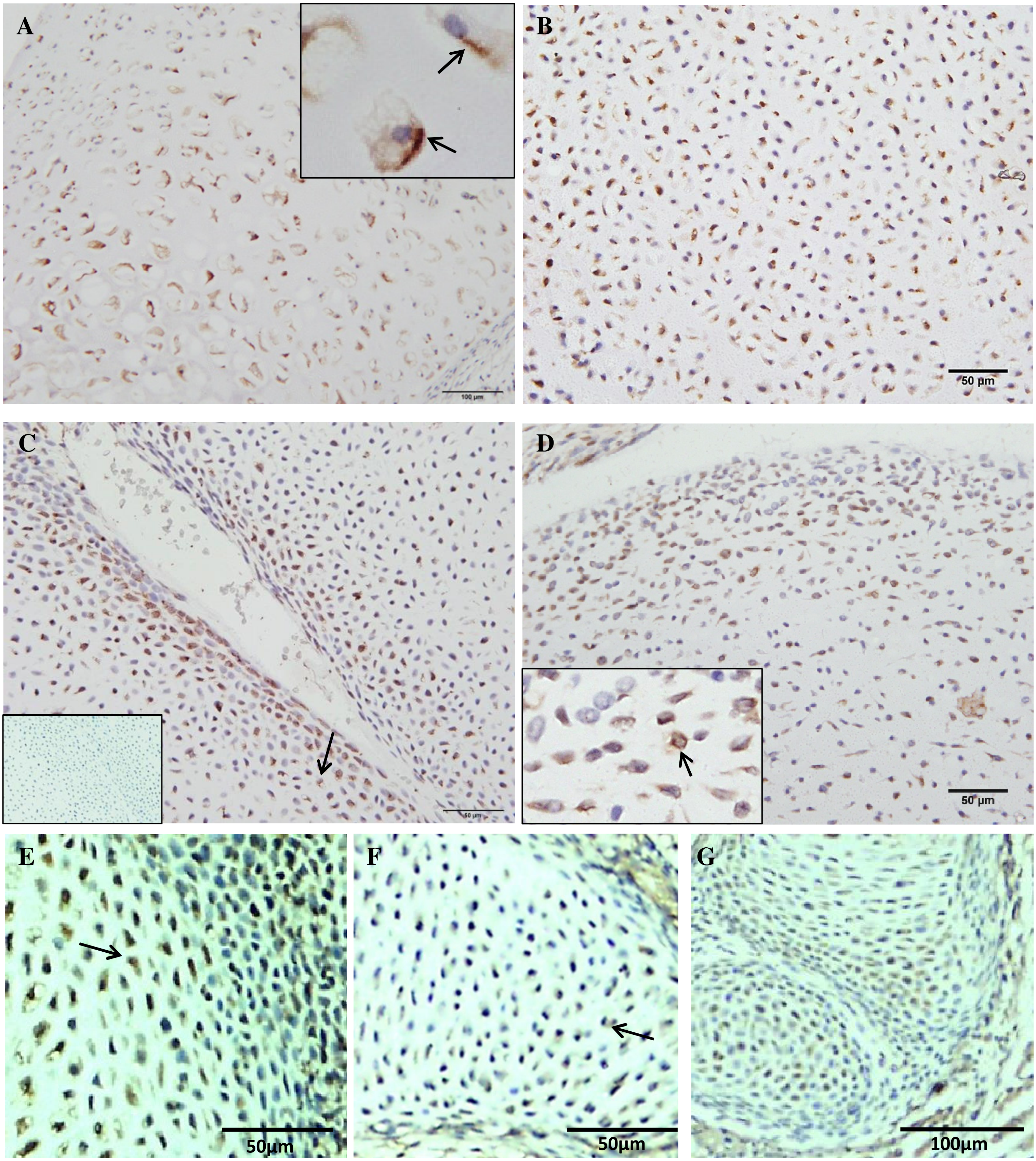
A
B
50 µm
C
D
50 µm
E
50µm
F
50µm
G
100µm

Figure 4.3-3: Human and murine fetal cartilage immunostained with goat polyclonal anti-GHSR1a antibody (Santa Cruz Biotechnology, F-16). GHSR1a is expressed in the hypertrophic chondrocytes of human fetal (10-12 weeks gestational age) vertebrae (A, 200x, scalebar= 500µm); insert shows a higher power image of A showing a lipid raft staining pattern (arrow) in some GHSR1a-positive chondrocytes (600x). (B) GHSR1a immunoreactivity in proliferating chondrocytes of fetal vertebrae (400x, scalebar= 50µm) and the hypertrophic chondrocytes of the (C) upper limb (arrow indicates hypertrophic region; 400x, scalebar= 50µm). Non-specific goat IgG negative control was non-immunoreactive in the upper limb (insert; C). (D) The proliferative chondrocyte zone of the fetal knee was positive for GHSR1a expression (400x, scalebar= 50µm); not all cells are immunoreactive (insert; arrow indicates GHSR1a expressing cell). (E) Mouse embryo chondrocytes (E14.5) showed immunoreactivity for GHSR1a (400x, scalebar= 50µm) as do (F) E16.5 chondrocytes (400x, scalebar= 50µm) and (G) E18.5 chondrocytes (20x, scalebar= 50µm).

sections of mouse liver immunostained for GHR expression demonstrated positive immunoreactivity with GHR expressing cells indicating that the rabbit polyclonal growth hormone receptor antibody (Santa Cruz Biotechnology, H-300) detected GHR (Figure 4.3-4A). Negative control sections of human fetal upper limb immunostained with non-specific rabbit IgG (Figure 4.3-2D) showed no immunoreactivity with the tissue sections indicating that the primary antibodies which were raised in rabbits did not immunoreact non-specifically with the tissue sections.

4.2.3 Expression of GHSR1a and GHR in mouse fetal cartilage

GHSR1a immunoreactivity was detected in mouse fetal chondrocytes. E14.5 (Figure 4.2.3E), E16.5 (Figure 4.2.3F) and E18.5 (Figure 4.2.3G) mouse fetal tissue sections immunostained for GHSR1a expression showed immunoreactivity with proliferating and hypertrophic chondrocytes of the cartilage templates. Immunoreactivity for GHSR1a was not observed in resting chondrocytes of the cartilage templates.

GHR expression was detected in mouse fetal chondrocytes. E14.5 (Figure 4.2.4B and Figure 4.2.4C), E16.5 (data not shown) and E18.5 (data not shown) mouse fetal tissue sections immunostained for GHR expression showed immunoreactivity with proliferating and hypertrophic chondrocytes of the cartilage templates. Immunoreactivity was not observed in resting chondrocytes of the cartilage templates.

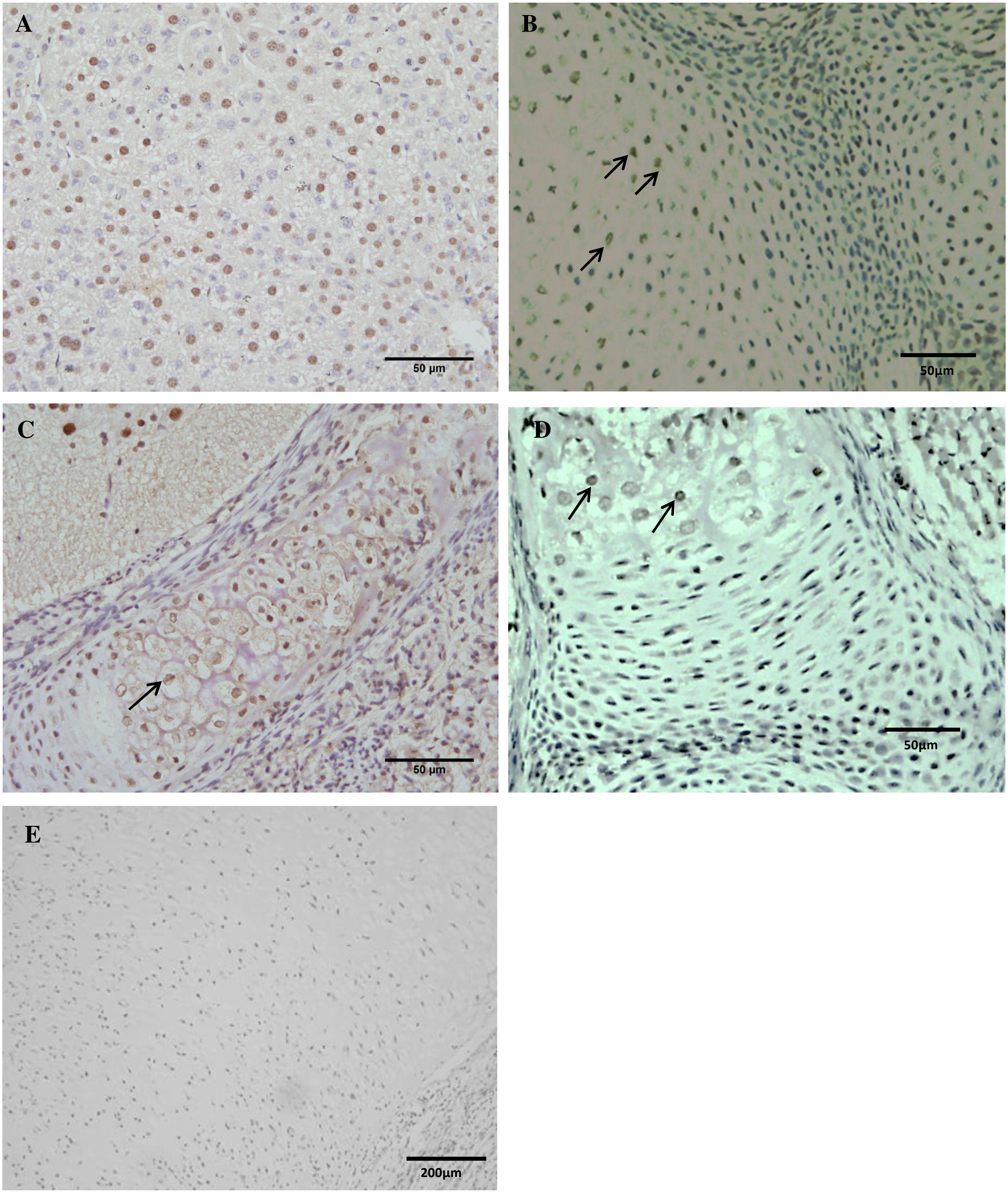
A
50 µm
B
50µm
C
50 µm
D
50µm
E
200µm

Figure 4.2-4: Murine and human fetal cartilage immunostained with rabbit polyclonal growth hormone receptor (GHR) antibody (Santa Cruz Biotechnology, H-300). (A) GHR is expressed in the nucleus of adult mouse liver hepatocytes (positive control; 400x). E14.5 mouse chondrocytes demonstrating immunoreactivity for GHR in hypertrophic chondrocytes (B, 400x), (C) GHR is also expressed in the chondrocytes of the mouse embryo E16.5 (400x), GHR in hypertrophic chondrocytes (arrow). (D) Hypertrophic chondrocytes of mouse embryo (E18.5) stained for GHR (arrows; 400x) Human fetal (10-12 weeks gestational age) lower limb chondrocytes (E) did not express GHR (200x). Scale bars are as shown.

4.3 Discussion

This study demonstrates for the first time that GHSR1a is expressed by chondrocytes of the cartilage templates of vertebrae, and primitive upper and lower limbs of first trimester human fetal skeletons and the cartilage templates of mouse embryo/fetuses aged 14.5, 16.5 and 18.5 days post-conception. This finding contradicts the conclusion by Caminos et al., (2005), which failed to detect GHSR1a in rat and human immortalised chondrocytes by RT-PCR and concluded that GHSR1a is not expressed by chondrocytes. In addition to immunohistochemical identification of GHSR1a, we have identified GHSR1a mRNA transcript expression using quantitative RT-PCR in chondrocytes which have been differentiated from human fetal mesenchymal stem cells (personal communication, P Jeffery). In the present study the antibody that was used to detect GHSR1a has been validated and does not show non-specific binding in GHSR knockout mouse tissues (Shin et al., 2010) or GHSR knockout human cells (Fung et al., 2013). We have also demonstrated that this antibody specifically detect GHSR1a in mouse brain. GHSR1a expression may also be species or cell type specific, as this study shows the expression of GHSR1a in chondrocytes of human and mouse. In contrast, Caminos et al., (2005) investigated expression in rat chondrocytes and immortalised human chondrocytes. We detected GHSR1a in cells showing morphological features of proliferation and hypertrophy, and expression was not seen in resting chondrocytes. The different cartilage cell types should be confirmed, however, using immunohistochemical markers such as SOX-9, Col2a and Agc1. Chondrocyte proliferation and maturation are the two drivers of cartilage tissue elongation (Mills, 2012).This suggest that GHSR1a activation may be responsible for chondrocyte proliferation and maturation in the cartilage templates that may result in cartilage growth. Hypertrophic chondrocytes synthesise vascular endothelial growth factors, and therefore could allow the invasion of blood vessels (Ferrara, et al., 2003). Blood vessel infiltration facilitates the degradation of the cartilage matrix by circulating osteoclasts and subsequent ossification (Karsenty, 1999). Therefore, expression of GHSR1a in hypertrophic chondrocytes suggests that GHSR1a activation may lead to endochondral ossification in addition to cartilage growth.

The endogenous ligand for GHSR1a is acylated ghrelin (Kojima et al., 1999), however, ghrelin expression was not detected in the chondrocytes in vertebrae and primitive upper and lower limbs of the human fetal tissues. Unlike Caminos et al., 2005, we could not detect ghrelin expression by the chondrocytes of the human fetal cartilage templates. This may be because of the different antibodies used for the different studies, but also may be because we investigated human chondrocytes whereas Caminos, et al., 2005 investigated rat chondrocytes. This suggests that an autocrine/paracrine ghrelin signalling pathway may be absent in human fetal cartilage templates. Ghrelin, however, is produced by fetal tissues (and the main source is the pancreas at this stage of development) (Chanoine & Wong, 2004; Wierup, Svensson, Mulder, & Sundler, 2002) and maternal ghrelin crosses the placenta (Nakahara et al., 2006) to be present in abundance to activate GHSR1a in chondrocytes by endocrine signalling. GHSR1a is a constitutively active receptor (Holst et al., 2003), therefore, GHSR1a may have a constitutive and ligand stimulated activity in chondrocytes.

Furthermore, most chondrocytes displayed a lipid raft staining pattern. Lipid rafts are plasma membrane micro-domains that are implicated in the assembly of diverse signalling pathways such as those mediated by growth factors (Simons and Toombre, 2000). The aggregated GHSR1a staining pattern that was observed in a small region of the chondrocyte, is characteristic of a lipid raft (Gupta and DeFranco, 2003) and indicates that GHSR1a may be activated and signal transduction is occurring. Caminos et al., (2005) showed that ghrelin treatment increased cAMP production and inhibited chondrocyte metabolic activity in human (T/C-28a2) and mouse (ATDC-5) immortalised chondrocytes, which do not express GHSR1a (Caminos et al., 2005). GHSR1a activation may lead to similar observations in human and mouse chondrocytes, however, further investigation is required to confirm the role of GHSR1a activation in human and mouse chondrocytes.

A direct action of GH on human fetal chondrocytes has been indicated due to the expression of GHR in second trimester human fetal chondrocytes (Werther, Haynes, Edmonson, et al., 1993; Werther, Haynes, & Waters, 1993; Werther et al., 1990). A major function of ghrelin is the stimulation of GH release. Therefore, this study investigated GHR expression in the first trimester human fetal chondrocytes. This study showed that GHR is not expressed by chondrocytes of the first trimester human fetal upper limbs, lower limbs and vertebrae, however, GHR is expressed by proliferating and mature chondrocytes of mouse fetuses aged 14.5, 16.5 and 18.5 days post-conception. Previous studies have shown that GHR is expressed by human fetal chondrocytes in the second trimester of pregnancy (Werther, Haynes, Edmonson, et al., 1993; Werther, Haynes, & Waters, 1993; Werther et al., 1990). Therefore, GHR may not be expressed until the second trimester of gestation. The standardised system of classifying the stages of gestation in the mouse compared to the human is the Carnegie system, however, this system only classifies the embryonic stage and is divided into 23 stages, which corresponds to day 58 post conception (stage 23) in humans (O'Rahilly & Müller, 1897) and 16 days post conception (stage 23) in mice (day 58 corresponding to mouse day 16 post-conception). Similarly, the Theiler and the Downs and Davies stages classification systems reflect how far the human and mouse embryos have progressed in their development (Downs & Davies, 1993; Goryanin & Goryachev, 2012). There is no classification system that relates the trimesters or stages of skeletal development and ossification of human gestation to mouse. The mouse fetuses used in this project were at late stages of pregnancy (E14.5, E16.5 and E18.5), and therefore GHR and GHSR1a expression may not be comparable to human chondrocytes of the first trimester. In addition, expression is likely to be species-specific. Identification of signalling receptors, and elucidating their function and mechanism of action, provides opportunities for therapeutic targeting. This study has shown that GHSR1a is expressed by human fetal chondrocytes in the first trimester of human pregnancy, a stage at which GHR is not expressed. This provides an opportunity to investigate therapeutical targeting of GHSR1a, such as down-regulation with inverse agonists or stimulation with ghrelin mimetics, for disorders of skeletal development, such as skeletal dysplasias in animal models.

In conclusion, this study has shown for the first time that GHSR1a is expressed by first trimester human fetal chondrocytes and mouse embryo/ fetal chondrocytes. Furthermore, we have shown that human fetal chondrocytes in the first trimester of pregnancy do not express ghrelin and GHR, indicating that an autocrine/ paracrine signalling pathway through GHSR1a may be absent. Direct growth hormone signalling is not involved in the modulation of behaviour of chondrocytes of first trimester cartilage templates.

Chapter 5

General Discussion and Future Directions

5.1 Discussion and future directions: characterisation of the bone micro-architecture of GOAT$^{-/-}$ mice.

The ghrelin axis appears to have direct and indirect regulatory effects on the bone and cartilage microenvironments (Caminos, et al., 2005; Delhanty, et al., 2013; Fukushima, et al., 2005; Kim, et al., 2005; van der Velde, et al., 2012). Positive correlations have been observed between ghrelin levels and bone mineral density (BMD) in several human populations ((Amini et al., 2013; Misra et al., 2005; Napoli et al., 2011; Nouh et al., 2012; Oh et al., 2005; Weiss et al., 2006), and administration of ghrelin increases BMD in rodents (Fukushima, et al., 2005). Ghrelin receptor (GHSR1a) knockout (GHSR$^{-/-}$) mice have shown significantly weaker bone micro-architectures with ageing due to increased osteoclast activity (van der Velde, et al., 2012). As GHSR1a only partly mediates acyl ghrelin signalling, the first part of this project characterised the 3D bone microarchitecture of adult GOAT$^{-/-}$ mice, which do not produce the acylated form of ghrelin. This was done in order to confirm whether acyl ghrelin signalling is critical for age-related maintainence of bone microarchitecture. This study demonstrated that the trabecular bone microarchitecture of GOAT$^{-/-}$ mice aged 6 months has a decreased bone volume fraction as a result of decreased trabecular connectivity. No difference in BMD was observed, indicating that acyl ghrelin is involved in the regulation of physiological bone remodelling affecting the trabecular microarchitecture. Reduced connectivity density may be a result of increased osteoclast activity due to the lack of acyl ghrelin signalling as reported with GHSR$^{-/-}$ mice (van der Velde et al., 2012). Due to time constraints and technical limitations, we could not reliably measure osteoclast numbers on the trabecular bone surface. Therefore, as a future direction, it is recommended that the resorption pits on the trabecular bone surface on 2D resin sections of the GOAT$^{-/-}$ and WT mice are measured, to determine whether osteoclast activity is affected by the lack of acyl ghrelin.

The mid-diaphyses of the femora and tibiae of cortical bone of 6 month old GOAT$^{-/-}$ mice had increased mineralisation indicating that acyl ghrelin signalling may negatively regulate cortical bone mineralisation. The periosteal perimeters were unaffected and endosteal perimeters were reduced in the GOAT$^{-/-}$ mice aged 6 months, indicating that osteoclast activity may be reduced. Further work is needed to evaluate osteoclast activity through the measurement of resorption pits, in the endosteal perimeter of femora and tibiae of GOAT$^{-/-}$ and WT mice. This will provide information on how osteoclast activity during bone modelling is affected by the lack of acyl ghrelin signalling. The geometric property providing resistance to fracture by torsion (pMOI) was reduced in the tibiae at an earlier age compared to the femora in the GOAT$^{-/-}$ mice. The results suggested that acyl ghrelin signalling modulates cortical bone metabolism, and tibial cortical bone is affected earlier than femora. The results also indicated that cellular activity is regulated differently during bone remodelling in the trabecular bone compared to bone modelling in the cortical bone. As remodelling is a tightly coupled activity between osteoclasts and osteoblasts (Sebba, 2013), we also recommend evaluating osteoblast activity on the trabecular bone through dynamic histomorphometry. The microarchitecture of the youngest adult GOAT$^{-/-}$ mouse (6 months old) used in this investigation showed a significant differences in trabecular and cortical bone compared to WT mice. Therefore, it would be ideal to investigate whether GOAT KO mice have less bone throughout lifespan or whether they also go through an age-related bone loss, similar to GHSR$^{-/-}$ mice. We recommend further work characterising the microarchitecture of younger GOAT$^{-/-}$ mice, such as neonatal and 8 week old mice.

We also characterised trabecular and cortical bone microarchitectures of 9 and 18 month old GOAT$^{-/-}$ mice, however, the limitation comparing GOAT$^{-/-}$ mice to WT mice was that the GOAT$^{-/-}$ mice were heavier at these ages. potentially due to deranged metabolic activity with age. Alternatively, the greater weights may be a result of the older GOAT$^{-/-}$ mice being maintained with smaller numbers per cage due to their increased susceptibility to stress compared to WT mice (Jeffery, P., personal communication). As increased strain resulting from increased weight causes adaptive bone remodelling and modelling in bone tissue (Ferretti et al., 1993; Frost, 1990b), the differences between 9 and 18 month old GOAT$^{-/-}$ mice and WT mice may have been compromised. If it would be possible to have matched weights of the GOAT$^{-/-}$ to WT in the future, further work may be carried out to investigate the impact of the lack of acyl ghrelin on bone in aged mice. In addition, due to the interaction of acyl ghrelin with other hormones, such as growth hormone, it is also possible that compensatory pathways may exist that may result in indirect effects on the GOAT$^{-/-}$ bones. Although it was attempted in this project to determine the expression of ghrelin, GHSR1a and GOAT in osteoblasts and osteoclasts in the paraffin embedded sections by immunohistochemistry, we could not optimise the protocol. Therefore, further attempts on optimising the protocol may provide information on whether acyl ghrelin acts in an autocrine/paracrine signalling pathway and whether it directly affects osteoblast and osteoclast activity.

5.2: Discussion and future directions: GHSR1a and GHR in chondrocytes

The ghrelin axis has been indicated to play a role in cartilage metabolism. Rat chondrocytes and human immortalised chondrocytes have been shown to express ghrelin, but lack GHSR1a (Caminos, et al., 2005). In this part of the project, we investigated whether ghrelin and GHSR1a is expressed by chondrocytes of the first trimester human fetal skeleton and mouse embryos and fetuses. Immunohistochemistry was performed on sections of first trimester human fetal upper limbs, lower limbs and vertebral columns, and mouse embryos and fetuses aged 14.5, 16.5 and 18.5 days post-conception, for the expression of ghrelin and GHSR1a. Ghrelin immunoreactivity was not seen in the chondrocytes of the first trimester human fetal upper limbs, lower limbs and vertebrae. This suggests that an autocrine/ paracrine ghrelin signalling pathway may be absent in the human cartilage microenvironment, however, ghrelin is expressed by many fetal tissues and maternal ghrelin also crosses the placenta to signal in an endocrine manner. Alternatively, due to very low expression levels, the ghrelin antibody concentration might have been too low to detect ghrelin in the chondrocytes. Therefore, we recommend as a future direction to investigate ghrelin expression in the cartilage templates using higher concentration of the ghrelin primary antibody or using use an anti-ghrelin antibody that is species-specific, and/or investigate an alternative methodology such as Western immunoblot.

Furthermore, due to time constraints with the project it was only possible to perform immunohistochemistry for ghrelin expression on human fetal chondrocytes. Therefore, as a future direction we recommend investigating ghrelin expression by immunohistochemistry on the mouse fetal chondrocytes. GHSR1a immunoreactivity was seen in the chondrocytes of the first trimester human fetal upper limbs, lower limbs and vertebrae, and mouse embryos/ fetuses aged E14.5, E16.5 and E18.5. Immunoreactivity was seen in proliferating and mature hypertrophic chondrocytes, and expression was not seen on resting chondrocytes of human vertebral columns, upper limbs and lower limbs, and mouse embryos/ fetuses. Even though, we identified chondrocytes based on their morphology, we recommend confirming the cells expressing GHSR1a are indeed chondrocytes and their proliferation, differentiation and maturation state, by immunohistochemical investigation using specific markers such as SOX-9, Col2a and Agc1. We recommend a future study to investigate GHSR1a activation by acyl ghrelin in chondrocytes expressing GHSR1a in culture to determine the effect on proliferation and maturation. This will provide information of the role GHSR1a activation may have on chondrocytes and elucidate the function of ghrelin and GHSR1a on cartilage homeostasis.

Furthermore, ghrelin is associated with GH release (Kojima, et al., 1999). GH mediates its function through GHR (DiGirolamo et al., 2007) and GHR has been reported to be expressed by second trimester human fetal chondrocytes (Werther, Haynes, Edmonson, et al., 1993; Werther, Haynes, & Waters, 1993; Werther et al., 1990). Therefore, in this project we further investigated whether GHR is expressed by first trimester human fetal chondrocytes to determine whether ghrelin may be indirectly linked to cartilage metabolism. GHR was not expressed by the first trimester human fetal chondrocytes of the upper limb, lower limb and vertebral column, however, expression was seen in proliferating and mature chondrocytes of mouse embryos/ fetuses. Further investigation is required to determine the degree of skeletal development or stage of chondrification/ossification of limb buds of the human fetuses and mouse embryos/fetuses to relate GHR expression on human fetal chondrocytes to the mouse fetal chondrocytes. Furthermore, mouse embryos at an earlier age could be investigated for GHR expression that may relate to the first trimester human fetus.

In conclusion, this project provides preliminary evidence for a role of the ghrelin axis in bone and cartilage metabolism. This study has shown for the first time that GHSR1a is expressed by first trimester human fetal chondrocytes and mouse embryo/ fetal chondrocytes. Furthermore, we have shown that human fetal chondrocytes in the first trimester of pregnancy do not express ghrelin and GHR, indicating that an autocrine/ paracrine signalling pathway through GHSR1a may be absent. Direct growth hormone signalling is not involved in the modulation of behaviour of chondrocytes of first trimester cartilage templates. This study demonstrates that the trabecular bone microarchitecture of bone of GOAT$^{-/-}$ mice aged 6 months has a decreased bone volume fraction as a result of decreased trabecular connectivity, indicating that acyl ghrelin is involved in the regulation of physiological bone remodelling by affecting the micro-structural properties of trabecular bone.. Reduced connectivity density may be a result of increased osteoclast activity due to the lack of acyl ghrelin signalling as reported with GHSR$^{-/-}$ mice (van der Velde et al., 2012).
The mid-diaphyses of the femora and tibiae of cortical bone of 6 month old GOAT$^{-/-}$ mice have increased mineralisation indicating that acyl ghrelin signalling may negatively regulate cortical bone mineralisation. The unaffected periosteal perimeters and reduced endosteal perimeters in the GOAT$^{-/-}$ mice aged 6 months, indicate that osteoclast activity may be reduced. The geometric property providing resistance to fracture by torsion (pMOI) is reduced in the tibiae at an ealier age compared to the femora in the GOAT$^{-/-}$ mice. These results suggest that acyl ghrelin signalling modulates cortical bone metabolism, and tibial cortical bone is affected earlier than femora. The results also indicate that cellular activity is regulated differently during bone remodelling in the trabecular bone compared to bone modelling in the cortical bone.
This study offers supporting evidence for exciting new research opportunities for the ghrelin axis to be investigated for the treatment and management of a wide range of bone and cartilage related disorders.

Appendix

6.1 Limb lengths of the GOAT$^{-/-}$ and WT mice

The lengths of the femora and tibiae harvested from each mouse aged 6 and 9 months were measured to check whether lack of ghrelin signalling may have any effect on longitudinal growth. The right tibiae of GOAT$^{-/-}$ mice were significantly shorter (p=0.002) than the WT tibiae. The length of the GOAT$^{-/-}$ right tibiae increased significantly with advancing age from 6 to 9 months (p=0.017). The left and right femora did not show any differences between the GOAT$^{-/-}$ mice and WT mice at any ages, neither did the left tibiae (Figure 6.1-1).

6.2 Evaluation of osteoclast activity

Osteoclast numbers on the bone surface of the secondary spongiosa of the left femora and tibiae of GOAT$^{-/-}$ and WT mice aged 6, 9 and 18 months were determined following TRAP staining of paraffin embedded sections, using the Osteomeasure program. The osteoclast number on the bone surface did not show any significant differences at any ages or with advancing age. The sample sizes were uneven for each group, as there were damages to tissue sections during tissue processing and staining. The drawbacks of the measurements were that it was carried out only on 1 section per mouse, the bone volume in the section was not representative of the bone volume measured by micro-CT, the volume of bone and osteoclast numbers varied greatly between each group as a result of the variation in the amount of bone of each section. Therefore, as future work, sections of right femora and tibiae representing the amount of bone determined by micro-CT should be used for evaluating the osteoclast activity.

a)

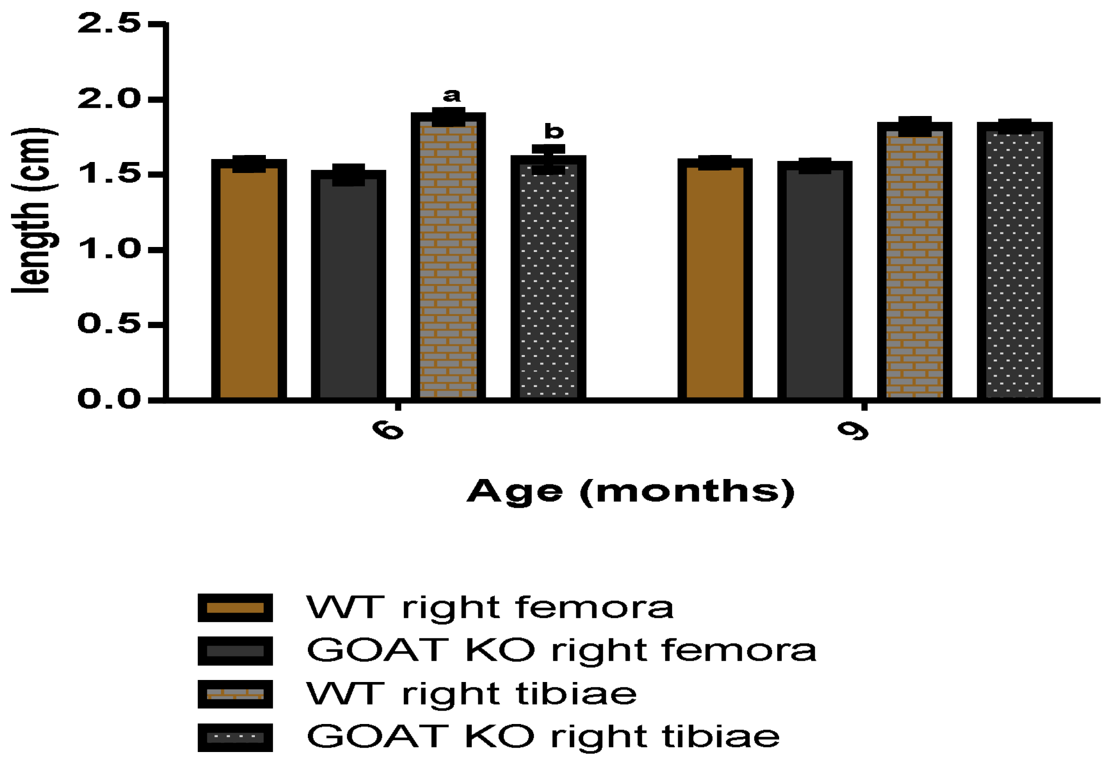

2.5
2.0
1.5
1.0
0.5
0.0
length (cm)
a
b
6
9
Age (months)
WT right femora
GOAT KO right femora
WT right tibiae
GOAT KO right tibiae

b)

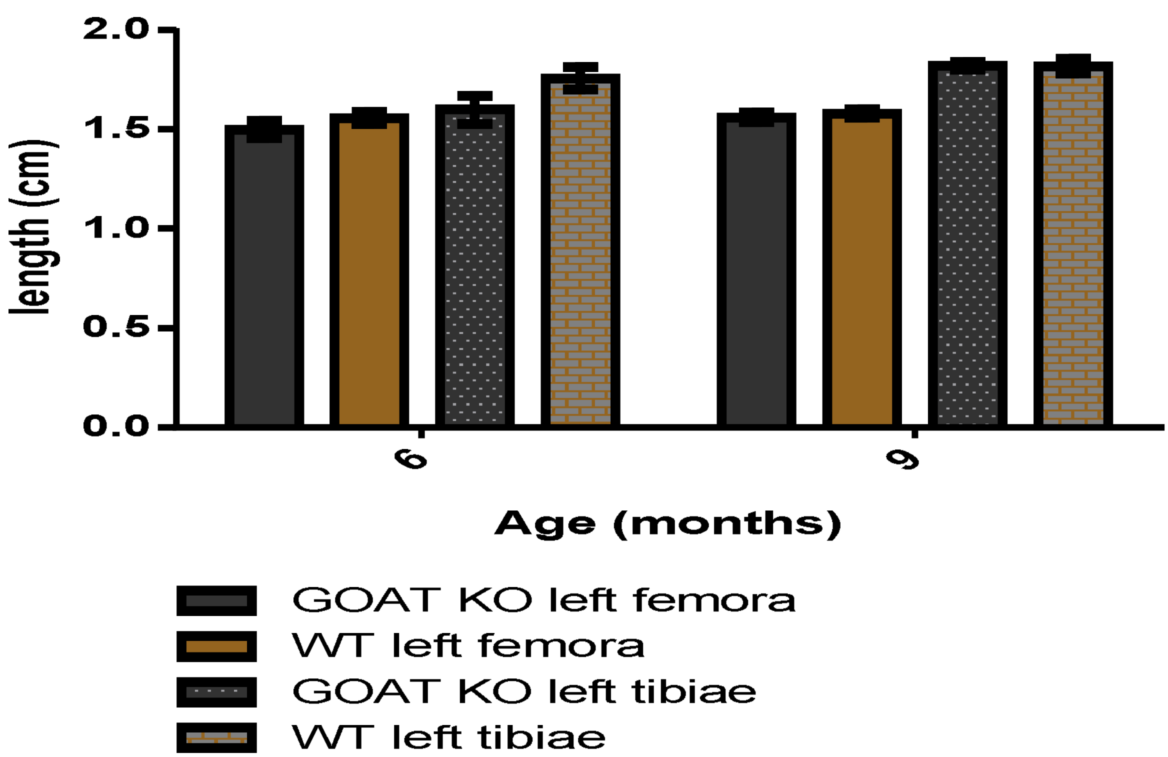

2.0
1.5
1.0
0.5
0.0
length (cm)
6
9
Age (months)
GOAT KO left femora
WT left femora
GOAT KO left tibiae
WT left tibiae

Figure 6.1-1 Lengths of the femora and tibiae of the GOAT$^{-/-}$ and WT mice of the a) right limb and b) left limb. Statistical significance between mean length of GOAT$^{-/-}$ and WTs was determined using independent t tests (GraphPad) and between the ages for each group using one-way ANOVA with Tukey's *post hoc* analysis (GraphPad). Data represented as mean +/- standard error of the mean (SEM); a=p<0.05 compared to GOAT KO right tibiae at 6 months of age, b=p<0.05 compared to GOAT KO right tibiae at 9 months.

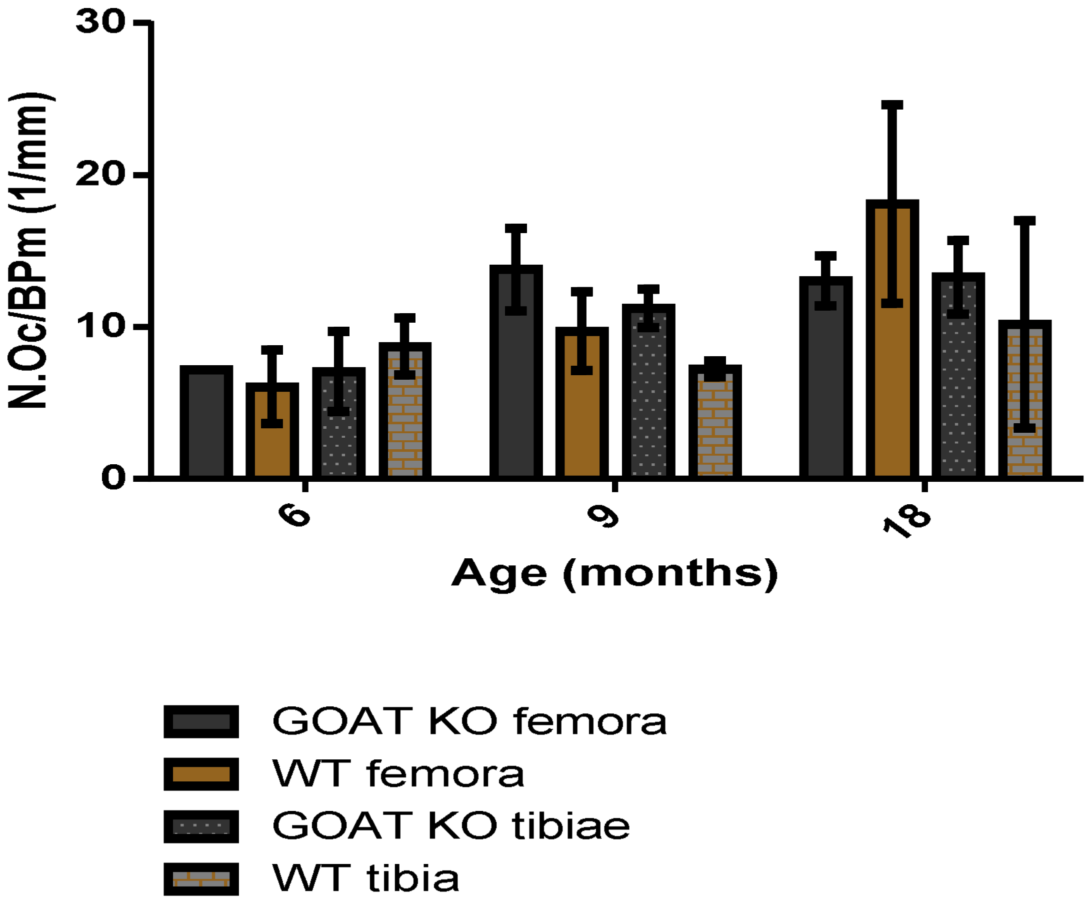

Figure 6.2-1 Osteoclast numbers on the surface of trabecular bone in the secondary spongiosa of the femora and tibiae between GOAT$^{-/-}$ and WT mice aged 6, 9 and 18 months. Osteoclasts were identified as pink stained cells on the surface of trabecular bone and quantified using Osteomeasure. Statistical significance between means of GOAT$^{-/-}$ and WTs was determined using independent Student's t tests (GraphPad) and

between the ages for each group using one-way ANOVA with Tukey's *post hoc* analysis (GraphPad). Data represented as mean +/- standard error of the mean (SEM); The

6.3 Immunohistochemistry for ghrelin, GOAT, GHSR1a, osteocalcin and runx2 in WT neonatal and 8 week old left tibia paraffin embedded sections

Immunohistochemistry was performed for the expression of ghrelin, GOAT, GHSR1a, osteocalcin and runx2 as described in chapter 2, 2.4.1. The primary ghrelin antibody (rabbit polyclonal anti- mouse ghrelin,Phoenix Pharmaceuticals Inc., H-031-31) could not be optimised as it immunoreacted non-specifically with marrow components. Dilutions of 1:100, 1:500 and 1:1000 were tested and all showed same response.

The primary GOAT antibodies (goat anti-human GOAT antibody, Abcam, ab-170690, goat anti-human MBOAT4 antibody, Santa Cruz Biotechnology, sc-98001), were used at dilutions of 1:100, 1:500 and 1:1000. The antibodies immunoreacted with GOAT knockout stomach tissues, indicating the antibodies were non-specific for detecting GOAT.

The primary GHSR1a antibody (goat polyclonal anti-human GHSR1a, Santa Cruz Biotechnology, F-16) bound non-specifically to the marrow components of the neonatal and 8 week old WT sections at concentrations of 1:100, 1:200 and 1:500. The osteocalcin (anti-human osteocalcin, Santa Cruz Biotechnology, sczsc-30044) and runx-2 antibodies (anti-human runx2 antibody, Abcam, ab23981) did not show any immunoreactivity with the sections.

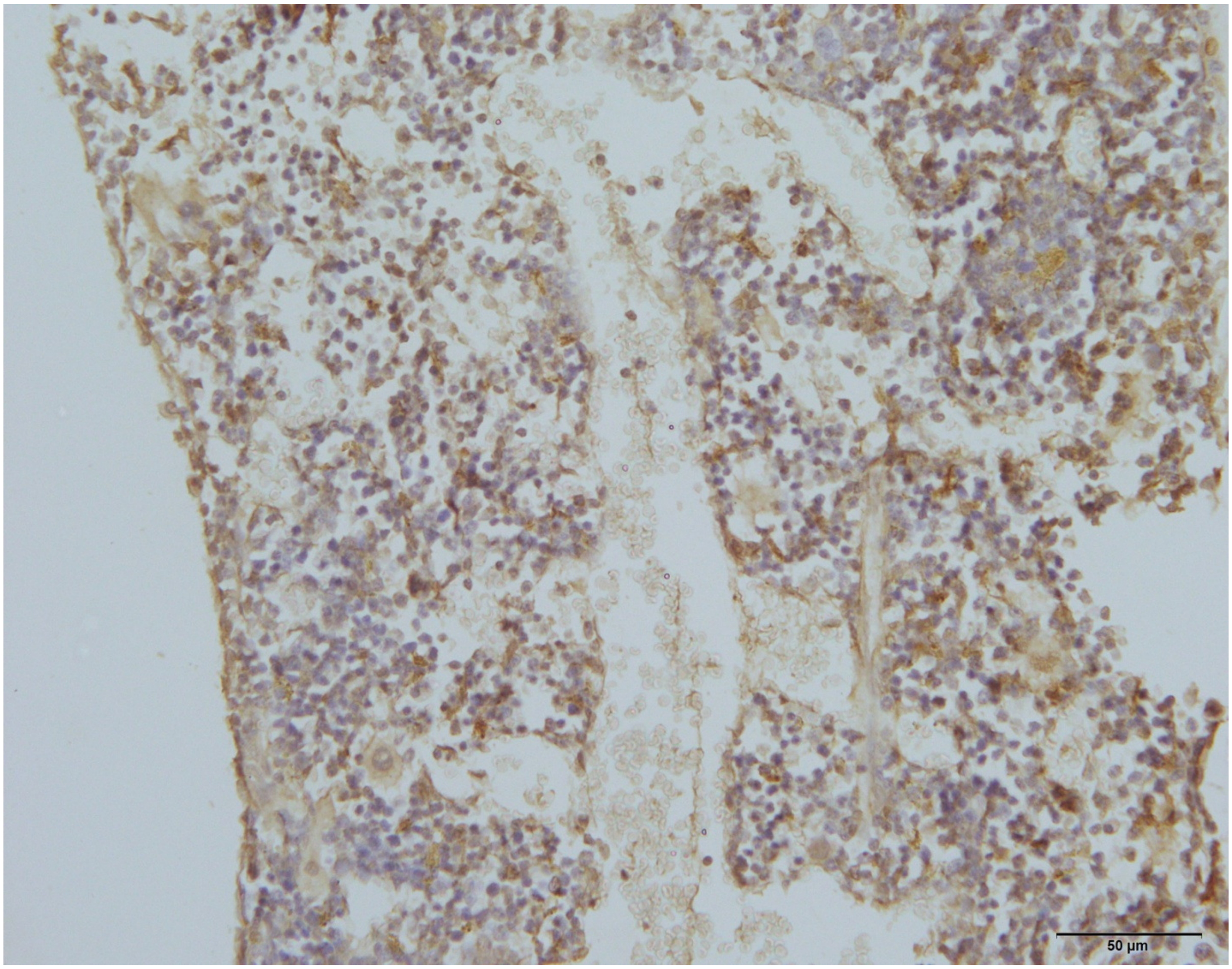

Figure 6.3-1. Neonatal section immunostained for GOAT at 1:1000 (Abcam, ab-170690). Non-specific immunoreactivity, brown staining on non-cellular background of marrow, antibody does not detect GOAT specifically. Magnification= x400, scalebar as shown.

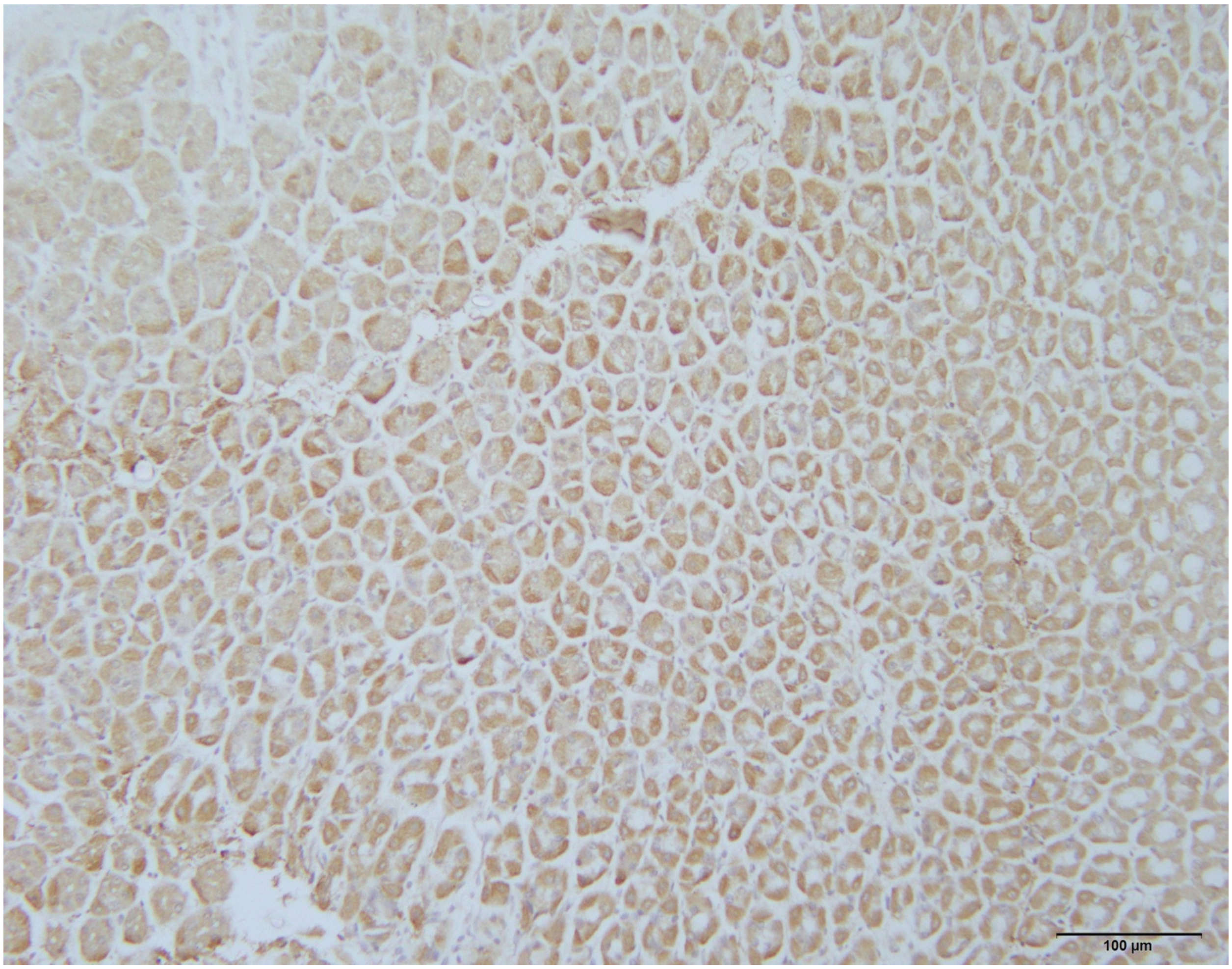

Figure 6.3-2. GOAT$^{-/-}$ mouse stomach section immunostained for GOAT at 1:1000 (Abcam, ab-170690). Brown staining of cells that do not express GOAT. Non-specific immunoreactivity seen. Magnification= x400, scalebar as shown.

6.4 Tables of results

Table 6.4-1: Weights of $GOAT^{-/-}$ and WT mice aged 6, 9 and 18 months. Values given as mean± standard error of mean (SEM), p values determined by Students *t* test.

		Age (months)		
		6	**9**	**18**
Weight (g)	$GOAT^{-/-}$	28.14±2.88	38.76 ±2.28	36.15 ±0.85
	WT	27.47 ±0.58	28.94±0.26	32.3±1.36
	p	0.7709	**0.0027**	**0.0317**

Table 6.4-2: Trabecular micro-architectural indices of the secondary spongiosa of the right distal femoral metaphysis and right proximal tibial metaphysis measured by micro-CT, between the $GOAT^{-/-}$ and WT mice aged 6, 9 and 18 months. Values given as mean± standard error of mean (SEM), p values determined by Students *t* test.

		Age (months)					
		6		**9**		**18**	
Limb		**Femur**	**Tibia**	**Femur**	**Tibia**	**Femur**	**Tibia**
Tb. BMD ($mgHA/cm^3$)	$GOAT^{-/-}$	880.28 ±6.15	879.61 ±16.8	896.92 ±9.82	941.80 ±8.63	921.01± 20.69	941.87± 48.84
	WT	864.05 ±12.58	918.21 ±8.164	877.61 ±11.53	922.21 ±13.73	947.88± 26.86	957.34± 9.95
	p	0.332	**0.100**	0.240	0.295	0.451	0.737
BV/TV (%)	$GOAT^{-/-}$	3.1 ±0.5	1.68 ±0.2	2.76 ±0.4	2.14 ±0.4	1.81 ±0.5	1.38 ±0.2
	WT	6.2 ±0.6	6.3 ±1.2	3.0 ±0.8	2.3 ±0.8	2.3 ±0.9	1.9 ±0.7
	p	**0.005**	**0.007**	0.713	0.903	0.670	0.481
Tb. N (1/mm)	$GOAT^{-/-}$	2.02 ±0.16	1.91 ±0.18	2.02 ±0.11	1.50 ±0.21	1.43 ±0.12	0.96 ±0.12
	WT	2.25 ±0.27	2.13 ±0.351	1.32 ±0.14	1.03 ±0.09	1.46 ±0.18	1.29 ±0.14
	p	0.538	0.634	**0.006**	0.102	0.903	0.140

Tb. Th (mm)	GOAT$^{-/-}$	0.058 ±0.004	0.056 ±0.003	0.053 ±0.002	0.058 ±0.004	0.053 ±0.005	0.056 ±0.001
	WT	0.062 ±0.003	0.059 ±0.002	0.065 ±0.002	0.067 ±0.002	0.067 ±0.003	0.066 ±0.003
	p	0.427	0.391	**0.001**	**0.094**	0.120	0.022
Tb.Sp (mm)	GOAT$^{-/-}$	0.51 ±0.05	0.46 ±0.04	0.49 ±0.02	0.71 ±0.09	0.73 ±0.05	1.09 ±0.11
	WT	0.48 ±0.05	0.53 ±0.06	0.85 ±0.12	1.02 ±0.09	0.72 ±0.10	0.81 ±0.08
	p	0.698	0.468	**0.017**	**0.053**	0.880	0.108
C. Den (1/mm^3)	GOAT$^{-/-}$	6.20 ±0.83	0.85 ±0.34	7.04 ±1.37	2.12 ±0.71	3.58 ±1.36	1.18 ±0.61
	WT	23.06 ±5.89	26.61 ±10.23	7.99 ±2.84	2.35 ±1.78	2.30 ±2.01	2.78 ±1.93
	p	**0.039**	**0.062**	0.757	0.902	0.598	0.411

Table 6.4-3: Cortical micro-architectural indices of the mid-diaphyses of the right femora and right tibia measured by micro-CT and Osteomeasure, between the $GOAT^{-/-}$ and WT mice aged 6, 9 and 18 months. Values given as mean± standard error of mean (SEM), p values determined by Students *t* test.

Age (months)		**6**		**9**		**18**	
Limb		**Femur**	**Tibia**	**Femur**	**Tibia**	**Femur**	**Tibia**
Ct. BMD ($mgHA/cm^3$)	$GOAT^{-/-}$	1208.99 ±17.61	1176.26 ±10.98	1241.22 ±14.33	1175.50 ±5.31	1243.86 ±7.48	1168.62 ±4.56
	WT	1155.15 ±16.33	1116.57 ±22.24	1197.81 ±8.77	1132.45 ±2.55	1238.3 ±16.80	1152.61 ±20.80
	p	**0.055**	**0.042**	**0.046**	**0.0003**	0.733	0.384
Ct.Th (µm)	$GOAT^{-/-}$	240.79 ±15.84	202.17 ±5.66	222.57 ±6.53	202.97 ±3.01	216.86±13.75	176.21 ±4.50
	WT	174.99 ±7.17	168.24 ±8.63	179.22 ±7.28	166.03 ±8.47	222.00 ±10.42	165.32 ±13.56
	p	**0.005**	**0.011**	**0.003**	**0.002**	0.803	0.394
Ps. Pm (mm)	$GOAT^{-/-}$	7.77 ±0.21	8.45 ±0.44	8.27 ±0.25	8.62 ±0.38	8.40 ±0.28	11.08 ±0.43
	WT	8.171 ±0.16	9.67 ±0.48	8.34 ±0.27	9.20 ±0.11	8.58 ±0.05	10.36 ±0.43
	p	0.180	0.103	0.852	0.242	0.691	0.295
Ec. Pm (mm)	$GOAT^{-/-}$	5.74 ±0.26	5.08 ±0.19	6.06 ±0.15	5.51 ±0.62	6.53 ±0.20	5.95 ±0.36
	WT	6.67 ±0.19	6.53 ±0.26	6.37 ±0.15	6.02 ±0.20	7.46 ±0.37	6.17 ±0.54
	p	**0.021**	**0.002**	0.209	0.515	**0.039**	0.732
Ct.Ar (mm^2)	$GOAT^{-/-}$	3.11 ±0.08	2.22 ±0.10	3.18 ±0.08	2.31 ±0.19	3.82 ±0.14	2.89 ±0.27
	WT	3.28 ±0.02	2.440 ±0.06	3.392 ±0.09	2.368 ±0.06	4.226 ±0.17	2.51 ±0.05
	p	0.071	0.122	0.135	0.825	0.118	0.271
pMOI	$GOAT^{-/-}$	0.40 ±0.03	0.28 ±0.02	0.39 ±0.02	0.28 ±0.01	0.51 ±0.03	0.37 ±0.01
	WT	0.37 ±0.008	0.40 ±0.017	0.40 ±0.021	0.39 ±0.015	0.69 ±0.07	0.436 ±0.010
	p	0.4273	**0.0062**	**0.8663**	**0.0032**	**0.0260**	**0.0287**

Table 6.4-4: Micro-architectural indices of 8 week old female (non-pregnant) WT mice, characterised for comparison with 8 week old GOAT$^{-/-}$ mice.

	8 week old WT	
limb	femora	tibiae
Tb. BMD (mg/HAcm^3)	97.28±10.8	90.99±11.69
BV/TV (%)	8.27±1.36	9.85±1.65
Tb.N (1/mm)	4.22±0.19	3.81±0.29
Tb.Th (mm)	0.049±0.001	0.049±0.001
Tb.Sp (mm)	0.235±0.01	0.269±0.021
Conn.Den (1/mm^3)	73.47±14.72	65.92±17.48
Cortical BMD	424.75±10.59	509.68±4.95

Table 6.4-5: Weights of neonatal and 8 week old WT mice, sacrificed for comparison with GOAT$^{-/-}$ mice.

Age	Weights
Female neonates-8 days	4.06±0.05
Male neonates- 8 days	3.72±0.24
Post-pregnant females 8 weeks	28.4±0.3
Non-pregnant females 8 weeks	19.74±0.21

Table 6.4-6: Limb lengths of WT neonates and post-pregnant female mice.

	Length (cm)			
Limb	Right femur	Right tibia	Left femur	Left tibia
Female neonates	0.58±0.02	0.86±0.02	0.58±0.02	0.89±0.03
Male neonates	0.53±0.04	0.78±0.03	0.54±0.04	0.77±0.05
8 wk post-pregnant females	1.47±0.18	1.75±0.05	1.55±0.05	1.75±0.05

References

Al Massadi, O., Tschop, M. H., & Tong, J. (2011). Ghrelin acylation and metabolic control. *Peptides, 32*(11), 2301-2308. doi: 10.1016/j.peptides.2011.08.020

Altenbach, H. (2013). Qin, Qing-Hua: Mechanics of Cellular Bone Remodeling – Coupled Thermal, Electrical, and Mechanical Field Effects. CRC Press: Taylor & Francis Group, Boca Raton, London, New York. *ZAMM - Journal of Applied Mathematics and Mechanics / Zeitschrift für Angewandte Mathematik und Mechanik, 93*(5), 345-345. doi: 10.1002/zamm.201390010

Amini, P., Cahill, F., Wadden, D., Ji, Y., Pedram, P., Vidyasankar, S., . . . Sun, G. (2013). Beneficial association of serum ghrelin and peptide YY with bone mineral density in the Newfoundland population. *BMC Endocr Disord, 13*(1), 35. doi: 10.1186/1472-6823-13-35

Ammann, P., & Rizzoli, R. (2003). Bone strength and its determinants. *Osteoporos Int, 14 Suppl 3*, S13-18. doi: 10.1007/s00198-002-1345-4

Arvat, E., Di Vito, L., Broglio, F., Papotti, M., Muccioli, G., Dieguez, C., . . . Ghigo, E. (2000). Preliminary evidence that Ghrelin, the natural GH secretagogue (GHS)-receptor ligand, strongly stimulates GH secretion in humans. *J Endocrinol Invest, 23*(8), 493-495.

Arvat, E., Maccario, M., Di Vito, L., Broglio, F., Benso, A., Gottero, C., . . . Ghigo, E. (2001). Endocrine activities of ghrelin, a natural growth hormone secretagogue (GHS), in humans: comparison and interactions with hexarelin, a nonnatural peptidyl GHS, and GH-releasing hormone. *J Clin Endocrinol Metab, 86*(3), 1169-1174. doi: 10.1210/jcem.86.3.7314

Bang, A. S., Soule, S. G., Yandle, T. G., Richards, A. M., & Pemberton, C. J. (2007). Characterisation of proghrelin peptides in mammalian tissue and plasma. *J Endocrinol, 192*(2), 313-323. doi: 10.1677/joe-06-0021

Bone Health and Osteoporosis: A Report of the Surgeon General. (2004). Rockville MD.

Bouxsein, M. L., Boyd, S. K., Christiansen, B. A., Guldberg, R. E., Jepsen, K. J., & Muller, R. (2010). Guidelines for assessment of bone microstructure in rodents using micro-computed tomography. *J Bone Miner Res, 25*(7), 1468-1486. doi: 10.1002/jbmr.141

Brandi, M. L. (2009). Microarchitecture, the key to bone quality. *Rheumatology (Oxford), 48 Suppl 4*, iv3-8. doi: 10.1093/rheumatology/kep273

Bruzzaniti, A., & Baron, R. (2006). Molecular regulation of osteoclast activity. *Rev Endocr Metab Disord, 7*(1-2), 123-139. doi: 10.1007/s11154-006-9009-x

Caminos, J. E., Gualillo, O., Lago, F., Otero, M., Blanco, M., Gallego, R., . . . Dieguez, C. (2005). The endogenous growth hormone secretagogue (ghrelin) is synthesized and secreted by chondrocytes. *Endocrinology, 146*(3), 1285-1292. doi: 10.1210/en.2004-1379

Cannata, D., Vijayakumar, A., Fierz, Y., & LeRoith, D. (2010). The GH/IGF-1 axis in growth and development: new insights derived from animal models. *Adv Pediatr, 57*(1), 331-351. doi: 10.1016/j.yapd.2010.09.003

Chan, C. B., & Cheng, C. H. (2004). Identification and functional characterization of two alternatively spliced growth hormone secretagogue receptor transcripts from the pituitary of black seabream Acanthopagrus schlegeli. *Mol Cell Endocrinol, 214*(1-2), 81-95. doi: 10.1016/j.mce.2003.11.020

Chanoine, J. P., & Wong, A. C. (2004). Ghrelin gene expression is markedly higher in fetal pancreas compared with fetal stomach: effect of maternal fasting. *Endocrinology, 145*(8), 3813-3820. doi: 10.1210/en.2004-0053

Chappard, D., Baslé, M. F., Legrand, E., & Audran, M. (2008). Trabecular bone microarchitecture: A review. *Morphologie, 92*(299), 162-170. doi: http://dx.doi.org/10.1016/j.morpho.2008.10.003

Chen, H., Zhou, X., Fujita, H., Onozuka, M., & Kubo, K. Y. (2013). Age-related changes in trabecular and cortical bone microstructure. *Int J Endocrinol, 2013*, 213234. doi: 10.1155/2013/213234

Chihara, K., & Sugimoto, T. (1997). The action of GH/IGF-I/IGFBP in osteoblasts and osteoclasts. *Horm Res, 48 Suppl 5*, 45-49.

Choi, H. J., Ki, K. H., Yang, J. Y., Jang, B. Y., Song, J. A., Baek, W. Y., . . . Shin, C. S. (2013). Chronic central administration of Ghrelin increases bone mass through a mechanism independent of appetite regulation. *PLoS One, 8*(7), e65505. doi: 10.1371/journal.pone.0065505

Chopin, L., Walpole, C., Seim, I., Cunningham, P., Murray, R., Whiteside, E., . . . Herington, A. (2011). Ghrelin and cancer. *Mol Cell Endocrinol, 340*(1), 65-69. doi: 10.1016/j.mce.2011.04.013

Chow, K. B. S., Sun, J., Man Chu, K., Tai Cheung, W., Cheng, C. H. K., & Wise, H. (2012). The truncated ghrelin receptor polypeptide (GHS-R1b) is localized in the endoplasmic reticulum where it forms heterodimers with ghrelin receptors (GHS-R1a) to attenuate their cell surface expression. *Mol Cell Endocrinol, 348*(1), 247-254. doi: http://dx.doi.org/10.1016/j.mce.2011.08.034

Clarke, B. (2008). Normal Bone Anatomy and Physiology. *Clinical Journal of the American Society of Nephrology, 3*(Supplement 3), S131-S139. doi: 10.2215/cjn.04151206

Cohen, M. M., Jr. (2006). The new bone biology: pathologic, molecular, and clinical correlates. *Am J Med Genet A, 140*(23), 2646-2706. doi: 10.1002/ajmg.a.31368

Costa, J. L., Naot, D., Lin, J. M., Watson, M., Callon, K. E., Reid, I. R., . . . Cornish, J. (2011). Ghrelin is an Osteoblast Mitogen and Increases Osteoclastic Bone Resorption In Vitro. *Int J Pept, 2011*, 605193. doi: 10.1155/2011/605193

Crockett, J. C., Rogers, M. J., Coxon, F. P., Hocking, L. J., & Helfrich, M. H. (2011). Bone remodelling at a glance. *J Cell Sci, 124*(Pt 7), 991-998. doi: 10.1242/jcs.063032

D'Elia, G., Caracchini, G., Cavalli, L., & Innocenti, P. (2009). Bone fragility and imaging techniques. *Clin Cases Miner Bone Metab, 6*(3), 234-246.

Date, Y., Kojima, M., Hosoda, H., Sawaguchi, A., Mondal, M. S., Suganuma, T., . . . Nakazato, M. (2000). Ghrelin, a novel growth hormone-releasing acylated peptide, is synthesized in a distinct endocrine cell type in the gastrointestinal tracts of rats and humans. *Endocrinology, 141*(11), 4255-4261.

Delhanty, P. J., van der Eerden, B. C., van der Velde, M., Gauna, C., Pols, H. A., Jahr, H., . . . van Leeuwen, J. P. (2006). Ghrelin and unacylated ghrelin stimulate human osteoblast growth via mitogen-activated protein kinase (MAPK)/phosphoinositide 3-kinase (PI3K) pathways in the absence of GHS-R1a. *J Endocrinol, 188*(1), 37-47. doi: 10.1677/joe.1.06404

Delhanty, P. J. D., van der Eerden, B. C. J., & van Leeuwen, J. P. T. M. (2013). Ghrelin and bone. *BioFactors*, n/a-n/a. doi: 10.1002/biof.1120

Deng, F., Ling, J., Ma, J., Liu, C., & Zhang, W. (2008). Stimulation of intramembranous bone repair in rats by ghrelin. *Exp Physiol, 93*(7), 872-879. doi: 10.1113/expphysiol.2007.041962

DiGirolamo, D. J., Mukherjee, A., Fulzele, K., Gan, Y., Cao, X., Frank, S. J., & Clemens, T. L. (2007). Mode of Growth Hormone Action in Osteoblasts. *Journal of Biological Chemistry, 282*(43), 31666-31674. doi: 10.1074/jbc.M705219200

Drake, W. M., Howell, S. J., Monson, J. P., & Shalet, S. M. (2001). Optimizing gh therapy in adults and children. *Endocr Rev, 22*(4), 425-450. doi: 10.1210/edrv.22.4.0438

Feng, X., & McDonald, J. M. (2011). Disorders of bone remodeling. *Annu Rev Pathol, 6*, 121-145. doi: 10.1146/annurev-pathol-011110-130203

Ferretti, J. L., Capozza, R. F., Mondelo, N., & Zanchetta, J. R. (1993). Interrelationships between densitometric, geometric, and mechanical properties of rat femora: inferences concerning mechanical regulation of bone modeling. *J Bone Miner Res, 8*(11), 1389-1396. doi: 10.1002/jbmr.5650081113

Frost, H. M. (1990a). Skeletal structural adaptations to mechanical usage (SATMU): 1. Redefining Wolff's law: the bone modeling problem. *Anat Rec, 226*(4), 403-413. doi: 10.1002/ar.1092260402

Frost, H. M. (1990b). Skeletal structural adaptations to mechanical usage (SATMU): 2. Redefining Wolff's law: the remodeling problem. *Anat Rec, 226*(4), 414-422. doi: 10.1002/ar.1092260403

Fukushima, N., Hanada, R., Teranishi, H., Fukue, Y., Tachibana, T., Ishikawa, H., . . . Kojima, M. (2005). Ghrelin directly regulates bone formation. *J Bone Miner Res, 20*(5), 790-798. doi: 10.1359/jbmr.041237

Fung, J. N., Jeffery, P. L., Lee, J. D., Seim, I., Roche, D., Obermair, A., . . . Chen, C. (2013). Silencing of ghrelin receptor expression inhibits endometrial cancer cell growth in vitro and in vivo. *Am J Physiol Endocrinol Metab, 305*(2), E305-313. doi: 10.1152/ajpendo.00156.2013

Gahete, M. D., Rincon-Fernandez, D., Villa-Osaba, A., Hormaechea-Agulla, D., Ibanez-Costa, A., Martinez-Fuentes, A. J., . . . Luque, R. M. (2014). Ghrelin gene products, receptors, and GOAT enzyme: biological and pathophysiological insight. *J Endocrinol, 220*(1), R1-R24. doi: 10.1530/joe-13-0391

Gentili, C., & Cancedda, R. (2009). Cartilage and bone extracellular matrix. *Curr Pharm Des, 15*(12), 1334-1348.

Gillberg, P., Mallmin, H., Petrén-Mallmin, M., Ljunghall, S., & Nilsson, A. G. (2002). Two Years of Treatment with Recombinant Human Growth Hormone Increases Bone Mineral Density in Men with Idiopathic Osteoporosis. *The Journal of Clinical Endocrinology & Metabolism, 87*(11), 4900-4906. doi: doi:10.1210/jc.2002-020231

Giustina, A., Mazziotti, G., & Canalis, E. (2008). Growth hormone, insulin-like growth factors, and the skeleton. *Endocr Rev, 29*(5), 535-559. doi: 10.1210/er.2007-0036

Gomez, R., Lago, F., Gomez-Reino, J. J., Dieguez, C., & Gualillo, O. (2009). Expression and modulation of ghrelin O-acyltransferase in cultured chondrocytes. *Arthritis Rheum, 60*(6), 1704-1709. doi: 10.1002/art.24522

Gotherstrom, G., Svensson, J., Koranyi, J., Alpsten, M., Bosaeus, I., Bengtsson, B., & Johannsson, G. (2001). A prospective study of 5 years of GH replacement therapy in GH-deficient adults: sustained effects on body composition, bone mass, and metabolic indices. *J Clin Endocrinol Metab, 86*(10), 4657-4665. doi: 10.1210/jcem.86.10.7887

Granata, R., Settanni, F., Biancone, L., Trovato, L., Nano, R., Bertuzzi, F., . . . Muccioli, G. (2007). Acylated and unacylated ghrelin promote proliferation and inhibit apoptosis of pancreatic beta-cells and human islets: involvement of 3',5'-cyclic adenosine monophosphate/protein kinase A, extracellular signal-regulated kinase 1/2, and phosphatidyl inositol 3-Kinase/Akt signaling. *Endocrinology, 148*(2), 512-529. doi: 10.1210/en.2006-0266

Gutierrez, J. A., Solenberg, P. J., Perkins, D. R., Willency, J. A., Knierman, M. D., Jin, Z., . . . Hale, J. E. (2008). Ghrelin octanoylation mediated by an orphan lipid transferase. *Proc Natl Acad Sci U S A, 105*(17), 6320-6325. doi: 10.1073/pnas.0800708105

Harvey, M. (2013). *Intuitive Biostatistics: A Nonmathematical Guide to Statistical Thinking, 3rd edition*: Oxford University Press.

Holst, B., Cygankiewicz, A., Jensen, T. H., Ankersen, M., & Schwartz, T. W. (2003). High constitutive signaling of the ghrelin receptor--identification of a potent inverse agonist. *Mol Endocrinol, 17*(11), 2201-2210. doi: 10.1210/me.2003-0069

Hosoda, H., Kojima, M., Matsuo, H., & Kangawa, K. (2000). Ghrelin and des-acyl ghrelin: two major forms of rat ghrelin peptide in gastrointestinal tissue. *Biochem Biophys Res Commun, 279*(3), 909-913. doi: 10.1006/bbrc.2000.4039

Howard, A. D., Feighner, S. D., Cully, D. F., Arena, J. P., Liberator, P. A., Rosenblum, C. I., . . . Van der Ploeg, L. H. (1996). A receptor in pituitary and hypothalamus that functions in growth hormone release. *Science, 273*(5277), 974-977.

Jeffery, P. L., Herington, A. C., & Chopin, L. K. (2003). The potential autocrine/paracrine roles of ghrelin and its receptor in hormone-dependent cancer. *Cytokine Growth Factor Rev, 14*(2), 113-122.

Kang, K., Zmuda, E., & Sleeman, M. W. (2011). Physiological role of ghrelin as revealed by the ghrelin and GOAT knockout mice. *Peptides, 32*(11), 2236-2241. doi: 10.1016/j.peptides.2011.04.028

Kim, S. W., Her, S. J., Park, S. J., Kim, D., Park, K. S., Lee, H. K., . . . Kim, S. Y. (2005). Ghrelin stimulates proliferation and differentiation and inhibits apoptosis in osteoblastic MC3T3-E1 cells. *Bone, 37*(3), 359-369. doi: 10.1016/j.bone.2005.04.020

Kini, U., & Nandeesh, B. N. (2012). Physiology of Bone Formation, Remodeling, and Metabolism. *Radionuclide and Hybrid Bone Imaging, I. Fogelman et al. (eds.)*.

Kirchner, H., Gutierrez, J. A., Solenberg, P. J., Pfluger, P. T., Czyzyk, T. A., Willency, J. A., . . . Tschop, M. H. (2009). GOAT links dietary lipids with the endocrine control of energy balance. *Nat Med, 15*(7), 741-745. doi: 10.1038/nm.1997

Kirchner, H., Heppner, K. M., & Tschop, M. H. (2012). The role of ghrelin in the control of energy balance. *Handb Exp Pharmacol*(209), 161-184. doi: 10.1007/978-3-642-24716-3_7

Kishimoto, I., Tokudome, T., Hosoda, H., Miyazato, M., & Kangawa, K. (2012). Ghrelin and cardiovascular diseases. *J Cardiol, 59*(1), 8-13. doi: 10.1016/j.jjcc.2011.11.002

Kojima, M., Hosoda, H., Date, Y., Nakazato, M., Matsuo, H., & Kangawa, K. (1999). Ghrelin is a growth-hormone-releasing acylated peptide from stomach. *Nature, 402*(6762), 656-660. doi: 10.1038/45230

Kojima, M., & Kangawa, K. (2005). Ghrelin: structure and function. *Physiol Rev, 85*(2), 495-522. doi: 10.1152/physrev.00012.2004

Koranyi, J., Svensson, J., Gotherstrom, G., Sunnerhagen, K. S., Bengtsson, B., & Johannsson, G. (2001). Baseline characteristics and the effects of five years of GH replacement therapy in adults with GH deficiency of childhood or adulthood onset: a comparative, prospective study. *J Clin Endocrinol Metab, 86*(10), 4693-4699. doi: 10.1210/jcem.86.10.7896

Landin-Wilhelmsen, K., Nilsson, A., Bosaeus, I., & Bengtsson, B.-Å. (2003). Growth Hormone Increases Bone Mineral Content in Postmenopausal Osteoporosis: A Randomized Placebo-Controlled Trial. *Journal of Bone and Mineral Research, 18*(3), 393-405. doi: 10.1359/jbmr.2003.18.3.393

Leung, P.-K., Chow, K. B. S., Lau, P.-N., Chu, K.-M., Chan, C.-B., Cheng, C. H. K., & Wise, H. (2007). The truncated ghrelin receptor polypeptide (GHS-R1b) acts as a dominant-negative mutant of the ghrelin receptor. *Cellular Signalling, 19*(5), 1011-1022. doi: http://dx.doi.org/10.1016/j.cellsig.2006.11.011

Liao L., & Wang, W. (2010). Effects of ghrelin on the proliferation and differentiation of human osteoblasts. *Journal of Clinical and Rehabilitative Tissue engineering Research, 14* (41), 7621-7625.

Lim, C. T., Kola, B., Grossman, A., & Korbonits, M. (2011). The expression of ghrelin O-acyltransferase (GOAT) in human tissues. *Endocr J, 58*(8), 707-710.

Lim, C. T., Kola, B., & Korbonits, M. (2011). The ghrelin/GOAT/GHS-R system and energy metabolism. *Rev Endocr Metab Disord, 12*(3), 173-186. doi: 10.1007/s11154-011-9169-1

Litwack, G. (2008). Ghrelin. *Vitam Horm, 77*.

Liu, B., Garcia, E. A., & Korbonits, M. (2011). Genetic studies on the ghrelin, growth hormone secretagogue receptor (GHSR) and ghrelin O-acyl transferase (GOAT) genes. *Peptides, 32*(11), 2191-2207. doi: 10.1016/j.peptides.2011.09.006

Liu, Z., Lavine, K. J., Hung, I. H., & Ornitz, D. M. (2007). FGF18 is required for early chondrocyte proliferation, hypertrophy and vascular invasion of the growth plate. *Dev Biol, 302*(1), 80-91. doi: 10.1016/j.ydbio.2006.08.071

Maccarinelli, G., Sibilia, V., Torsello, A., Raimondo, F., Pitto, M., Giustina, A., . . . Cocchi, D. (2005). Ghrelin regulates proliferation and differentiation of osteoblastic cells. *J Endocrinol, 184*(1), 249-256. doi: 10.1677/joe.1.05837

Mackie, E. J., Ahmed, Y. A., Tatarczuch, L., Chen, K. S., & Mirams, M. (2008). Endochondral ossification: how cartilage is converted into bone in the developing skeleton. *Int J Biochem Cell Biol, 40*(1), 46-62. doi: 10.1016/j.biocel.2007.06.009

Mackie, E. J., Tatarczuch, L., & Mirams, M. (2011). The skeleton: a multi-functional complex organ: the growth plate chondrocyte and endochondral ossification. *J Endocrinol, 211*(2), 109-121. doi: 10.1530/joe-11-0048

McKee, K. K., Palyha, O. C., Feighner, S. D., Hreniuk, D. L., Tan, C. P., Phillips, M. S., . . . Howard, A. D. (1997). Molecular analysis of rat pituitary and hypothalamic growth hormone secretagogue receptors. *Mol Endocrinol, 11*(4), 415-423. doi: 10.1210/mend.11.4.9908

Misra, M., Miller, K. K., Stewart, V., Hunter, E., Kuo, K., Herzog, D. B., & Klibanski, A. (2005). Ghrelin and bone metabolism in adolescent girls with anorexia nervosa and healthy adolescents. *J Clin Endocrinol Metab, 90*(9), 5082-5087. doi: 10.1210/jc.2005-0512

Mondal, M. S., Toshinai, K., Ueno, H., Koshinaka, K., & Nakazato, M. (2008). Characterization of obestatin in rat and human stomach and plasma, and its lack of acute effect on feeding behavior in rodents. *J Endocrinol, 198*(2), 339-346. doi: 10.1677/joe-08-0082

Morel, G., Chavassieux, P., Barenton, B., Dubois, P. M., Meunier, P. J., & Boivin, G. (1993). Evidence for a direct effect of growth hormone on osteoblasts. *Cell Tissue Res, 273*(2), 279-286.

Muccioli, G., Pons, N., Ghe, C., Catapano, F., Granata, R., & Ghigo, E. (2004). Ghrelin and des-acyl ghrelin both inhibit isoproterenol-induced lipolysis in rat adipocytes via a non-type 1a growth hormone secretagogue receptor. *Eur J Pharmacol, 498*(1-3), 27-35. doi: 10.1016/j.ejphar.2004.07.066

Nakahara, K., Nakagawa, M., Baba, Y., Sato, M., Toshinai, K., Date, Y., . . . Murakami, N. (2006). Maternal ghrelin plays an important role in rat fetal development during pregnancy. *Endocrinology, 147*(3), 1333-1342. doi: 10.1210/en.2005-0708

Napoli, N., Pedone, C., Pozzilli, P., Lauretani, F., Bandinelli, S., Ferrucci, L., & Incalzi, R. A. (2011). Effect of ghrelin on bone mass density: the InChianti study. *Bone, 49*(2), 257-263. doi: 10.1016/j.bone.2011.03.772

Nishi, Y., Hiejima, H., Hosoda, H., Kaiya, H., Mori, K., Fukue, Y., . . . Kojima, M. (2005). Ingested medium-chain fatty acids are directly utilized for the acyl modification of ghrelin. *Endocrinology, 146*(5), 2255-2264. doi: 10.1210/en.2004-0695

Nouh, O., Abd Elfattah, M. M., & Hassouna, A. A. (2012). Association between ghrelin levels and BMD: a cross sectional trial. *Gynecol Endocrinol, 28*(7), 570-572. doi: 10.3109/09513590.2011.593663

Oh, K. W., Lee, W. Y., Rhee, E. J., Baek, K. H., Yoon, K. H., Kang, M. I., . . . Park, S. W. (2005). The relationship between serum resistin, leptin, adiponectin, ghrelin levels and bone mineral density in middle-aged men. *Clin Endocrinol (Oxf), 63*(2), 131-138. doi: 10.1111/j.1365-2265.2005.02312.x

Ohlsson, C., Bengtsson, B. A., Isaksson, O. G., Andreassen, T. T., & Slootweg, M. C. (1998). Growth hormone and bone. *Endocr Rev, 19*(1), 55-79. doi: 10.1210/edrv.19.1.0324

Olsen, B. R., Reginato, A. M., & Wang, W. (2000). Bone development. *Annu Rev Cell Dev Biol, 16*, 191-220. doi: 10.1146/annurev.cellbio.16.1.191

Oxlund, H., Ejersted, C., Andreassen, T. T., Torring, O., & Nilsson, M. H. (1993). Parathyroid hormone (1-34) and (1-84) stimulate cortical bone formation both from periosteum and endosteum. *Calcif Tissue Int, 53*(6), 394-399.

Pacheco-Pantoja, E. L., Ranganath, L. R., Gallagher, J. A., Wilson, P. J., & Fraser, W. D. (2011). Receptors and effects of gut hormones in three osteoblastic cell lines. *BMC Physiol, 11*, 12. doi: 10.1186/1472-6793-11-12

Parfitt, A. M. (1984). Age-related structural changes in trabecular and cortical bone: cellular mechanisms and biomechanical consequences. *Calcif Tissue Int, 36 Suppl 1*, S123-128.
Parkinson, I. H., & Fazzalari, N. L. (2013). Characterisation of Trabecular Bone Structure. *Stud Mechanobiol Tissue Eng Biomater, 5*, 31–51.
Parra-Torres, A. Y., Valdés-Flores, M., Orozco, L., & Velázquez-Cruz, R. (2013). *Molecular Aspects of Bone Remodeling*.
Pemberton, C., Wimalasena, P., Yandle, T., Soule, S., & Richards, M. (2003). C-terminal pro-ghrelin peptides are present in the human circulation. *Biochem Biophys Res Commun, 310*(2), 567-573.
Raisz, L. G. (1999). Physiology and pathophysiology of bone remodeling. *Clin Chem, 45*(8 Pt 2), 1353-1358.
Root, A. W., & Root, M. J. (2002). Clinical pharmacology of human growth hormone and its secretagogues. *Curr Drug Targets Immune Endocr Metabol Disord, 2*(1), 27-52.
Sakata, I., Yang, J., Lee, C. E., Osborne-Lawrence, S., Rovinsky, S. A., Elmquist, J. K., & Zigman, J. M. (2009). Colocalization of ghrelin O-acyltransferase and ghrelin in gastric mucosal cells. *Am J Physiol Endocrinol Metab, 297*(1), E134-141. doi: 10.1152/ajpendo.90859.2008
Sato, T., Nakamura, Y., Shiimura, Y., Ohgusu, H., Kangawa, K., & Kojima, M. (2011). Structure, regulation and function of ghrelin. *J Biochem*. doi: 10.1093/jb/mvr134
Sattler, F. R. (2013). Growth hormone in the aging male. *Best Practice & Research Clinical Endocrinology & Metabolism, 27*(4), 541-555. doi: http://dx.doi.org/10.1016/j.beem.2013.05.003
Seeman, E. (2009). Bone modeling and remodeling. *Crit Rev Eukaryot Gene Expr, 19*(3), 219-233.
Seeman, E. (2013). Age- and menopause-related bone loss compromise cortical and trabecular microstructure. *J Gerontol A Biol Sci Med Sci, 68*(10), 1218-1225. doi: 10.1093/gerona/glt071
Seim, I., Josh, P., Cunningham, P., Herington, A., & Chopin, L. (2011). Ghrelin axis genes, peptides and receptors: recent findings and future challenges. *Mol Cell Endocrinol, 340*(1), 3-9. doi: 10.1016/j.mce.2011.05.002
Shin, Y. K., Martin, B., Kim, W., White, C. M., Ji, S., Sun, Y., . . . Egan, J. M. (2010). Ghrelin is produced in taste cells and ghrelin receptor null mice show reduced taste responsivity to salty (NaCl) and sour (citric acid) tastants. *PLoS One, 5*(9), e12729. doi: 10.1371/journal.pone.0012729
Skerry, T. M. (2006). One mechanostat or many? Modifications of the site-specific response of bone to mechanical loading by nature and nurture. *J Musculoskelet Neuronal Interact, 6*(2), 122-127.
Skibicka, K. P., Hansson, C., Egecioglu, E., & Dickson, S. L. (2012). Role of ghrelin in food reward: impact of ghrelin on sucrose self-administration and mesolimbic dopamine and acetylcholine receptor gene expression. *Addict Biol, 17*(1), 95-107. doi: 10.1111/j.1369-1600.2010.00294.x
Stevens, D. A., & Williams, G. R. (1999). Hormone regulation of chondrocyte differentiation and endochondral bone formation. *Mol Cell Endocrinol, 151*(1-2), 195-204.
Sun, Y., Ahmed, S., & Smith, R. G. (2003). Deletion of ghrelin impairs neither growth nor appetite. *Mol Cell Biol, 23*(22), 7973-7981.
Sun, Y., Garcia, J. M., & Smith, R. G. (2007). Ghrelin and growth hormone secretagogue receptor expression in mice during aging. *Endocrinology, 148*(3), 1323-1329. doi: 10.1210/en.2006-0782
Sun, Y., Wang, P., Zheng, H., & Smith, R. G. (2004). Ghrelin stimulation of growth hormone release and appetite is mediated through the growth hormone secretagogue receptor. *Proc Natl Acad Sci U S A, 101*(13), 4679-4684. doi: 10.1073/pnas.0305930101
Taichman, R. S. (2005). Blood and bone: two tissues whose fates are intertwined to create the hematopoietic stem-cell niche. *Blood, 105*(7), 2631-2639. doi: 10.1182/blood-2004-06-2480
Takahashi, T., Ida, T., Sato, T., Nakashima, Y., Nakamura, Y., Tsuji, A., & Kojima, M. (2009). Production of n-octanoyl-modified ghrelin in cultured cells requires prohormone processing protease and ghrelin O-acyltransferase, as well as n-octanoic acid. *J Biochem, 146*(5), 675-682. doi: 10.1093/jb/mvp112

Takeda, R., Nishimatsu, H., Suzuki, E., Satonaka, H., Nagata, D., Oba, S., . . . Hirata, Y. (2006). Ghrelin improves renal function in mice with ischemic acute renal failure. *J Am Soc Nephrol, 17*(1), 113-121. doi: 10.1681/asn.2004080626

Tanck, E., Homminga, J., van Lenthe, G. H., & Huiskes, R. (2001). Increase in bone volume fraction precedes architectural adaptation in growing bone. *Bone, 28*(6), 650-654.

Thielemans, L., Peeters, P. J., Jonckheere, H., Luyten, W., de Hoogt, R., Coulie, B., & Aerssens, J. (2007). The hepatocarcinoma cell line HepG2 does not express a GHS-R1a-type ghrelin receptor. *J Recept Signal Transduct Res, 27*(4), 309-322. doi: 10.1080/10799890701519587

Tschop, M., Smiley, D. L., & Heiman, M. L. (2000). Ghrelin induces adiposity in rodents. *Nature, 407*(6806), 908-913. doi: 10.1038/35038090

Tuan, R. S. (2004). Biology of developmental and regenerative skeletogenesis. *Clin Orthop Relat Res*(427 Suppl), S105-117.

Van Der Linden, J. C., Verhaar, J. A., & Weinans, H. (2001). A three-dimensional simulation of age-related remodeling in trabecular bone. *J Bone Miner Res, 16*(4), 688-696. doi: 10.1359/jbmr.2001.16.4.688

van der Velde, M., Delhanty, P., van der Eerden, B., van der Lely, A. J., & van Leeuwen, J. (2008). Ghrelin and bone. *Vitam Horm, 77*, 239-258. doi: 10.1016/s0083-6729(06)77010-8

van der Velde, M., van der Eerden, B. C., Sun, Y., Almering, J. M., van der Lely, A. J., Delhanty, P. J., . . . van Leeuwen, J. P. (2012). An age-dependent interaction with leptin unmasks ghrelin's bone-protective effects. *Endocrinology, 153*(8), 3593-3602. doi: 10.1210/en.2012-1277

Volante, M., Allia, E., Fulcheri, E., Cassoni, P., Ghigo, E., Muccioli, G., & Papotti, M. (2003). Ghrelin in fetal thyroid and follicular tumors and cell lines: expression and effects on tumor growth. *Am J Pathol, 162*(2), 645-654. doi: 10.1016/s0002-9440(10)63858-8

Volante, M., Fulcheri, E., Allia, E., Cerrato, M., Pucci, A., & Papotti, M. (2002). Ghrelin expression in fetal, infant, and adult human lung. *J Histochem Cytochem, 50*(8), 1013-1021.

Weiss, L. A., Langenberg, C., & Barrett-Connor, E. (2006). Ghrelin and Bone: Is There an Association in Older Adults?: The Rancho Bernardo Study. *Journal of Bone and Mineral Research, 21*(5), 752-757. doi: 10.1359/jbmr.060209

Werther, G. A., Haynes, K., Edmonson, S., Oakes, S., Buchanan, C. J., Herington, A. C., & Waters, M. J. (1993). Identification of growth hormone receptors on human growth plate chondrocytes. *Acta Paediatr Suppl, 82 Suppl 391*, 50-53.

Werther, G. A., Haynes, K., & Waters, M. J. (1993). Growth hormone (GH) receptors are expressed on human fetal mesenchymal tissues--identification of messenger ribonucleic acid and GH-binding protein. *J Clin Endocrinol Metab, 76*(6), 1638-1646.

Werther, G. A., Haynes, K. M., Barnard, R., & Waters, M. J. (1990). Visual demonstration of growth hormone receptors on human growth plate chondrocytes. *J Clin Endocrinol Metab, 70*(6), 1725-1731.

Wierup, N., Svensson, H., Mulder, H., & Sundler, F. (2002). The ghrelin cell: a novel developmentally regulated islet cell in the human pancreas. *Regulatory Peptides, 107*(1–3), 63-69. doi: http://dx.doi.org/10.1016/S0167-0115(02)00067-8

Wit, J. M., & Camacho-Hubner, C. (2011). Endocrine regulation of longitudinal bone growth. *Endocr Dev, 21*, 30-41. doi: 10.1159/000328119

Wren, A. M., Small, C. J., Ward, H. L., Murphy, K. G., Dakin, C. L., Taheri, S., . . . Bloom, S. R. (2000). The novel hypothalamic peptide ghrelin stimulates food intake and growth hormone secretion. *Endocrinology, 141*(11), 4325-4328. doi: 10.1210/endo.141.11.7873

Yang, J., Brown, M. S., Liang, G., Grishin, N. V., & Goldstein, J. L. (2008). Identification of the acyltransferase that octanoylates ghrelin, an appetite-stimulating peptide hormone. *Cell, 132*(3), 387-396. doi: 10.1016/j.cell.2008.01.017

Yi, C. X., Heppner, K. M., Kirchner, H., Tong, J., Bielohuby, M., Gaylinn, B. D., . . . Pfluger, P. T. (2012). The GOAT-ghrelin system is not essential for hypoglycemia prevention during prolonged calorie restriction. *PLoS One, 7*(2), e32100. doi: 10.1371/journal.pone.0032100

Zhang, J. V., Ren, P.-G., Avsian-Kretchmer, O., Luo, C.-W., Rauch, R., Klein, C., & Hsueh, A. J. W. (2005). Obestatin, a Peptide Encoded by the Ghrelin Gene, Opposes Ghrelin's Effects on Food Intake. *Science, 310*(5750), 996-999. doi: 10.1126/science.1117255

Zhu, X., Cao, Y., Voogd, K., & Steiner, D. F. (2006). On the processing of proghrelin to ghrelin. *J Biol Chem, 281*(50), 38867-38870. doi: 10.1074/jbc.M607955200